5-1992

Development of a Generalized Quartic Equation of State for Pure Fluids

Vinod M. Shah
University of Tennessee - Knoxville

To the Graduate Council:

I am submitting herewith a dissertation written by Vinod M. Shah entitled "Development of a Generalized Quartic Equation of State for Pure Fluids." I have examined the final electronic copy of this dissertation for form and content and recommend that it be accepted in partial fulfillment of the requirements for the degree of Doctor of Philosophy, with a major in Chemical Engineering.

Paul R. Bienkowski, Hank D. Cochran, Major Professor

We have read this dissertation and recommend its acceptance:

H. W. Hsu, W. A. VanHook

Accepted for the Council:

Carolyn R. Hodges

Vice Provost and Dean of the Graduate School

(Original signatures are on file with official student records.)

To the Graduate Council:

I am submitting herewith a dissertation written by Vinod M. Shah entitled "Development of a Generalized Quartic Equation of State for Pure Fluids." I have examined the final copy of this dissertation for form and content and recommend that it be accepted in partial fulfillment of the requirements for the degree of Doctor of Philosophy, with a major in Chemical Engineering.

Paul R. Bienkowski, Co-Major Professor

Hank D. Cochran, Co-Major Professor

We have read this dissertation
and recommend its acceptance:

Accepted for the Council:

Associate Vice Chancellor
and Dean of The Graduate School

DEVELOPMENT OF A GENERALIZED QUARTIC EQUATION OF STATE FOR PURE FLUIDS

A Dissertation

Presented for the

Doctor of Philosophy

Degree

The University of Tennessee, Knoxville

Vinod M. Shah

May 1992

DEDICATION

This dissertation is dedicated to my parents

Mr. Mavjibhai V. Shah

and

Mrs. Maniben M. Shah

ACKNOWLEDGEMENTS

I would like to express my sincere thanks to Dr. Paul Bienkowski for his guidance, help and encouragement during the course of this work. I would also like to express my deepest gratitude and thanks to Dr. Hank Cochran for helpful suggestions and the use of computing facilities at the Oak Ridge National Laboratory without which this work could not have been completed. I am grateful to Dr. H. W. Hsu and Dr. W. A. VanHook for serving on my committee and giving useful suggestions. I would like to thank my brother Bipin his support and help. Finally, I would like to thank my wife, Shilpa, for her love, support and patience.

ABSTRACT

A generalized quartic equation of state has been developed for pure simple fluids. It is a four parameter perturbed hard sphere equation of state. The four parameters of the equation of state for any fluid depend only on three properties of the fluid, namely critical temperature, critical volume and the acentric factor. The repulsive contribution to the pressure has been modelled using an mathematical approximation of a hard-sphere equation of state. An empirical equation is used to model the attractive contributions to the pressure. Being a quartic equation of state, it yields four roots when solved. One root of the quartic equation is always less than the close packed volume of the fluid and hence has no physical meaning. The remaining three roots behave like the three roots of a cubic equation of state. Thus, the equation of state has the advantages of the cubic equation of state, namely, simplicity and unequivocal identification of the roots. The quartic equation of state models the attractive and repulsive contributions to the pressure correctly, unlike cubic equations of state.

The constants in the equation of state have been obtained by performing multiproperty regressions using data for 16 pure fluids. These constants have been generalized and are functions of the acentric factor of the fluid. Comparison of the new equation of state with the Peng-Robinson and the Kubic's quartic equation of state has been presented. Density and thermodynamic properties such as the second virial coefficient and residual enthalpy predictions have been compared. The new equation of state is more accurate than the Peng-Robinson and the Kubic equation of state, particularly, in the supercritical region and the compressed liquid region.

TABLE OF CONTENTS

LIST OF FIGURES

LIST OF TABLES

Nomenclature

a = parameter of the quartic equation of state, MPa/dm^6

b = van der Waals volume, mol/dm^3

B_{vir} = Second virial coefficient, cm^3/mol

c = parameter of the quartic equation of state, MPa/dm^6

d = parameter of the quartic equation of state, mol/dm^3

e = parameter of the quartic equation of state, mol/dm^3

f = fugacity, MPa

g^E_∞ = Excess Gibbs energy at infinite pressure

H_r = Residual Enthalpy, J/mol

H_v = Enthalpy of vaporization, J/mol

k_0, k_1 = quartic equation of state constants

N = Number of data points

P = Pressure, MPa

R = Universal gas constant, $\frac{MPadm^3}{molK}$

T = Temperature, K

V = Molar volume, dm^3/mol

x, y = mole fractions

X_i = quartic equation of state constants

y = packing fraction

Z = compressibility of a fluid

α = nonsphericity parameter used in hard-convex body equations

$\alpha(T_r)$ = temperature dependence of parameter a

β = hard core volume, dm^3/mol

ω = acentric factor

Ω = dimensionless parameters of the equation of state

ρ = Density, mol/dm^3

$\xi(T_r)$ = temperature dependence of parameter c

Subscripts and Superscripts

c = value at the critical temperature or the critical point

$calc$ = calculated value value

exp = experimental value

g = gas, single phase region

hs = hard-sphere

hc = hard-core

l = liquid phase

v = vapor phase

r = reduced property or constant

s = saturated, two-phase envelope

sl = saturated liquid phase

sv = saturated vapor phase

$\star$ = reduced variable

CHAPTER 1

Introduction

Mathematical equations that describe the state (phase) of a substance are called Equations of State (EOS). These equations can be used to calculate the physical properties such as pressure and molar volume of substances at different temperatures. Thermodynamic properties such as specific heat, isothermal compressibility and enthalpy can also be calculated. These equations are widely used in the chemical industry to model and predict phase equilibria and in process design calculations. Different equations of state predict these properties with different degrees of accuracy.

The main objective of this research was to develop a simple, yet, accurate equation of state. Cubic equations of state model the repulsive forces incorrectly. In order to model the repulsive forces accurately an equation of degree greater than three was necessary. A quartic equation was chosen as an analytical solution exists. Thus, it could be subjected to a mathematical analysis and the behavior of its roots could be studied and characterized. This could be useful in formulating rules for the correct identification of the roots. Fifth degree polynomial equations cannot be solved analytically.

A background on the existing equations of state is presented in Chapter 2. The focus has been restricted to generalized equation of state, i.e., those equations that are not specific to a particular chemical substance. Particular emphasis has been give to cubic equations of state. These have been widely accepted in the chemical industry because of their simplicity and reasonable accuracy. A survey of the recent advances

in the various mixing rules used in the cubic equations of state has been presented. A survey of the applications of cubic equations of state for the prediction of critical points of multicomponent mixtures is also presented in chapter 2.

Chapter 3 contains the methodology used to develop the quartic equation of state. The deficiencies of cubic equations of state have been pointed out. The development of a simple hard-sphere repulsive term based on reported molecular dynamics simulations has been presented. The procedure of finding an attractive term and combining it with the repulsive term to form a quartic equation of state is given. Chapter 3 also shows the development of the nonlinear regression programs used for estimating the constants of the equation of state. Chapter 4 deals with the results of regressions and the final forms of the equation of state. Comparison of thermodynamic properties calculated by the new equation of state with those from the Peng-Robinson equation of state and Kubic's quartic equation of state are presented. Chapter 5 deals with the conclusions of this work. Recommendations for future work on extending the equation of state to a larger variety of fluids have been given.

Additional work performed on two topics during the course of this research has been presented in the appendices. Appendix E deals with correlating the solubility of the antibiotic Penicillin V in supercritical CO_2. The Peng-Robinson equation of state and the Kirkwood-Buff model were used for the correlations. Appendix F deals with Monte Carlo simulations in the grand canonical ensemble for dilute supercritical fluid mixtures. Simulations were performed to study the clustering behavior of the solvent molecules about the solute molecule. Comparison of the results with molecular dynamic simulations reported in literature have been done.

CHAPTER 2

Background

Pressure explicit equations of state are the most commonly used equations of state. In these equations, repulsive and attractive forces between the molecules contribute to the pressure. It is desirable to have independent terms describe these contributions to the pressure in a fluid. Most equations of state try to model these two contributions independently. This chapter provides a background on the various equations of state. These include, the cubic, hard-sphere, hard-core equations, and perturbed hard-sphere equations. A brief introduction to the perturbation theories of liquids has been given. Cubic equations of state are the simplest of all equations of state which work for real fluids over a wide range of conditions.

Equations of state are widely used in the chemical industry to describe the phase behavior of mixtures. These equations can be used for mixtures by using 'rules' to describe the interactions between molecules of different types. These rules are called 'Mixing Rules'. This chapter provides a summary of some of the new types of mixing rules, particularly developed for cubic equations of state.

2.1 Cubic Equations of State

Cubic equations of state have gained widespread popularity in the chemical industry over the last two decades for predicting phase equilibria of pure compounds and mixtures. Van der Waals [1] proposed the first cubic equation of state in 1873, which is

given by :

$$P = \frac{RT}{(V-b)} - \frac{a}{V^2} \tag{2.1}$$

where

P is the pressure of the substance,

T is the temperature of the substance,

V is the molar volume of the substance,

R is the universal gas constant,

a is the attraction parameter,

b is the van der Waals volume of the substance.

In most cubic equations of state the contribution to the pressure due to repulsive forces between molecules is given by the van der Waals repulsive term

$$P_{rep} = \frac{RT}{(V-b)} \tag{2.2}$$

where

P_{rep} is the contribution to the pressure due to the repulsion between the molecules.

It was based on the assumption that only collisions between a pair of molecules occur in dilute gases. As a result, four times the volume of one molecule was not available to any other molecule. While this assumption is true for dilute gases, it is no longer

valid at higher densities. The Redlich-Kwong equation of state [2] was proposed in 1949. It was considerably superior to the equations of state available at that time. The Redlich-Kwong (RK) equation is given by :

$$P = \frac{RT}{(V-b)} - \frac{a}{\sqrt{T}(V+b)V} \tag{2.3}$$

The RK equation retained the van der Waals P_{rep} term, a practice followed in all the popular cubic equations of state. Soave [3] introduced a temperature dependence in a parameter of the RK equation and let it be a function of the acentric factor of the fluid. Peng and Robinson [4] proposed an equation of state in 1976. The Peng-Robinson (PR) equation of state (equation 2.4) had improved liquid density predictions as compared to the Soave equation of state.

$$P = \frac{RT}{(V-b)} - \frac{a}{(V+b)V + b(V-b)} \tag{2.4}$$

Presently, the Soave equation and the Peng-Robinson equation are the most popular of all the cubic equations of state. These are two-parameter equations of state whose parameters, a and b, are determined by assuming an analytical behavior of the equation of state at the critical point. Then, a and b are related to the critical pressure and temperature of a fluid by applying the conditions

$$\left(\frac{\partial P}{\partial V}\right)_{T_c,P_c} = 0 \tag{2.5}$$

$$\left(\frac{\partial^2 P}{\partial V^2}\right)_{T_c,P_c} = 0 \tag{2.6}$$

Parameter a is a measure of the attractive forces between molecules and b represents the excluded volume of the molecules in the same form as used by van der Waals.

The two-parameter equations of state predict a fixed critical compressibility for all the substances. However, different substances have different critical compressibilities.

As a result, these two-parameter cubic equations of state perform poorly in the vicinity of the critical point. Abbot [5] showed that the critical compressibility predicted by cubic equations had to be greater than the actual compressibility. This was necessary for improved accuracy in predicting the molar volumes, at high pressures, along the critical isotherm. Another two-parameter equation of state is the PRSV (Peng-Robinson-Stryjek-Vera) [6] equation of state. The PRSV equation has the same form as the Peng-Robinson equation of state except for a different temperature dependence of a. Adachi and Sugie [7, 8], showed that the heat of vaporization of the substance in cubic equations of state depends only on the parameter a. Melhem et al. [9] used Adachi's ideas to determine the temperature dependence of a for the Peng-Robinson equation.

To account for the component-dependent critical compressibility, a third parameter used in the equation of state was introduced by Usdin and McAuliffe [10], Martin [11], Schmidt and Wenzel [12], Harmens and Knapp [13], Heyen [14], Patel and Teja [15], Kubic [16] and Freze et al. [17]. The Patel-Teja equation of state gave better estimates of liquid molar volumes than the Soave and the Peng-Robinson equations of state. Yu et al. [18] proposed a three parameter cubic equation of state that had only one temperature-dependent parameter. Yu, Lu, and Iwai [19] proposed a cubic equation of state that was extended to polar fluids by Iwai, Margerum and Lu [20].

Four-parameter cubic equations of state have been proposed by Adachi, Lu, and Sugie [21], Guo, Kim, Lin, and Chao [22] and Trebble and Bishnoi [23]. A five-parameter cubic equation of state has been proposed by Adachi and Sugie [24]. Justification for using five parameters was based on the analysis of the behavior of the attractive contribution of the equation of state with the reduced density. In this equation of state,

all the parameters were expressed as functions of the reduced temperature and/or the acentric factor of the pure fluid.

Temperature dependence of the b parameter has been incorporated in the Heyen [14], Watson [25] and Trebble-Bishnoi (TB) [23] equations of state. Trebble and Bishnoi [26] performed a critical evaluation of 10 equations of state using pure component data for 75 fluids. They showed that decreasing b with increasing temperature led to negative heat capacity predictions by the Heyen EOS above the critical temperature. Hence, they used a value of b which increased with temperature in their four-parameter equation of state. Trebble and Salim [27] have recently removed the temperature dependency from b completely from the TB equation of state, as it lead to prediction of negative heat capacities at reduced temperatures below 0.5.

Zudkevitch and Joffe [28], Yarborough [29], and Morris and Turek [30] allowed the parameters a and b to be polynomial functions of temperature. The temperature dependence of a and b was obtained by fitting the Soave equation of state to the pure component properties at various temperatures. To obtain temperature-dependent parameters a and b, Panagiotopoulos and Kumar [31] extended the technique used by Zudkevitch and Joffe [28]. The temperature dependence of a and b was independent of the nature of the substance. Cisternas [32] proposed a method to determine the pure component temperature-dependent parameters of the three parameter Usdin-McAuliffe [10] equation of state.

Martin [11] showed that a simple translation along the volume axis

$$v = \tilde{v} - c \tag{2.7}$$

where

$\tilde{v}$ is the translated volume,

v is the actual volume,

c is a translation constant.

can improve the performance of a cubic equation of state. Peneloux et al. [33] showed that such a volume translation does not affect the phase equilibria predicted by these equations. They also showed that a considerable improvement in the calculated molar volumes can be obtained for the Peng-Robinson and Soave equations of state using volume translation. Mathias, Naheiri and Oh [34] used this idea to develop a density correction for the Peng-Robinson equation of state. They used an empirical additive term to correct the liquid molar volumes. Guo, Kim, Lin, and Chao [22] have proposed a unique hard-sphere repulsive term which takes into account contributions due to the rotational motion of hard chains. Being an cubic equation of state it is called the Cubic Chain of Rotators (CCOR) equation of state. Kubic, proposed the first quartic equation of state [35] and extended it to mixtures [36]. He used the repulsive term used in the CCOR equation of state. It was a three parameter equation of state, with the temperature dependence of the parameters based on the temperature dependence of the second virial coefficients. Soave [37] has also proposed a quartic equation of state for pure fluids.

Most of the cubic equations of state fail to predict high pressure phase equilibria accurately. One of the problems is that the cubic equations of state yield only one solution for the compressibility of a mixture at high pressures, even in a two phase region. This happens when the psuedocritical temperature of the mixture is exceeded. Several techniques [38], [39], [40] have been proposed to allow the identification of the

roots of the cubic equation under such conditions.

2.2 Other Equations of State

They are more accurate than the cubic equations of state. A number of these equations of state are theoretically more correct. Almost all the other equations of state are functionally more complicated than the cubic equations of state. They also give rise to multiple solutions and are difficult to use for phase equilibrium calculations. This makes these equations of state less attractive for use when compared with the cubic equations of state.

2.2.1 Hard-Sphere and Hard-Core Equations of State

It has been pointed out [41] that the van der Waals equation of state is more correct in its attractive $\frac{a}{V^2}$ term than in its repulsive $\frac{RT}{(V-b)}$ term. The Carnahan-Starling [42] equation for hard-spheres is in agreement with molecular dynamic and Monte Carlo simulations for hard-spheres. The Carnahan-Starling equation is given by,

$$\left(\frac{PV}{RT}\right)_{hs} = \frac{1 + y + y^2 - y^3}{(1-y)^3} \tag{2.8}$$

where

hs represents the hard-sphere contribution,

y is the packing fraction of the fluid and is given by the equation

$$y = \rho\frac{N_A \pi d^3}{6} \tag{2.9}$$

where

ρ is the density of the fluid,

d is the hard-sphere diameter, and

N_A is the Avagadro's number.

Alder et al. [43] performed molecular dynamics simulations of hard spheres at high densities. At high densities their results no longer agreed with those predicted by the Carnahan-Starling Equation (2.8). Kenneth Hall [44] proposed a hard-sphere equation of state which agreed with the results of Alder et al. at high densities. The Carnahan-Starling Equation (2.8) and the Hall equation differ from each other only at packing fractions greater than 0.5. Erpenbeck and Wood [45] have proposed a hard-sphere equation of state based on extensive Monte Carlo-molecular dynamic simulations. Zhou and Stell [46] have also proposed an hard-sphere equation of state. Both these equations are more accurate than the Carnahan-Starling equation as more accurate simulation data were used to test and develop these equations.

Gibbons [47] applied the Scaled Particle Theory (SPT) to pure convex bodies. Later, Gibbons [48] showed that it was difficult to extend the SPT to mixtures of convex bodies of different shapes. Boublik [49], [50] presented a hard-core equation of state that could be applied to hard convex bodies. Boublik's equation is given by

$$\left(\frac{PV}{RT}\right)_{hc} = \frac{1}{(1-y)} + \frac{3\alpha y}{(1-y)^2} + \frac{3\alpha^2 y^2 - \alpha^2 y^3}{(1-y)^3} \tag{2.10}$$

where

y is the packing fraction of the fluid,

α is the non-sphericity parameter of the convex molecule, and

hc represents the hard convex body contribution only.

Nezbeda [51] proposed a similar hard core equation of sate for convex bodies. Nezbeda's equation is given by :

$$\left(\frac{PV}{RT}\right)_{hc} = \frac{1}{(1-y)} + \frac{3\alpha y}{(1-y)^2} + \frac{(\alpha^2 + 4\alpha - 2)\, y^2 - (5\alpha^2 - 4\alpha)\, y^3}{(1-y)^3} \tag{2.11}$$

Boublik and Nezbeda's equations used a non-sphericity parameter α, which has a value of one for a sphere and greater than one for convex bodies. Monte Carlo simulation studies [52] on spherocylinders have shown that both the Nezbeda and Boublik's equation of state are quite accurate up to a L/D (length to diameter) ratio of 2. Nezbeda and Boublik[53] showed the non-equivalence of a variety of hard convex body fluids at high densities; that is convex bodies having the same α but different shapes do not necessarily obey the same equation of state. Naumann et al. [54] proposed a hard-core equation of state with an additional parameter τ, which is a measure of the 'needleness' characterizing the shape of the convex body. Azevedo and Prausnitz [55] studied the effect of molecular size and shape on the thermodynamic properties of binary mixtures. The Naumann equation of state was used for their studies.

2.2.2 Perturbed Hard-Sphere Equations of State

Based on molecular dynamic studies of a square well fluid, Alder et al. [56] proposed that the residual Helmholtz energy for a fluid can be described by a power series of the density of the fluid. Chen and Kreglewski [57] combined the Boublik's hard-core Equation (2.10) with the attractive terms of Alder's equation to form an equation of state, called the BACK equation (for **B**oublik-**A**lder-**C**hen-**K**reglewski). Equations of state developed with a hard-sphere reference pair potential are called Perturbed hard-sphere equations

of state. Several perturbed hard-sphere equations of state have been proposed which use the Carnahan-Starling (CS) hard-sphere Equation (2.8) to represent the repulsive contributions to the pressure. Carnahan and Starling [58] used the attractive term of the Redlich-Kwong equation of state and obtained a remarkable improvement in PVT and enthalpy predictions at high pressures.

Beret and Prausnitz [59] proposed the Perturbed Hard Chain Theory (PHCT). An unique attraction term was used with a hard-sphere repulsion term, to form a three parameter equation of state for hard chains. The third parameter was introduced to account for the rotational and vibrational motions of long chained molecules. Donohue and Prausnitz [60] extended this equation of state to mixtures. De Santis [61] used the Clausius attraction term with the CS hard-sphere term to form a two parameter equation of state. Both the parameters were allowed to be temperature dependent. Nakamura et al. [62] proposed a perturbed hard-sphere equation of state for polar and nonpolar substances. Oellrich et al. [63] proposed a simple perturbed hard-sphere equation of state based on the Carnahan-Starling-van der Waals (CSvdW) equation of state. Donohue and Vimalchand [64] have reviewed the development and applications of PHCT and several equations of state based on PHCT.

To describe the behavior of simple fluids, Bienkowski et al. [65] combined the Carnahan-Starling equation 2.8 with a virial expansion. The hard-core volumes for the simple fluids were deduced from isothermal compressibility data and its extrapolation to infinite pressures [66]. Svejda and Kohler [67] used Boublik's hard-core equation 2.10 and the van der Waals equation's attractive term to form an equation of state. They treated the molecules as having a temperature independent core surrounded by a temperature-dependent hard layer. Marchand et al. [68] analyzed the temperature de-

pendence of the a parameter of the Carnahan-Starling-Redlich-Kwong (CSRK) equation of state for the prediction of vapor pressures of pure substances.

2.2.3 Perturbation Theories of Liquids

In the liquid state, the repulsive interactions between molecules play an important role. The properties of a hard-sphere fluid have been studied using statistical thermodynamics and computer simulations. While simple potential models such as hard-spheres cannot adequately describe the liquid phase, they could serve as reference potentials, and attractive interactions could be treated as perturbations on the reference system.

Perturbation theories of liquids treat the real fluids as having a reference intermolecular potential with a perturbed potential representing the attractive part of the intermolecular potential. Thus, the pair potential is divided as

$$v(r_{12}) = v_0(r_{12}) + w(r_{12}) \tag{2.12}$$

where

$v(r_{12})$ is the pair potential of the molecules 1 and 2,

r_{12} is the distance between the two molecules,

$v_0(r_{12})$ is the pair potential of the reference system, and

$w(r_{12})$ is the perturbation.

Several theories use a "soft-core" reference potential, particularly important are that of Barker and Henderson (BH) and that of Weeks, Chandler, and Andersen (WCA). In the Barker-Henderson theory, the reference system is defined by the part of the Lennard-Jones potential that is positive ($r < \sigma$) , while the perturbation consists of the part that

is negative ($r > \sigma$). The hard-sphere diameter in the BH treatment can be obtained by a analytical expression and is a function of temperature only. The BH perturbation theory was the first of its kind capable of yielding accurate results for the liquid state. In the WCA method the Lennard-Jones potential is split at the minimum of the potential, $r = r_m$, into its purely repulsive ($r < r_m$) and purely attractive ($r > r_m$) parts. The hard-sphere diameter in the WCA treatment depends on the temperature and density of the reference system.

2.3 Equations of State and Mixtures

Equations of state are widely used in the chemical industry to calculate the phase behavior of mixtures. As mentioned earlier, mixing rules are used with an equation of state to describe the behavior of mixtures. The performance of the equations of state for mixtures depends considerably on the type of mixing rules used. Cubic equations of state have been widely used for mixtures because of their simplicity, the unequivocal identification of the roots and the ease with which they could be used for increasing number of components in the mixture.

Before the widespread use of equations of state, the behavior of liquid mixtures had been successfully described using Excess Gibbs Energy Models. Equations of state with conventional mixing rules cannot describe liquid mixtures as accurately as excess Gibbs energy models. The next section describes the recent advances made to incorporate the knowledge of excess Gibbs energy models into the mixing rules for equations of state. This has been done largely with cubic equations of state in an attempt to improve their performance for liquid mixtures.

2.3.1 Mixing Rules and Excess Gibbs Energy in Cubic Equations of State

The most commonly used mixing rules with the cubic equation of state are the one-fluid van der Waals mixing rules shown below.

$$a_m = \sum_i \sum_j x_i x_j a_{ij} \tag{2.13}$$

$$a_{ij} = \sqrt{a_i a_j}\,(1 - k_{ij}) \tag{2.14}$$

$$b_m = \sum_i \sum_j x_i x_j b_{ij} \tag{2.15}$$

$$b_{ij} = \left(\frac{b_i + b_j}{2}\right)(1 - \eta_{ij}) \tag{2.16}$$

where

x_i is the mole fraction of the component i,

a_i is the attractive parameter for component i,

b_i is the excluded volume parameter for component i,

a_m is the attractive parameter for the mixture,

b_m is the excluded volume parameter for the mixture,

h_{ij} is an adjustable parameter,

k_{ij} is an adjustable parameter.

η_{ij} and k_{ij} are determined by fitting the equation of state to experimental data.

If η_{ij} is set to zero, Equation (2.16) reduces to

$$b_{ij} = \left(\frac{b_i + bj}{2}\right) \tag{2.17}$$

Vidal [69] showed that the van der Waals constants for a mixture are related to the excess Gibbs free energy for the mixture at infinite pressure. Huron and Vidal [70] used the NRTL model, assuming that it could be applied at an infinite pressure, to relate the parameters of cubic equations of state for polar mixtures. A linear mixing rule was used for the volume parameter b_m given by Equation (2.17); however, a_m was given by :

$$a_m = b_m \left(\sum_i x_i \frac{a_i}{b_i} - \frac{g^E_\infty}{\ln 2}\right) \tag{2.18}$$

where

g^E_∞ is the excess Gibbs free energy at infinite pressure.

They reported a considerable improvement in the prediction of high pressure vapor-liquid equilibria with polar compounds using the new mixing rule. Won [71] used the excess Gibbs free energy at infinite pressure approach with the Soave equation of state. The g^E_∞ was derived using the NRTL model to explain the solubility of high boiling organic solutes in supercritical fluids.

Soave [72] used the new mixing rule with the van der Waals and Redlich-Kwong equations of state. Tochigi et al. [73], [74] and Pandit et al. [75] have applied these rules to the Soave, the Peng-Robinson, and the Martin equations of state. The ASOG group contribution method was used to obtain the values of excess Gibbs free energy for the mixtures. Soave [76] proposed procedures to obtain the activity coefficients at infinite pressure from liquid phase activity coefficients. Mollerup [77] proposed a modified form

of Soave's mixing rule. Gupte et al. [78] used the excess Gibbs free energy at infinite pressure approach with the van der Waals equation of state. A modified UNIFAC group-contribution method [79] was used to predict g^E_∞. However, when any of the components was supercritical, the NRTL model was used instead of UNIFAC. Stryjek [80] used this approach with the PRSV [6] equation of state. Kurihara et al. [81] used these mixing rules with the Soave equation of state. To obtain values for g^E_∞, they used the Redlich-Kister expansion. These mixing rules do not transform to the classical quadratic mixing rules at low pressures, thus limiting the accuracy of vapor phase calculations at low pressures. However, it has been argued that at low pressures a large portion of the non-ideality, in the vapor-liquid calculations, arises from the liquid phase and not the vapor phase.

2.3.2 Mixing Rules in Other Equations of State

The behavior of liquid mixtures cannot be described accurately by simple equations of state and simple mixing rules. Such behavior can be accurately described by excess Gibbs energy and activity coefficient models. Using the local-composition concept, Mollerup [82] showed that the excess Gibbs energy models and activity coefficient models could be derived from van der Waals equation of state. The excess Gibbs energy models included the van Laar, the Scatchard-Hildebrand, and the Flory-Huggins models. The activity coefficient models included the NRTL, the Wilson and the UNIQUAC models. Based on these concepts Mollerup proposed local-composition versions of the van der Waals, Soave and the Peng-Robinson equations of state. Whiting and Prausnitz [83] developed a local-composition model for van der Waals type equations of state. The mixing rules developed by Mollerup [82] and Whiting and Prausnitz incorporated

density dependence. Thus, their mixing rules interpolated between the low density limit (quadratic behavior with mole fractions) and a high density (liquid like) limit.

Lee et al. [84] used statistical-mechanical treatment to show that the local-composition models could be defined in terms of the pair-correlation functions and the potential of mean force. Sandler [85] proposed the theory of the generalized van der Waals partition function and showed its relation to the equations of state, their mixing rules and excess Gibbs energy models. Lee, Lombardo and Sandler [86] applied this theory to square-well fluids to obtain an equation of state. To determine how the coordination number varied with temperature and density, they used Monte Carlo simulation on square-well fluids. Lee, Sandler and Patel [87] performed Monte Carlo simulations for binary mixtures of equal sized molecules of square-well fluids. They proposed new local-composition models for such mixtures. Lee and Sandler [88] proposed a new local-composition activity coefficient model based on Monte Carlo simulations for binary mixtures of square-well molecules. The molecules were of equal energy but different sizes. They also proposed a new density dependent mixing rule for an equation of state, which was then used to develop a cubic equation of state.

Kanchanakpan, Lee and Twu [89] developed an equation of state for non-spherical molecules based on distribution function theories. A two-step form of the square-well potential was used to describe the behavior of real fluids. Using statistical mechanics, Lee [90] reformulated the Scatchard-Hildebrand theory of solubility parameters and applied it to polar mixtures. By using the hard-core mixing terms developed by Nezbeda and mixing rules given by Boublik [91], Lee allowed entropic effects to be included.

2.4 Multicomponent Phase Equilibria and Critical Points

The following section only deals with vapor-liquid phase equilibria. Beegle, Modell and Reid [92] developed a criterion, using Legendre transforms, to determine the thermodynamic stability for pure substances and mixtures. Reid and Beegle [93] used Legendre transforms to derive a general criterion to determine the critical points for multicomponent mixtures. Peng and Robinson [94] used the Gibbs criterion to predict the critical properties of multicomponent mixtures, using the Peng-Robinson equation of state. A more general procedure to calculate the critical points of multicomponent mixtures using a single equation of state was developed by Heidemann and Khalil [95]. The Heidemann-Khalil procedure is easier to implement than the Peng-Robinson procedure. The Heidemann-Khalil procedure only requires the partial derivatives of the Helmholtz free energy of the mixture with respect to the mole fractions. The Peng-Robinson procedure however uses the partial derivatives of the internal energy as well as the partial derivatives of the Gibbs free energy with respect to the mole fractions of the components. Michelsen and Heidemann [96] suggested an easier procedure to implement the Heidemann-Khalil procedure for two-parameter cubic equations of state.

Hong, Modell and Tester [97] applied the Beegle-Modell-Reid criterion with the Peng-Robinson equation of state to predict binary phase equilibria. The binary systems studied were supercritical carbon dioxide-naphthalene, carbon dioxide-n-hexadecane and ethylene-naphthalene. Palenchar, Erickson and Leland [98] studied the predictions of critical properties of binary mixtures using five cubic equations of state. Sadus and Young [99] used the Svejda-Kohler [67]73 hard convex body equation of state to determine the critical properties of binary mixtures. For binary and ternary mixtures,

Mainwaring et al. [100] showed that a hard convex body equation of state does not yield significantly better prediction of critical properties as compared to a simple hard-sphere equation of state.

Baker, Pierce and Luks [101] showed why an equation of state can predict incorrect phase equilibria. They formulated the tangent-plane criterion, which helps in deciding whether the predicted equilibrium is true or false. Michelsen used a modified Gibbs tangent-plane criterion to study phase stability in multicomponent mixtures [102], [103] and to calculate phase boundaries in the critical region [104]. Techniques to locate and construct phase boundaries in multiphase systems, with special emphasis to two and three phase regions using a single equation of state, have been presented [105].

This chapter provided a background on the various equations of state and their extensions to mixtures. An attempt was made to point out the recent trends and advances in equations of states and their applications. There is considerable research going on in this field at the present. The information provided in this chapter is only representative of the recent trends in this area of research. Before a new equation of state is widely accepted by the chemical industry and researchers it has to be tested for its ability to describe a large variety of mixtures and the behavior of multiphase systems. The cubic equations of state have been widely tested with considerable success in these regards. Thus a new equation of state has to outperform cubic equations of state in a number of these areas before it will replace cubic equations.

CHAPTER 3

Development of the Equation of State

Almost all cubic equations of state model the repulsive forces between the molecules incorrectly. Other equations of state use the correct hard-sphere equation to model the repulsive forces. However, some of them use the wrong hard-sphere volumes and hence model the repulsive forces incorrectly. This chapter explains the methodology used to develop the new equation of state. The main idea was to use the correct hard-sphere equation with the correct hard-sphere volumes to model the repulsive interactions between molecules. An empirical term was developed to model the attractive forces between molecules. A quartic equation was chosen because its behavior could be analyzed. Rules could be setup based on such an analysis to identify the roots of the quartic equation. The unequivocal identification of roots of cubic equations of state make them very popular. The quartic equation of state was developed with the idea that its roots could be identified unequivocally.

3.1 Development of the Repulsive Term

In most cubic equations of state, the contribution to the pressure due to repulsion between molecules is given by the van der Waals repulsive term (2.2). This term does not agree closely with Monte Carlo simulations for hard-spheres. The Carnahan-Starling Equation (2.8) represents the simulation data for hard-spheres accurately. A common misconception about the van der Waals repulsive term, when used in cubic equations of

state, is that the volume parameter 'b' is four times the true hard-sphere volume of the molecule. Based on this figures such as Figure 3.1 have been drawn, emphasizing the invalidity of the van der Waals repulsive term at higher densities. According to Figure 3.1 the van der Waals type cubic equations of state fail completely beyond packing fractions of 0.25. In reality, imposing the critical constraints on the van der Waals type cubic equations of state leads to a value of 'b' which is much smaller. As a result, all the cubic equations of state work better than would be expected from Figure 3.1 for higher densities. Table 3.1 shows the relationship between the hard sphere volumes for a simple fluid (argon), determined by various equations of state (at the triple point of argon) and the hard-sphere volumes derived from perturbation theory [107]. The hard-sphere volume is calculated from the value of Ω_b by using Equation (3.1).

$$V_{hs} = \frac{b}{4} = \frac{\Omega_b R T_c}{P_c 4} \tag{3.1}$$

where

$\Omega_b = \frac{b_c P_c}{R T_c}$ is the dimensionless volume parameter calculated at the critical temperature of the fluid,

V_{hs} is the hard-sphere molar volume predicted by the equation of state,

P_c is the critical pressure of argon ,

T_c is the critical temperature of argon.

From Table 3.1 it can be seen that only the CCOR (Cubic Chain of Rotators) equation of state, the CS-vdW and the Dohrn-Prausnitz [106] equation of state predict hard-sphere volumes comparable with used in perturbation theories. Bondi's volume shown

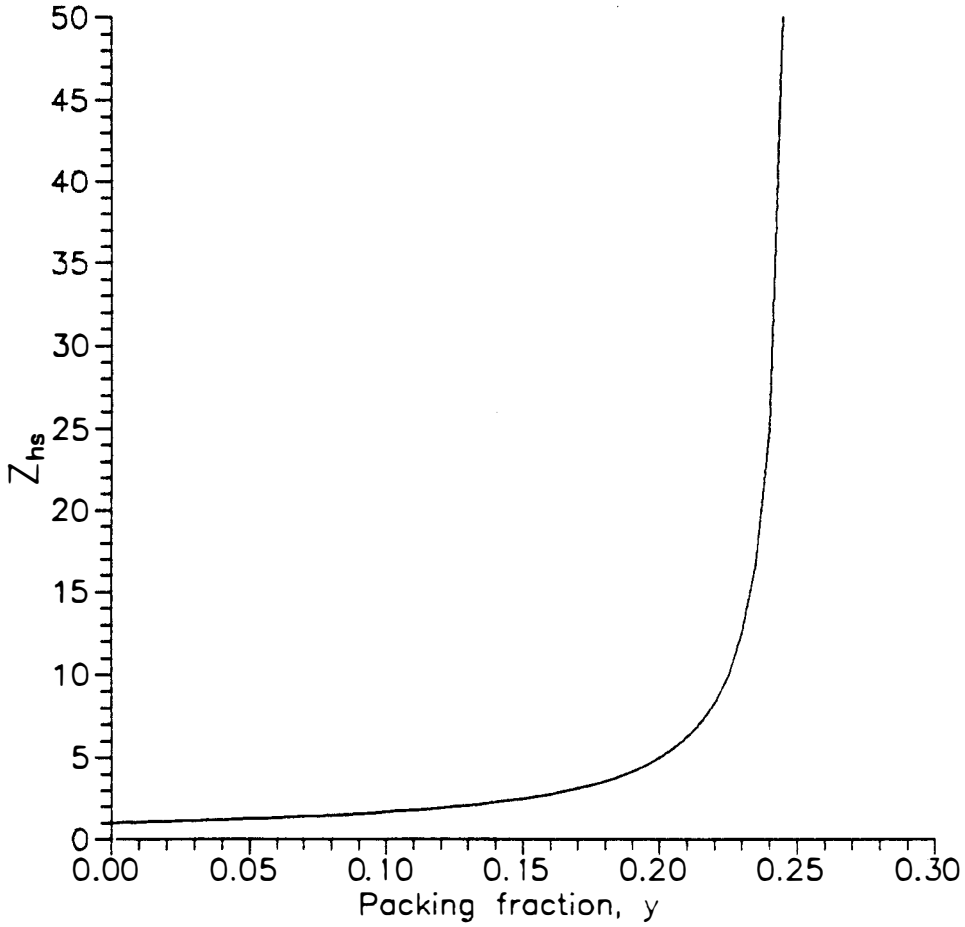

Figure 3.1: Hard-sphere compressibility for a van der Waals fluid

Table 3.1: Hard-sphere volume of argon at its triple point temperature (83.78 K)

Equation	Z_c	Ω_b	V_{hs} cm^3/mol
Dohrn-Prausnitz (DP) [106]	0.298	0.18728	12.05
CS-van der Waals (CS-vdW)	0.366	0.18730	12.06
CS-Redlich Kwong (CS-RK)	0.324	0.10500	6.75
CS-Peng Robinson (CS-PR)	0.273	0.09775	6.29
Redlich Kwong (RK)	0.327	0.08664	5.58
Peng-Robinson (PR)	0.307	0.07780	5.01
CCOR	0.298	0.19000	12.23
Quartic (Kubic) (QK)	0.333	0.13735	8.84
Quartic(Soave) (QS)	0.307	0.09500	6.11
Aim-Nezbeda (hBH Perturbation Theory)	-	-	13.18
Bondi's volume at 0.0 K	-	-	16.80

in Table 3.1 is the hard-sphere volume of a substance at 0 K. Bondi [108] developed a group contribution technique for estimating the hard-sphere volume of substances at 0 K. The volume calculated by this technique is often called 'Bondi's van der Waals volume'. This volume will be referred to as 'Bondi's volume' to avoid confusion with the van der Waals volume parameter used in cubic equations of state.

Figure 3.2 shows the calculations of the hard-sphere compressibility (Z_{hs}) by some of the equations of state as a function of density for argon. The Z_{hs} for the van der Waals (vdW) type equations of state is given by

$$Z_{hs} = \frac{1}{(1 - b\rho)} \tag{3.2}$$

where

b is the van der Waals volume for argon predicted by the equation of state,

ρ is the molar density of argon.

The Z_{hs} for the Carnahan-Starling type (CS) equations of state is given by Equation (2.8). Figure 3.2 also shows the liquid density of argon at its triple point and also at 260 K and 1000 MPa. The packing fraction y of argon shown in Figure 3.2 is based on the hard-sphere volume of Aim and Nezbeda [107]. It can be clearly seen that the Z_{hs} determined by all the van der Waals and the Carnahan-Starling type equations of state do not agree at high densities with that determined by perturbation theory.

The cubic equations of state do a reasonable job of predicting PVT properties of real fluids in spite of the incorrect repulsive contribution. It has required a distortion in the attractive term in the cubic equations of state to compensate for the deficiencies

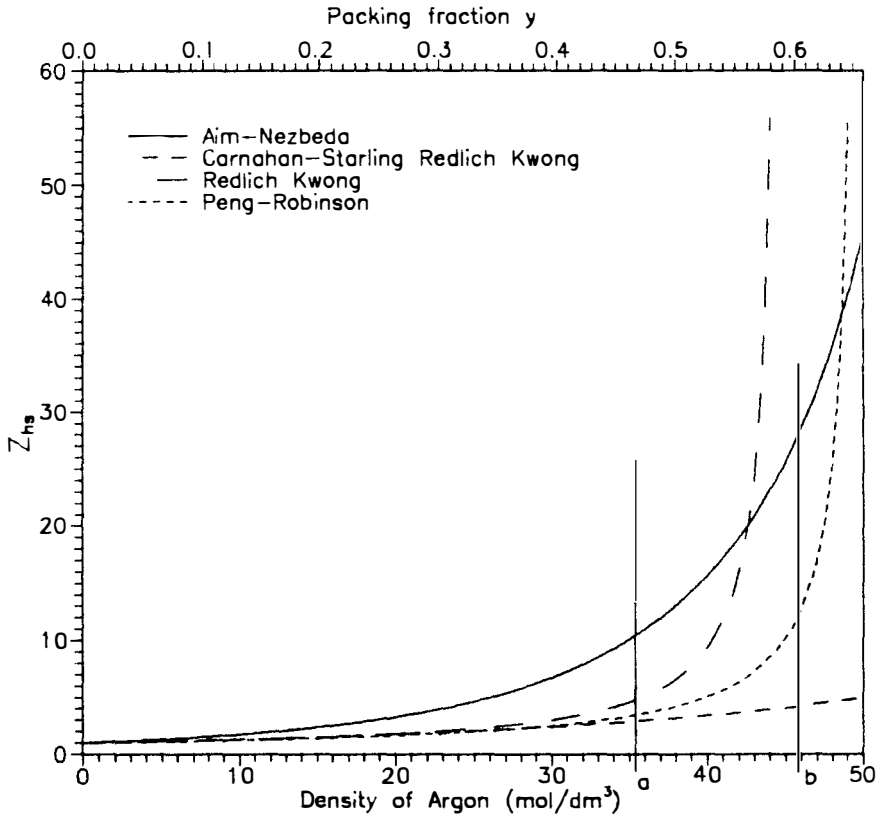

Figure 3.2: Hard-sphere compressibility calculations from various equations of state as a function of packing fraction and density

Vertical line marked (a) shows the density of liquid argon at its triple point and (b) shows the density at 260 K and 1000 MPa.

of the repulsive term. This also explains the fact, that equations of state which used the Carnahan-Starling repulsive term along with the Soave attractive term or the Peng-Robinson attractive term do not perform well.

Because of their algebraic complexity, the Carnahan-Starling Equation (2.8) or the Hall hard-sphere equation [44] could not be used to develop a quartic equation of state. As pointed out earlier, the Hall hard-sphere equation of state agreed with the molecular dynamic results of Alder et al. [43] at high densities. It was found that a mathematically simple term

$$P_{rep} = \frac{RT}{(V - k_0\beta)} + \frac{\beta k_1 RT}{(V - k_0\beta)^2} \tag{3.3}$$

where

β is the hard-sphere molar volume of the fluid.

could be made to fit the molecular dynamics data of Alder et al. [43] closely in the packing fraction range of 0.0 to 0.6. Regression was used to determine the constants k_0 and k_1.

The values of k_0 and k_1 so obtained were 1.2864 and 2.8225 respectively. Figure 3.3 shows the plot of the MD data and the calculated hard-sphere compressibility using Equation (3.3). It can be seen that Equation (3.3) provides a very good approximation to the hard-sphere compressibility data of Alder et al. Because of the algebraic simplicity of Equation (3.3), it could be used to develop a simple quartic equation of state. Equation (3.3) was to be used as a repulsive pressure term in an equation of state.

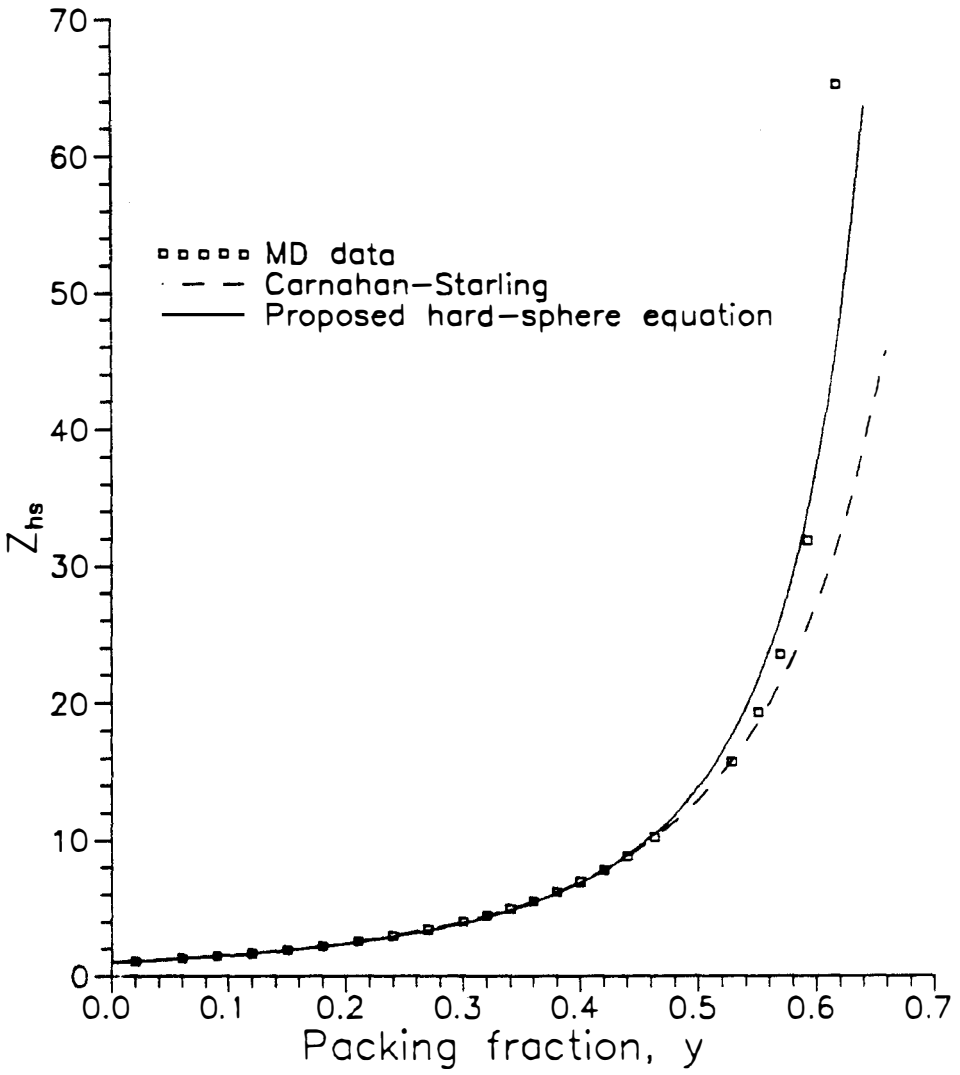

Figure 3.3: Hard-sphere compressibility predicted by the proposed equation
Data source: Alder et al. *J. Chem. Phys.*, 33:1439, 1960.

3.2 Development of an Empirical Attractive Term

The contribution to the pressure due to attractive forces between the molecules has been modelled in perturbation theories using series expansions in densities. The algebraic complexity of these series expansions in densities prevented them from being used with the proposed hard-sphere equation to form a quartic equation of state. Hence, a functional form had to be selected for the attractive term of the equation of state. In order to determine a functional form which could represent attractive forces, the following approach was used. Using real fluid data for argon and hard sphere compressibilities calculated using Equation (3.3), plots of Z_{att} vs ρ^* (reduced density) were prepared for various reduced temperatures.

$$Z_{att} = Z_{exp} - Z_{hs} \tag{3.4}$$

where

Z_{att} is the attractive contribution to the compressibility,

Z_{exp} is the experimental compressibility value.

Z_{hs} is the hard-sphere contribution to the compressibility, and is given by :

$$Z_{hs} = \frac{V}{(V - k_0\beta)} + \frac{k_1\beta V}{(V - k_0\beta)^2} \tag{3.5}$$

$$= \frac{1}{(1 - k_0\beta^*\rho^*)} + \frac{k_1\beta^*\rho^*}{(1 - k_0\beta^*\rho^*)^2} \tag{3.6}$$

where

V is the molar volume of argon,

$\rho^* = \frac{\rho}{\rho_c}$ is the reduced density of argon,

ρ_c is the critical molar density of argon,

$\beta^* = \beta\rho_c$ is the reduced hard-sphere volume of argon.

Figure 3.4 shows such a plot for argon for different reduced temperatures. Nonlinear regression was used to chose one out of several functional forms that gave the best fit to these curves. The functional form was chosen to be dependent on the reduced density and reduced temperature only. Only the functional forms that would lead to a quartic equation of state, when used with the proposed hard-sphere Equation (3.3), were used.

The functional form for Z_{att} given by

$$Z_{att} = -\frac{(\bar{a}V^2)}{(V+d)(V+e)(V-k_0\beta)} + \frac{\bar{c}V}{(V+d)(V+e)} \tag{3.7}$$

where

d and e are substance dependant constants, and

$\bar{a}$ and $\bar{c}$ are substance dependent parameters which are functions of the temperature.

gave the best fits. During the early stages a, c, d, and e were parameters estimated by the nonlinear regression. Thus the equation of state used in the early stages was

$$P = \frac{RT}{(V-k_0\beta)} + \frac{\beta k_1 RT}{(V-k_0\beta)^2} - \frac{\bar{a}VRT}{(V+d)(V+e)(V-k_0\beta)} + \frac{\bar{c}RT}{(V+d)(V+e)} \tag{3.8}$$

Equation (3.8) can be written in another, more convenient form

$$P = \frac{RT}{(V-k_0\beta)} + \frac{\beta k_1 RT}{(V-k_0\beta)^2} - \frac{aV + k_0\beta c}{(V+d)(V+e)(V-k_0\beta)} \tag{3.9}$$

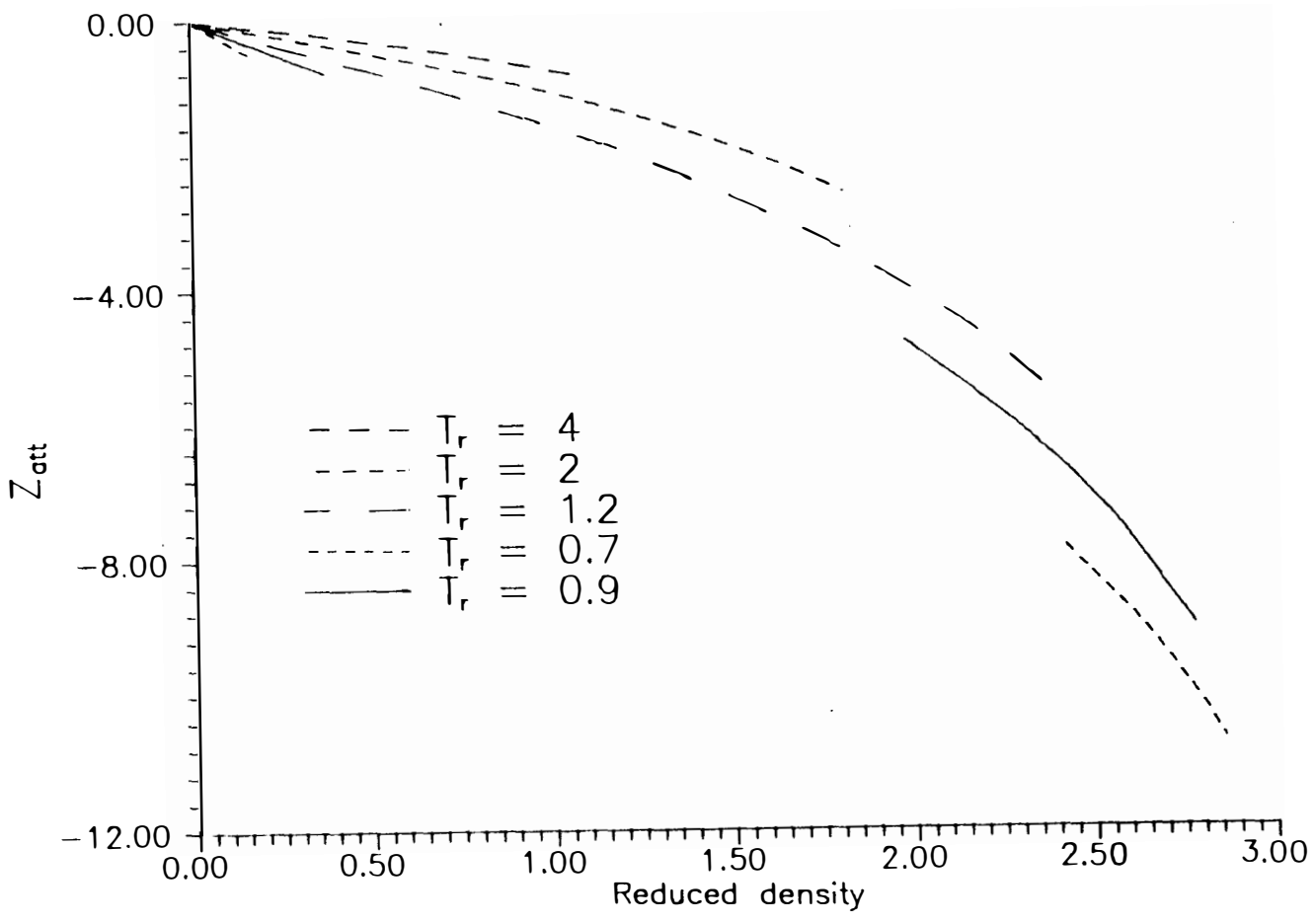

Figure 3.4: Attractive compressibility as a function of reduced temperature for argon

where

$$a = (\bar{a} - \bar{c})\, RT$$

$$c = \bar{c} RT$$

Equation (3.9) can be rewritten as a quartic equation in the volume V of the fluid as shown below :

$$V^4 + q_3 V^3 + q_2 V^2 + q_1 V + q_0 = 0 \tag{3.10}$$

where

$$q_3 = \left(-2k_0\beta + (d+e) - \frac{RT}{P}\right) \tag{3.11}$$

$$q_2 = \left(\frac{RT}{P}\left(\beta\left(k_0 - k_1\right) - d - e\right) + k_0\beta\left(k_0\beta - 2(d+e)\right) + de\right) + \frac{a}{P} \tag{3.12}$$

$$q_1 = (d+e)\left(k_0^2\beta^2 + \frac{RT}{P}\beta\left(k_0 - k_1\right)\right) + \frac{k_0\beta}{P}(c-a) - de\left(\frac{RT}{P} + 2k_0\beta\right) \tag{3.13}$$

$$q_0 = \frac{RT}{P}\beta\left(de\left(k_0 - k_1\right)\right) + k_0^2\beta^2\left(de - \frac{c}{P}\right) \tag{3.14}$$

The parameters a, β, c, d, and e could be related to the critical properties of a fluid by applying the critical point criteria (2.5) and (2.6) to Equation (3.9) and solving the resulting equations simultaneously. Hard-sphere volumes of fluids could be obtained alternatively from Bondi's volume. Figure 3.5 shows the linear relationship between Bondi's volume and the critical volume of some simple and normal fluids. The slope of the best line fitted through the data, shown in Figure 3.5, was 0.181. Since Bondi's volume is the hard-sphere volume at 0 K, the hard-sphere volume of a fluid was selected to be 0.165 times the critical volume of the pure component at the critical temperature

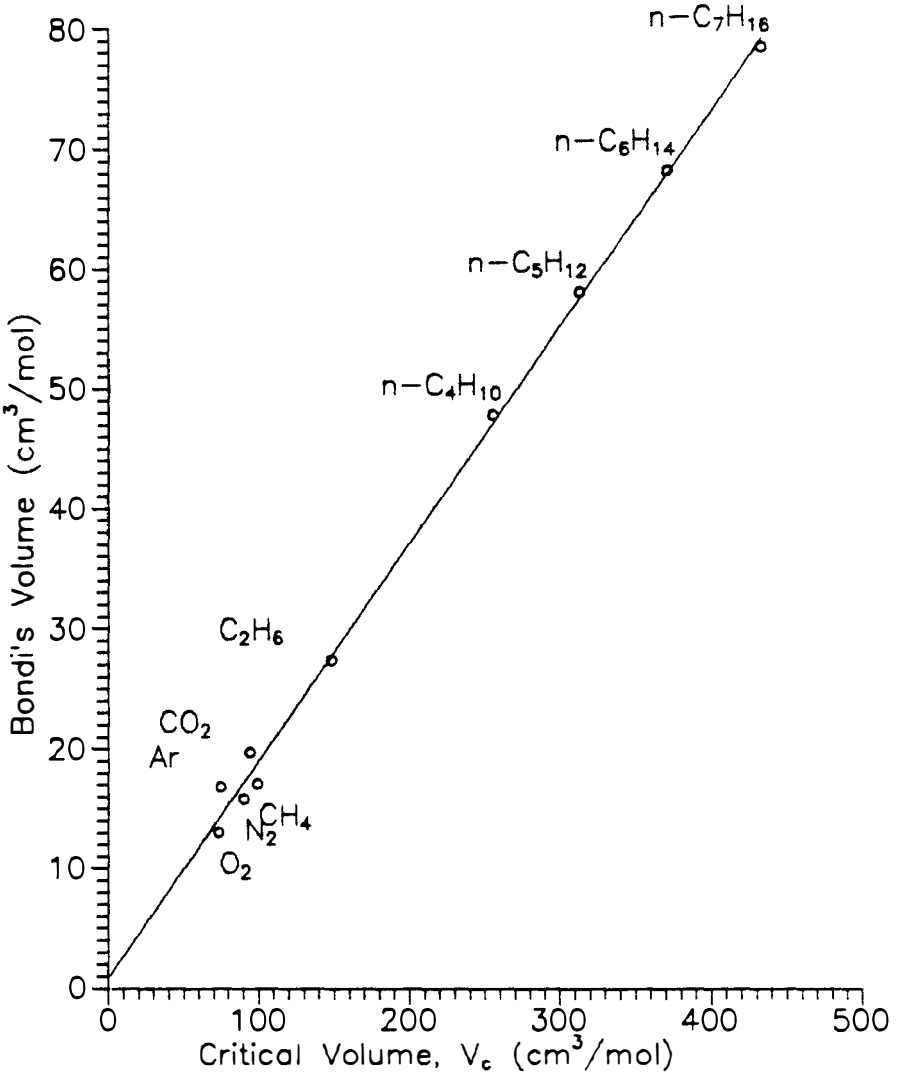

Figure 3.5: Plot of Bondi's volume vs. critical volume.
Data Source: Daubert, et. al. *Physical and Thermodynamic Properties of Pure Chemicals.*, Vols 1-4, Hemisphere Publishing Corp., 1989.

of the fluid. That is, the value of β at $T_r = 1.0$ was fixed to 0.165 V_c, where V_c is the critical volume of the pure component.

Fixing the value of β left only a, c, d, and e to be determined. As mentioned earlier, these parameters could be related to the critical properties of the fluid. There were four parameters to be estimated from the Equation (3.9), (2.5) and (2.6). It was decided to leave e as a parameter to be fixed later and obtaining a, c, and d from the chosen value of e. Applying the critical constraints (2.5) and (2.6) on the proposed quartic Equation (3.9) gave the following relations between the various parameters in the equation of state.

$$\Omega_e = -\frac{\left[\begin{array}{c} 3Z_c^4 + (\Omega_d - 10k_0\Omega_\beta - 1)Z_c^3 \\ + (-3k_0\Omega_\beta\Omega_d + 12k_0^2\Omega_\beta^2 + 3k_0\Omega_\beta)Z_c^2 \\ + (3k_0^2\Omega_\beta^2\Omega_d - 6k_0^3\Omega_\beta^3 - 3k_0^2\Omega_\beta^2)Z_c \\ + (-k_0^3\Omega_\beta^3 - k_0k_1\Omega_\beta^2)\Omega_d + k_0^4\Omega_\beta^4 + (k_0^3 - k_0^2k_1)\Omega_\beta^3 \end{array}\right]}{\left((Z_c - k_0\Omega_\beta)^3 - k_1\Omega_\beta\Omega_d - k_0k_1\Omega_\beta^2\right)} \tag{3.15}$$

$$\begin{aligned}\Omega_a = -6Z_c^2 + (-3\Omega_e - 3\Omega_d + 6k_0\Omega_\beta + 3)Z_c + (-\Omega_d + 2k_0\Omega_\beta + 1)\Omega_e \\ +(2k_0\Omega_\beta + 1)\Omega_d - k_0^2\Omega_\beta^2 + (k_1 - k_0)\Omega_\beta\end{aligned} \tag{3.16}$$

$$\Omega_c = \frac{\left[\begin{array}{c} 8Z_c^3 + (3\Omega_e + 3\Omega_d - 12k_0\Omega_\beta - 3)Z_c^2 \\ + (-3k_0\Omega_\beta\Omega_e - 3k_0\Omega_\beta\Omega_d + 6k_0^2\Omega_\beta^2 + 3k_0\Omega_\beta)Z_c \\ + ((k_0\Omega_\beta + 1)\Omega_d + k_0^2\Omega_\beta^2 + k_1\Omega_\beta)\Omega_e \\ + (k_0^2\Omega_\beta^2 + k_1\Omega_\beta)\Omega_d - k_0^3\Omega_\beta^3 + (k_0k_1 - k_0^2)\Omega_\beta^2 \end{array}\right]}{k_0\Omega_\beta} \tag{3.17}$$

where

$\Omega_\beta = \frac{\beta_c P_c}{RT_c}$ is the dimensionless hard sphere volume parameter,

$\Omega_c = \frac{c_c P_c}{R^2 T_c^2}$ is the dimensionless c parameter,

$\Omega_a = \frac{a_c P_c}{R^2 T_c^2}$ is the dimensionless a parameter,

$\Omega_e = \frac{e_c P_c}{RT_c}$ is the dimensionless e parameter,

$\Omega_d = \frac{d_c P_c}{RT_c}$ is the dimensionless d parameter,

Z_c is the critical compressibility of the fluid,

β_c, a_c, and c_c are the values of the parameters β , a, and c, respectively, at the critical temperature of the fluid.

Appendix A describes the general theory of quartic equations and gives an alternative and much simpler procedure for deriving Equations (3.15) through (3.17).

3.3 Identification of Roots

A quartic equation poses the problem of assigning the roots obtained after solving the equation of state. Although an analytical solution can be found for a quartic equation, a polynomial root finding routine was used to solve the quartic Equation (3.10). It was found that the following set of rules could be applied for the assignment of roots obtained by solving Equation (3.10).

1. For subcritical temperatures :

(a) The largest root in volume corresponds to the molar volume of the vapor phase.

(b) The smallest root which is positive and greater than $\sqrt{2}$ times the hard-sphere volume corresponds to the molar volume of the liquid phase.

2. Critical and Supercritical temperatures :

The largest root in volume corresponds to the molar volume of the single phase.

In addition, at all the valid roots to the quartic equation the derivative of pressure with respect to volume was required to be negative. It was found that this condition was never violated while developing the quartic equation of state (3.9). The above set of rules were used in the final nonlinear regression routines.

A temperature dependence was incorporated in the parameters β, a, and c. The temperature dependence of β was chosen to be

$$\beta = \beta_c \left\{ \exp \left[-0.03125 \ln (T_r) - 0.0054 [\ln (T_r)]^2 \right] \right\}^3 \tag{3.18}$$

where

β_c is the hard-sphere volume at the critical temperature.

The temperature dependence used here was very similar to that used by Aim and Nezbeda [107]. Aim and Nezbeda used Equation (3.18) with the triple point of the fluid as the reference temperature. The temperature dependence of β was assumed to be independent of the nature of the fluid.

The temperature dependence of a and c was to be determined so as to give the best calculation of various thermodynamic properties of a pure fluid. Thus for a given pure fluid the parameters e and d and the temperature dependence of a and c were to be

obtained by regression. Various functional forms for the temperature dependence of a and c were tried out. One of the best functional forms for a was

$$a = a_c \alpha(T_r) \tag{3.19}$$

where

$$\alpha(T_r) = \left[1 + X_2\left(1 - \sqrt{Tr}\right) + X_3\left(1 - \sqrt{Tr}\right)^2 + X_4\left(1 - \sqrt{Tr}\right)^3\right]^2 \quad \text{for } T_r \leq 1 \tag{3.20}$$

$$= \left[1 + X_2\left(1 - \sqrt{Tr}\right) + X_5\left(1 - \sqrt{Tr}\right)^2 + X_6\left(1 - \sqrt{Tr}\right)^3\right]^2 \quad \text{for } T_r > 1 \tag{3.21}$$

where

a_c is the value of a at the critical temperature of the fluid,

X_2, X_3, X_4, X_5, and X_6 are constants to be determined by nonlinear regression.

The functional form chosen for $\alpha(T_r)$ was such that it is continuous at $T_r = 1$ and the first derivative of $\alpha(T_r)$ with respect to temperature is continuous at $T_r = 1$. The temperature dependence of c used in the nonlinear regressions was

$$c = c_c \xi(T_r) \tag{3.22}$$

$$\xi(T_r) = \left[1 + X_7\left(1 - \sqrt{Tr}\right)\right]^2 \tag{3.23}$$

where

c_c is the value of c at the critical temperature of the fluid,

X_7 is a constant to be determined by nonlinear regression.

Thus the constants X_2, X_3, X_4, X_5, X_6, and X_7 had to be determined for various fluids. In order to perform the nonlinear regressions two other characteristic properties of the fluid had to be specified. The critical temperature had to be specified to get reduced temperatures used in Equations (3.20) and (3.23). The critical volume of a fluid had to be specified in order to obtain a value for β.

3.4 Nonlinear Regressions

A secant-based nonlinear least squares technique [109] was used in the initial nonlinear regressions. The following objective function was minimized using nonlinear regression

$$OBJ1 = \sum_{i=1}^{N_1} \left(\left(\frac{\Delta P_{si}}{P_{si}} \right)^2 + \left(\frac{\Delta \rho_{si}}{\rho_{si}} \right)^2 + \left(\frac{\Delta \rho_{li}}{\rho_{li}} \right)^2 \right) + \sum_{j=1}^{N_2} \left(\frac{\Delta \rho_{gj}}{\rho_{gj}} \right)^2 \tag{3.24}$$

where

N_1 is the number of saturation data points in the two phase region,

N_2 is the number of density data points in the single phase (gas) region,

P_{si} is the saturation pressure,

ρ_{vi} is the vapor density,

ρ_{li} is the liquid density,

ρ_{gj} is the gas density,

$\Delta P_{si} = \left(P_{si}^{calc} - P_{si}^{data}\right)$ is the error in the saturation pressure,

$\Delta \rho_{vi} = \left(\rho_{vi}^{calc} - \rho_{vi}^{data}\right)$ is the error in the vapor density,

$\Delta \rho_{li} = \left(\rho_{li}^{calc} - \rho_{li}^{data}\right)$ is the error in the liquid density, and

$\Delta \rho_{gj} = \left(\rho_{gi}^{calc} - \rho_{gi}^{data}\right)$ is the error in the gas density.

In the two phase region, the saturation pressure, the saturated vapor density and the saturated liquid density were obtained by equating the fugacity of the two phases to be equal. That is,

$$f_v = f_l \tag{3.25}$$

where

f_v is the fugacity of the vapor phase, and

f_l is the fugacity of the liquid phase.

The saturation pressure at a given temperature was determined by an iterative process until the vapor and liquid volumes, obtained on solving the quartic equation of state, satisfied Equation (3.25). The Newton-Raphson method was used to determine the saturation pressure at a given temperature. The fugacity for the proposed quartic equation of state is given by

$$\begin{aligned} RT \ln\left|\frac{f}{P}\right| &= -RT \ln\left(\frac{V - k_0\beta}{V}\right) + \frac{k_1 \beta RT}{(V - k_0\beta)} \\ &\quad + \frac{(ad - k_0\beta c)}{(k_0\beta + d)(e - d)} \ln\left(\frac{V + d}{V - k_0\beta}\right) \\ &\quad - \frac{(ae - k_0\beta c)}{(k_0\beta + e)(e - d)} \ln\left(\frac{V + e}{V - k_0\beta}\right) - RT \ln Z + RT(Z - 1) \end{aligned} \tag{3.26}$$

where

f is the fugacity of the fluid.

The objective function (3.24) was not a smooth function of the constants being estimated. This was due to the fact that certain values of the constants could result in

1. Failure to obtain valid root(s) upon solving the quartic equation. That is, two valid roots could not be found in the two phase region or one valid root could not be found in the single phase region.

2. Failure to calculate the fugacity or enthalpy for the pure component. This resulted mainly because certain values of constants caused the programs to take the logarithm of a negative number.

3. Failure of the Newton-Raphson procedure to converge in 300 iterations in order to satisfy Equation (3.25) in the two-phase region.

Additionally, it was found that the objective function had a number of local minima and the nonlinear least squares routine often converged to one of these local minima. A fortran routine was written to implement the Nelder-Mead simplex [110, 111] algorithm for the purpose of nonlinear regressions. The Nelder-Mead method is a direct search method used for finding the minimum of a function. The method is well suited for discontinuous or non-smooth functions. The Nelder-Mead method proved useful to get out of a local minimum and move towards a better minimum. However, the method had very a very slow rate of convergence and required a very large number of function evaluations. Thus, the Nelder-Mead method was used to move outside of the local

minima region and the secant-based method used from there on to rapidly converge to the final minimum.

During the early stages of the development of the EOS the critical compressibility of a real fluid was set equal to the experimentally observed value. Whereas, good density calculations could be obtained, calculations of the second virial coefficient had large errors in them. It became obvious that the quartic equation of state was incapable of accurately determining density, the second virial coefficient and the critical compressibility of a fluid at the same time. This is also true, to some degree, for the popular cubic equations of state.

The CCOR equation calculates orthobaric liquid densities very well for most fluids. The calculations for the two-phase envelope by the CCOR EOS for nitrogen can be seen in Figure 3.6. Orthobaric liquid density calculations are very good compared to the Peng-Robinson EOS up to the critical point. The CCOR EOS predicts the critical compressibility of a fluid exactly. Figure 3.7 shows the second virial coefficient calculations for Nitrogen by the CCOR EOS. It can be seen that the CCOR equation of state has the correct functional form needed to accurately determine the critical compressibility, orthobaric liquid densities and the second virial coefficients. However, density calculations are very poor, particularly, at temperature slightly above the critical temperature. Figure 3.8 shows the $P - \rho - T$ calculations by the CCOR EOS and the Peng-Robinson EOS for nitrogen. It appears that the CCOR EOS achieves a remarkable performance at the critical point of the fluid at the expense of accuracy at temperatures slightly above the critical and high pressures.

Martin [11] has shown that the second virial coefficient of a fluid at its critical temperature is related to the critical compressibility, critical temperature and critical

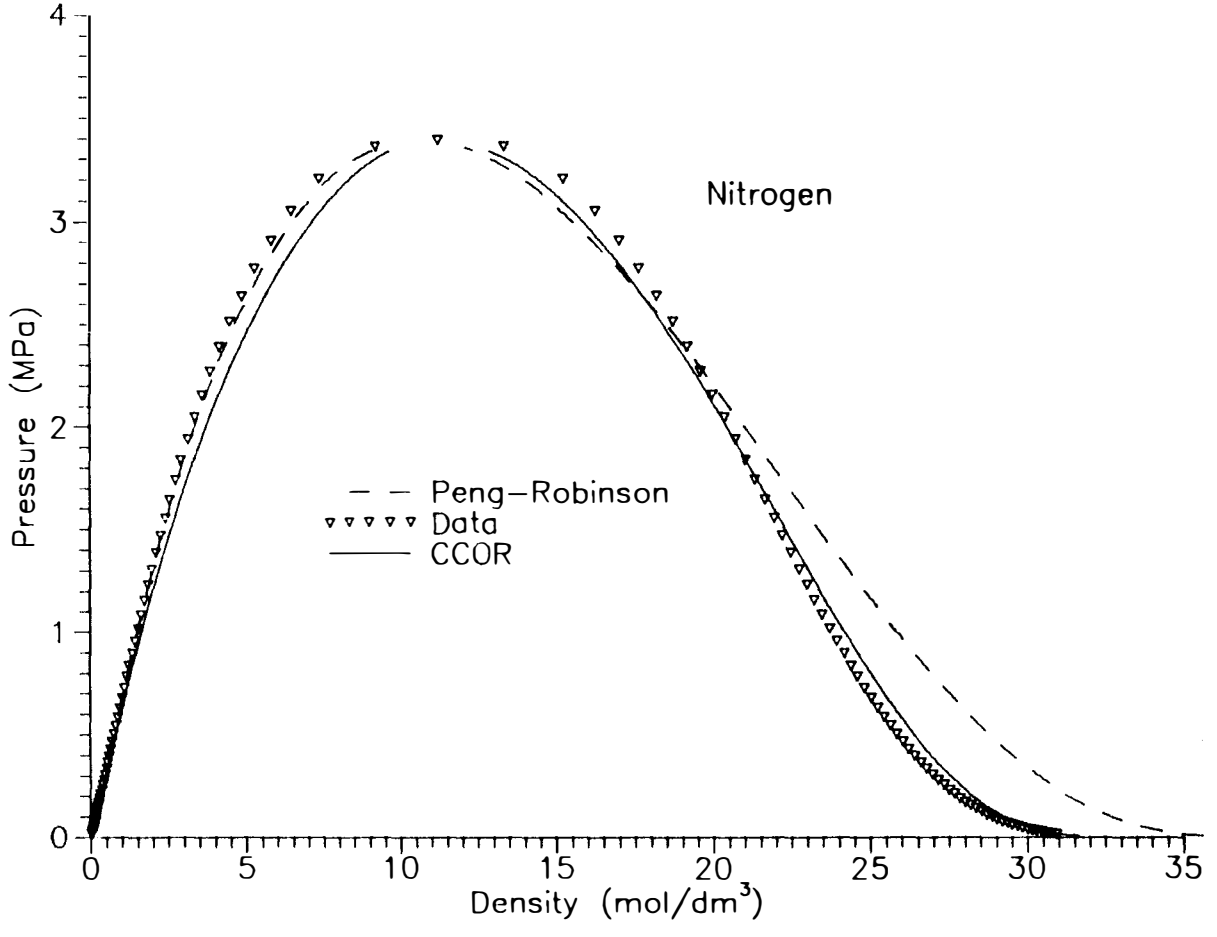

Figure 3.6: CCOR calculation of the two-phase envelope of nitrogen
Data Source: Jacobsen et al. *J. Phys. Chem. Ref. Data*, 15:735. 1986.

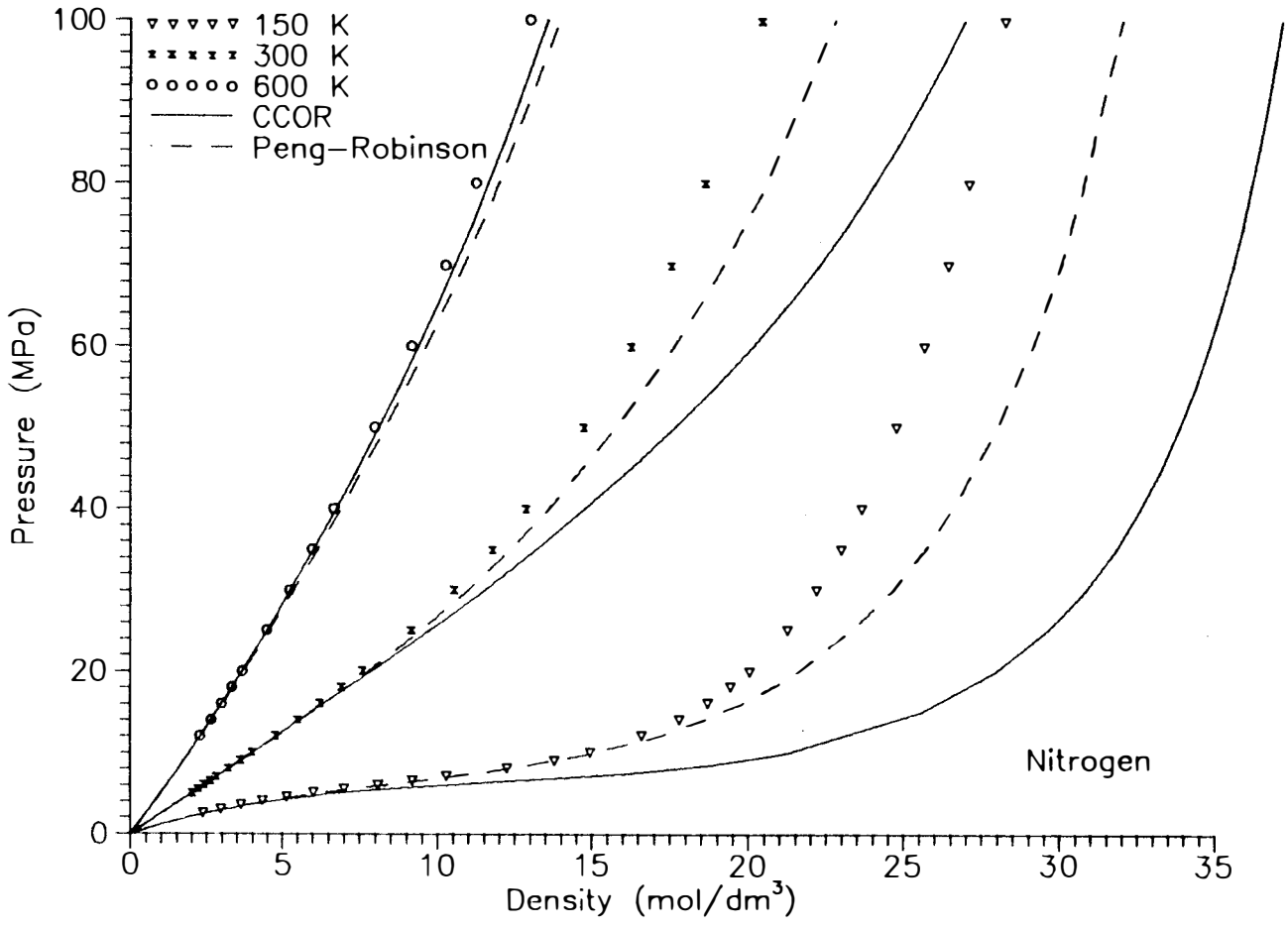

Figure 3.7: Pressure-density calculations by the Peng-Robinson and the CCOR equations of state for nitrogen
Data Source: Jacobsen et al. *J. Phys. Chem. Ref. Data*, 15:735. 1986.

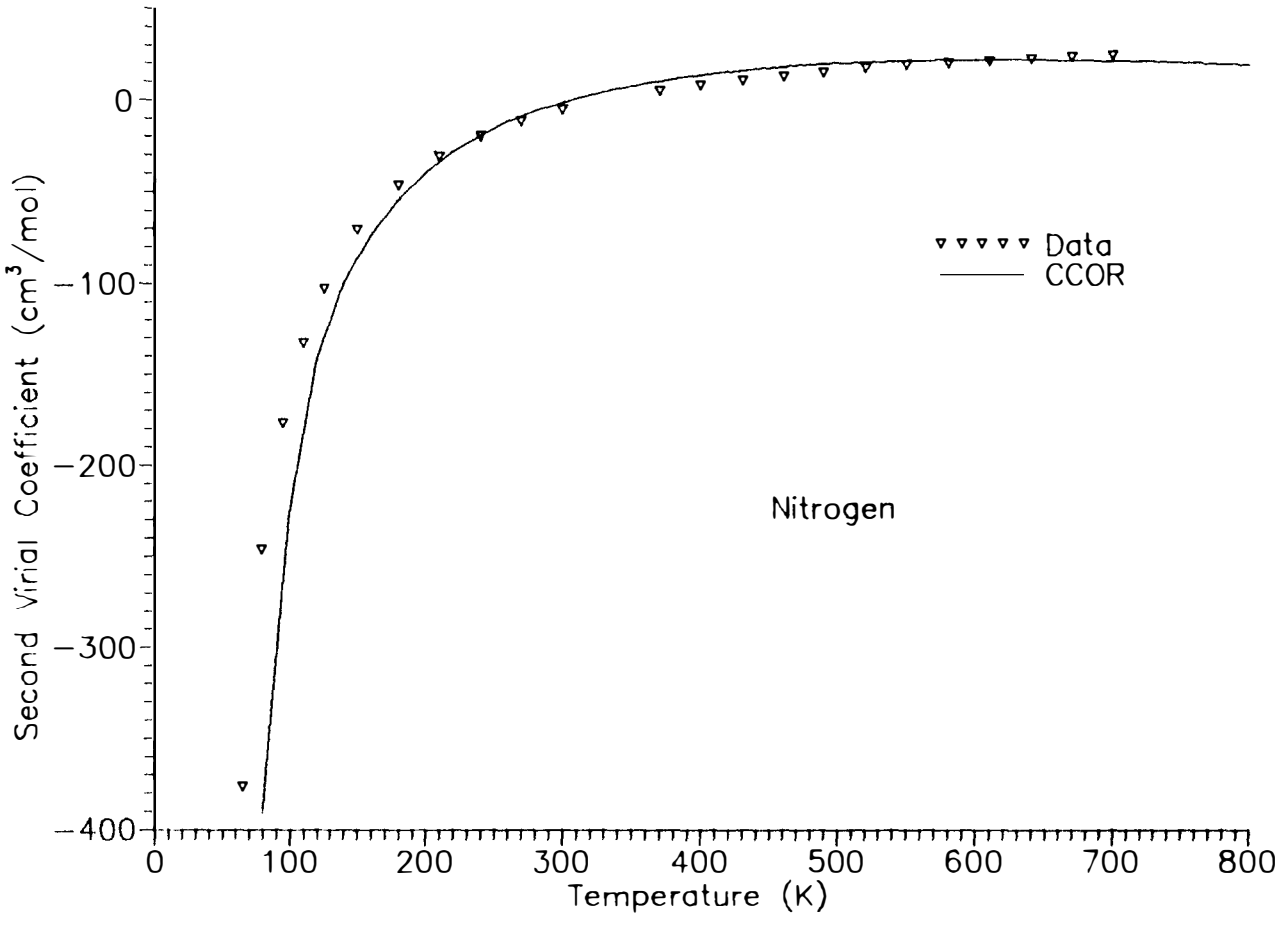

Figure 3.8: CCOR calculation of second virial coefficient of nitrogen.
Data Source: Jacobsen et al. *J. Phys. Chem. Ref. Data*, 15:735. 1986.

pressure by

$$Z_c - \frac{B_{vir,c}P_c}{RT_c} = \text{constant} \tag{3.27}$$

where

$B_{vir,c}$ is the second virial coefficient at the critical temperature of the fluid.

He showed that the constant had a value of 0.62 ± 0.1 for 39 different fluids. The new quartic EOS was not capable of satisfying equation (3.27) and determine various physical and thermodynamic properties accurately.

It is well known [112] that an analytical equation of state cannot represent the critical region of a fluid accurately. Hence, instead of attempting to change the functional form of the quartic EOS to satisfy the experimental critical compressibility, the constraints on the critical compressibility were completely removed. This implied that the Equations (3.16), (3.15), and (3.17) could not be used. Hence, a, c, d, and e were left as parameters to be obtained by regressions without any constraints on them.

Initial parameter estimations were performed using only $P-\rho-T$ data for pure fluids. The results of the parameter estimations showed that the density predictions over the entire P and T region were good. However, second virial coefficient and residual enthalpy calculations (particularly at $T_r > 3$) were not very good. The residual enthalpy for the quartic EOS is given by Equation (3.28), and the second virial coefficient by Equation (3.29).

$$H_r = \int_V^\infty \left[P - T\left(\frac{\partial P}{\partial T}\right)_v\right] dV + (PV - RT)$$

$$
\begin{aligned}
= & -\frac{RT^2\beta'(k_0+k_1)}{(V-k_0\beta)}+\frac{(a+c)Tk_0^2\beta'\beta}{(k_0\beta+e)(k_0\beta+e)(V-k_0\beta)}-\frac{k_1k_0\beta'\beta RT^2}{(V-k_0\beta)^2} \\
& -\left\{\frac{(a'T-a)d-k_0[(c'\beta+c\beta')T-c\beta]}{(e-d)(k_0\beta+d)}-\frac{Tk_0\beta'(ad-ck_0\beta)}{(e-d)(k_0\beta+d)^2}\right\} \\
& \quad \times \ln\left(\frac{V+d}{V-k_0\beta}\right) \\
& +\left\{\frac{(a'T-a)e-k_0[(c'\beta+c\beta')T-c\beta]}{(e-d)(k_0\beta+e)}-\frac{Tk_0\beta'(ae-ck_0\beta)}{(e-d)(k_0\beta+e)^2}\right\} \\
& \quad \times \ln\left(\frac{V+e}{V-k_0\beta}\right) \\
& +(PV-RT)
\end{aligned}
\tag{3.28}
$$

$$
B_{vir}=(k_0+k_1)\beta-\frac{a}{RT} \tag{3.29}
$$

Second virial coefficient data and high temperature residual enthalpy data were used, along with density data for parameter estimation. Second virial coefficient data was generated using reported correlations developed for each pure fluid [113]. Hence, the new objective function to be minimized was given by :

$$
\begin{aligned}
OBJ2 = & \sum_{i=1}^{N_1}\left(\left(\frac{\Delta P_{si}}{P_{si}}\right)^2+\left(\frac{\Delta\rho_{si}}{\rho_{si}}\right)^2+\left(\frac{\Delta\rho_{li}}{\rho_{li}}\right)^2\right)+\sum_{j=1}^{N_2}\left(\frac{\Delta\rho_{gj}}{\rho_{gj}}\right)^2 \\
& +\sum_{k=1}^{N_3}\left(\frac{\Delta H_{vk}}{H_{vk}}\right)^2+\sum_{l=1}^{N_4}\left(\frac{\Delta H_{rl}}{H_{rl}}\right)^2+\sum_{m=1}^{N_5}\left(\frac{\Delta B_{vir\,m}}{B_{vir\,m}}\right)^2
\end{aligned}
\tag{3.30}
$$

where

N_3 is the number of H_v data points in the two phase region,

N_4 is the number of residual enthalpy data points,

H_{vk} is the enthalpy of vaporization,

H_{rl} is the residual enthalpy,

$B_{vir\,m}$ is the second virial coefficient,

$\Delta H_{rl} = \left(H_{rl}^{calc} - H_{rl}^{data}\right)$ is the error in the residual enthalpy,

$\Delta H_{vk} = \left(H_{vk}^{calc} - H_{vk}^{data}\right)$ is the error in the vaporization enthalpy,

$\Delta B_{vir\,m} = \left(B_{vir\,m}^{calc} - B_{vir\,m}^{data}\right)$ is the error in the second virial coefficient.

The equation of state had too many constants to be estimated for every fluid. The idea was to eventually obtain constants for several simple and normal pure fluids and make an attempt to correlate them to some characteristic property of the fluid. The law of corresponding states of fluids states that behavior of simple fluids can be completely specified by two parameters. These two parameters are the size parameter and the energy parameter. The size parameter can be represented by the hard-sphere volume of the fluid. The energy parameter is representative of the attractive forces between molecules. The critical temperature of the fluid may be used to represent this parameter. In order to characterize normal fluids which no longer have a spherical shape, a third parameter needs to be specified. Pitzer's acentric factor (ω) was chosen as the third parameter needed to characterize normal fluids. The acentric factor of a fluid can be calculated by the equation

$$\omega = -\log_{10}\left(\frac{P_s}{P_c}\right)_{T/T_c=0.7} \tag{3.31}$$

where

P_s is the saturated vapor pressure of the fluid at a reduced temperature of 0.7.

The various constants of the equation of state were obtained for a few simple and normal fluids. Several conclusions were drawn based on regressions for individual fluids. They were

1. The constants were highly cross-correlated.

2. Two or more different sets of constant estimates were equally good at minimizing the objective function.

3. Some constants became statistically insignificant for some fluids.

Constants such as X_7 often became statistically insignificant for a fluid like n-butane. This was due to the fact that density data available for regressions was for temperatures less than $1.5\,T_r$. It can be seen by looking at Equation (3.20) that the value of X_7 would not have a significant effect on the value of α. This coupled with the high degree of cross-correlation between the constants, made attempts to obtain a correlation between an individual constant and the acentric factor of the fluid very difficult.

To overcome this problem, the estimation of constants for several fluids was undertaken at the same time. The constants X_2 through X_7 were assumed to be linear functions of ω as shown in Equation (3.32).

$$X_i = X_{i1} + X_{i2}\,\omega \quad \text{for } i = 2,3,4,5,6 \text{ and } 7 \tag{3.32}$$

The parameter d was assumed to be zero and the reduced parameters a_r, e_r and c_r were assumed to be quadratic functions of ω. The parameters a, b and c are related to the

reduced parameters as follows:

$$a_r = \frac{a_c \rho_c}{R T_c} \tag{3.33}$$

$$c_r = \frac{c_c \rho_c}{R T_c} \tag{3.34}$$

$$e_r = e\,\rho_c \tag{3.35}$$

$$\beta_r = \beta_c \rho_c \tag{3.36}$$

$$a_r = a_{r0}\left(1 + a_{r1}\omega + a_{r2}\omega^2\right) \tag{3.37}$$

$$e_r = e_{r0}\left(1 + e_{r1}\omega + e_{r2}\omega^2\right) \tag{3.38}$$

$$c_r = c_{r0}\left(1 + c_{r1}\omega + c_{r2}\omega^2\right) \tag{3.39}$$

The hard-sphere volume was fixed to a constant times V_c at the critical temperature of the fluid and had a temperature dependency as described in Equation (3.18). Thus, multiproperty regression, using physical property data and thermodynamic data of sixteen simple and normal fluids, was to be used to determine all the constants needed to completely specify the equation of state.

This chapter provided in detail the methodology used to develop the quartic equation of state. An algebraically simple term was used to model the repulsive forces between molecules. This term modeled the repulsive forces correctly as it used the correct hard-sphere volumes of the molecules. The attractive forces between molecules were modelled using an empirical term. The resulting equation of state was a quartic equation in the volume of the fluid. The quartic equation of state had five parameters, one of which was eliminated. Three of the remaining four parameters, β, a and c, were functions of temperature. The fourth parameter, e, was independent of temperature. In order

to generalize the equation of state to normal fluids, the parameters a, c, and e were assumed to be functions of the acentric factor of the fluid. All fluids were assumed to have a temperature-dependent spherical hard-core. The temperature-dependency of the hard-sphere volume did not depend on the nature of the fluid. Finally, the equation of state was set up so that the constants that describe the dependence of the parameters a, c, and e on the temperature and the acentric factor of the fluid, could be determined using multiproperty regressions.

CHAPTER 4

Results and Discussion

This chapter deals with the results of multiproperty regressions performed to determine the various constants used in the generalized equation of state. Pure fluid data of sixteen simple and normal fluids was used to obtain the constants. The resulting equation of state was tested for three additional fluids. The new equation of state reproduces $P - \rho - T$ and thermodynamic properties of simple and normal fluids very well. Comparision of the new equation of state was done with the Peng-Robinson and Kubic's quartic equation of state. The new equation of state is remarkably superior to both the equations of state.

The various constants of the new equation of state were estimated using $P - \rho - T$, heat of vaporization, residual enthalpy and second virial coefficient data of sixteen pure fluids. Table 4.1 shows the fluids and the range of data and their sources used in obtaining the constants. A detailed table of the different thermodynamic properties used in the regressions for each of the fluid can be obtained from Appendix B. Table 4.2 shows the pure component properties used during the regressions. Pure component properties are taken from Reid et al. [120]. The final set of constants so obtained is presented in Table 4.3. The equation of state is completely specified by the set of Equations (3.9), (3.19), (3.20), (3.22), (3.23), (3.18) and Equations (3.32) through (3.39).

Another set of constants for the equation of state gave a remarkable improvement

Table 4.1: Pure component data used in regressions and their sources

Fluid	Temperature range (K)	Pressure range (MPa)	Source
Argon	84 – 1000	0 – 100	[114]
Krypton	116 – 1000	0 – 100	[115]
Xenon	164 – 1000	0 – 100	[115]
Oxygen	56 – 1000	0 – 100	[115]
Nitrogen	64 – 1000	0 – 100	[116]
Methane	100 – 600	0 – 100	[117]
Ethane	140 – 600	0 – 100	[117]
Propane	170 – 600	0 – 100	[117]
n-Butane	130 – 600	0 – 70	[117]
Carbon Dioxide	220 – 1000	0 – 100	[118]
n-Pentane	299 – 455		[119]
n-Hexane	266 – 494		[119]
n-Octane	277 – 533		[119]
n-Nonane	253 – 573	0 – 20	[115]
n-Decane	263 – 393	0 – 10	[115]
n-Undecane	303 – 573	0 – 100	[115]

Table 4.2: Pure component physical properties of the fluids used in the regressions [120].

Fluid	Critical Temperature (K)	Critical Volume (dm^3/mol)	Acentric Factor
Argon	150.8	0.0749	0.001
Krypton	209.4	0.0912	0.005
Xenon	289.7	0.1184	0.008
Methane	190.4	0.0992	0.011
Oxygen	154.6	0.0734	0.025
Nitrogen	126.2	0.0898	0.039
Ethane	305.4	0.1483	0.099
Propane	369.8	0.203	0.153
n-Butane	425.2	0.255	0.199
Carbon dioxide	304.1	0.0939	0.225
n-Pentane	469.7	0.304	0.251
n-Hexane	507.5	0.370	0.299
n-Octane	568.8	0.492	0.398
n-Nonane	594.6	0.548	0.445
n-Decane	617.7	0.603	0.489
n-Undecane	638.8	0.660	0.535

Table 4.3: Equation of state constants obtained by regressions (Quartic A)

Parameter		Parameter	
a_{r0}	1.84713	X_{21}	0.14988
a_{r1}	−0.05218	X_{22}	0.97848
a_{r2}	1.06446	X_{31}	−0.32379
c_{r0}	1.78336	X_{32}	1.84591
c_{r1}	−1.29690	X_{41}	0.14833
c_{r2}	2.78945	X_{42}	−3.46693
e_{r0}	0.63189	X_{51}	0.11048
e_{r1}	−0.81660	X_{52}	0.57743
e_{r2}	3.25246	X_{61}	0.02581
		X_{62}	−0.02700
β_r^*	0.165	X_{71}	−0.77357
k_0^*	1.2865	X_{72}	−1.45342
k_1^*	2.8225	d^*	0.0000

* These quantities were kept fixed during regressions.

in liquid density calculations. This set of constants was obtained when the hard core volume to fixed as $0.175\,V_c$. The values of this second set of constants are given in Appendix C.1. The quartic EOS with the first set of constants (Table 4.3) will be referred to as Quartic A and the quartic EOS with the second set of constants (Appendix C.1) will be referred to as Quartic B. The overall AAD and sum of squares summary for the two quartics has been presented in Table 4.4. The overall sum of squares shown in Table 4.4 is the minimum value of the objective function (3.30). It can be seen that Quartic B is better than Quartic A only as far as liquid density and gas density calculations are concerned. Quartic B shows reduced accuracy for all the other properties.

Comparison between the two EOS's Quartic A and B shows that both of them are almost identical in the supercritical region. Figure 4.1 shows the density calculations by both the EOS's for Nitrogen. Figure 4.2 shows the two-phase envelope calculations for Argon. Quartic B does not perform as well as Quartic A in the critical region. As pointed out in the previous chapter, the critical compressibility calculated by the quartic EOS was not constrained in any way. Also, pure fluid data near the critical point were not used in obtaining the set of constants of the EOS. Hence, the new EOS's do not perform particularly well near the critical point of the fluid. Evidently, the critical compressibility calculated by Quartic B is larger than that calculated by Quartic A.

As Quartic B is not as accurate as Quartic A in the critical region, the latter was accepted as the new EOS. The figures shown in this chapter are representative of the superior performance of the new EOS. The density calculations in the supercritical region by Quartic A for Carbon Dioxide can be seen in Figures 4.3. Pressure-density diagrams such as Figure 4.3 cannot show the performance of the EOS at low pressures. However, log-log plots of pressure versus density such as Figure 4.4 show that the new

Table 4.4: Overall sum of squares and AAD summary for the regressions

Thermodynamic property	Quartic A AAD (%)	Quartic B AAD (%)	No. of Data points
P_{sat}	1.56	2.06	502
ρ_{sv}	1.75	1.89	449
ρ_l	3.46	2.05	581
H_{vap}	2.00	2.47	465
ρ_g	0.61	0.55	2886
H_r	3.92	4.11	742
B_{vir}	5.15	5.44	554
	Quartic A	Quartic B	No. of Data points
Sum of Squares	8.11	8.35	6179

$$AAD(\%) = \frac{1}{N_d} \sum_{i}^{N_d} \left| \frac{y_i^{calc} - y_i^{exp}}{y_i^{exp}} \right| 100$$

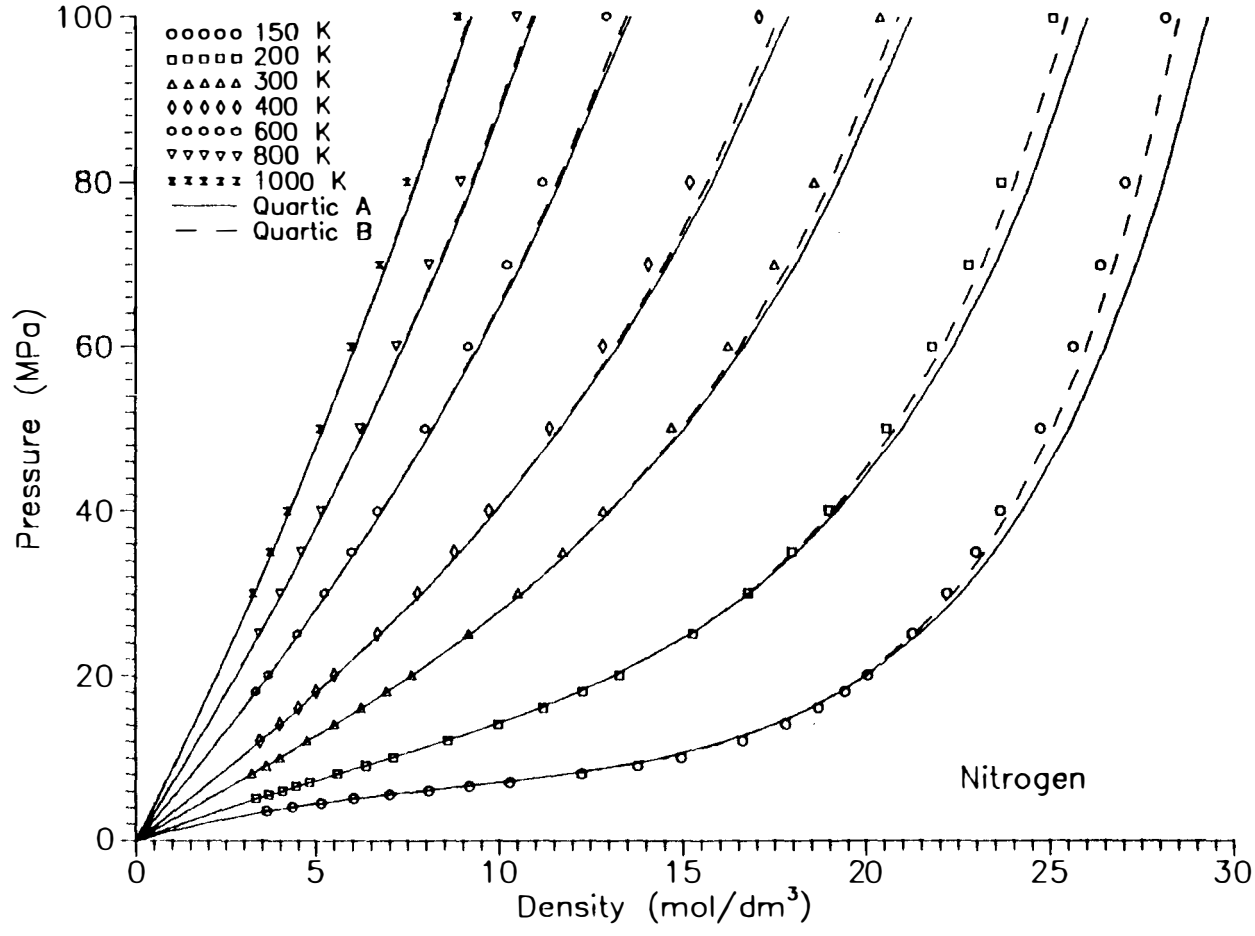

Figure 4.1: Pressure-density calculations for Nitrogen.
Data Source: Jacobsen et al. *J. Phys. Chem. Ref. Data*, 15:735, 1986.

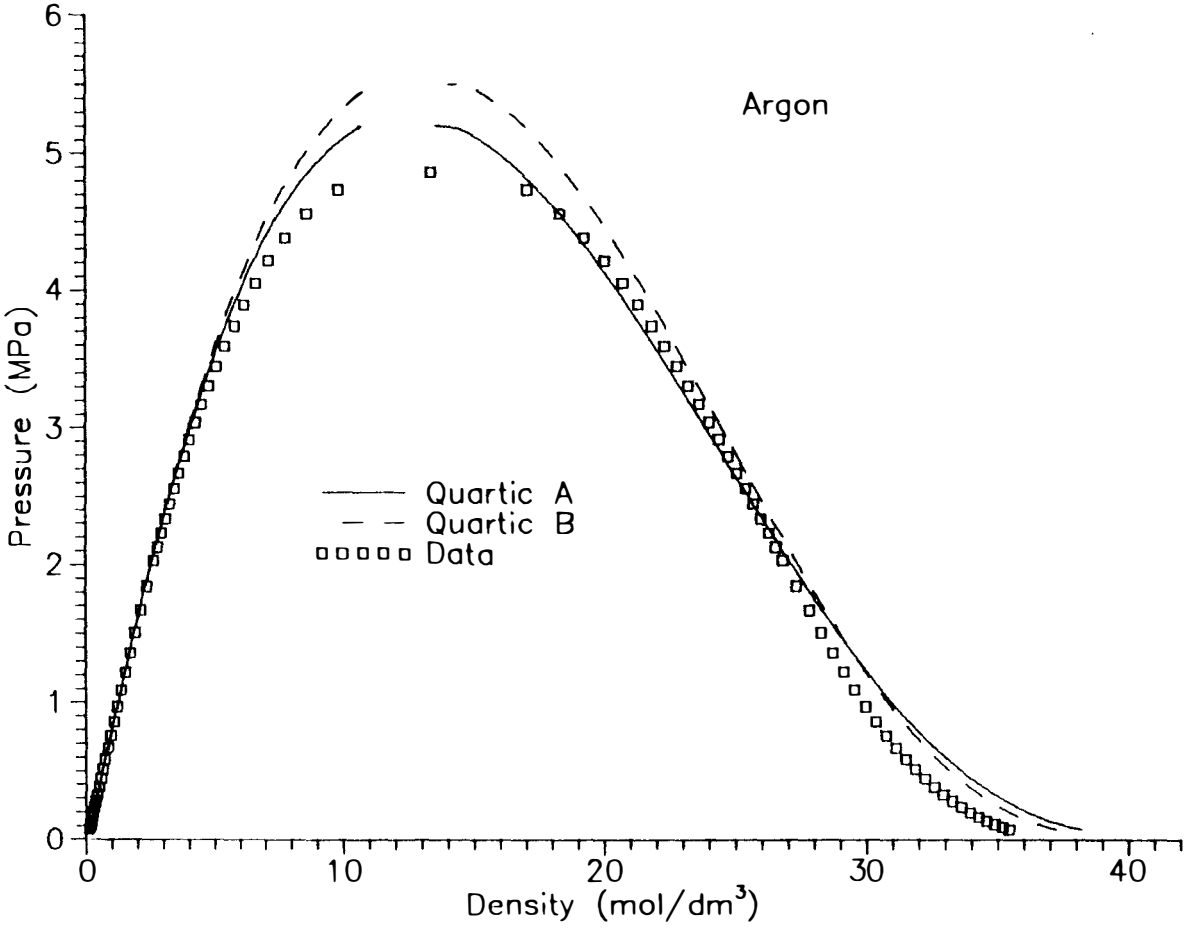

Figure 4.2: Saturated VLE calculations for Argon.
Data Source: Stewart et al. *J. Phys. Chem. Ref. Data*, 18:640, 1989.

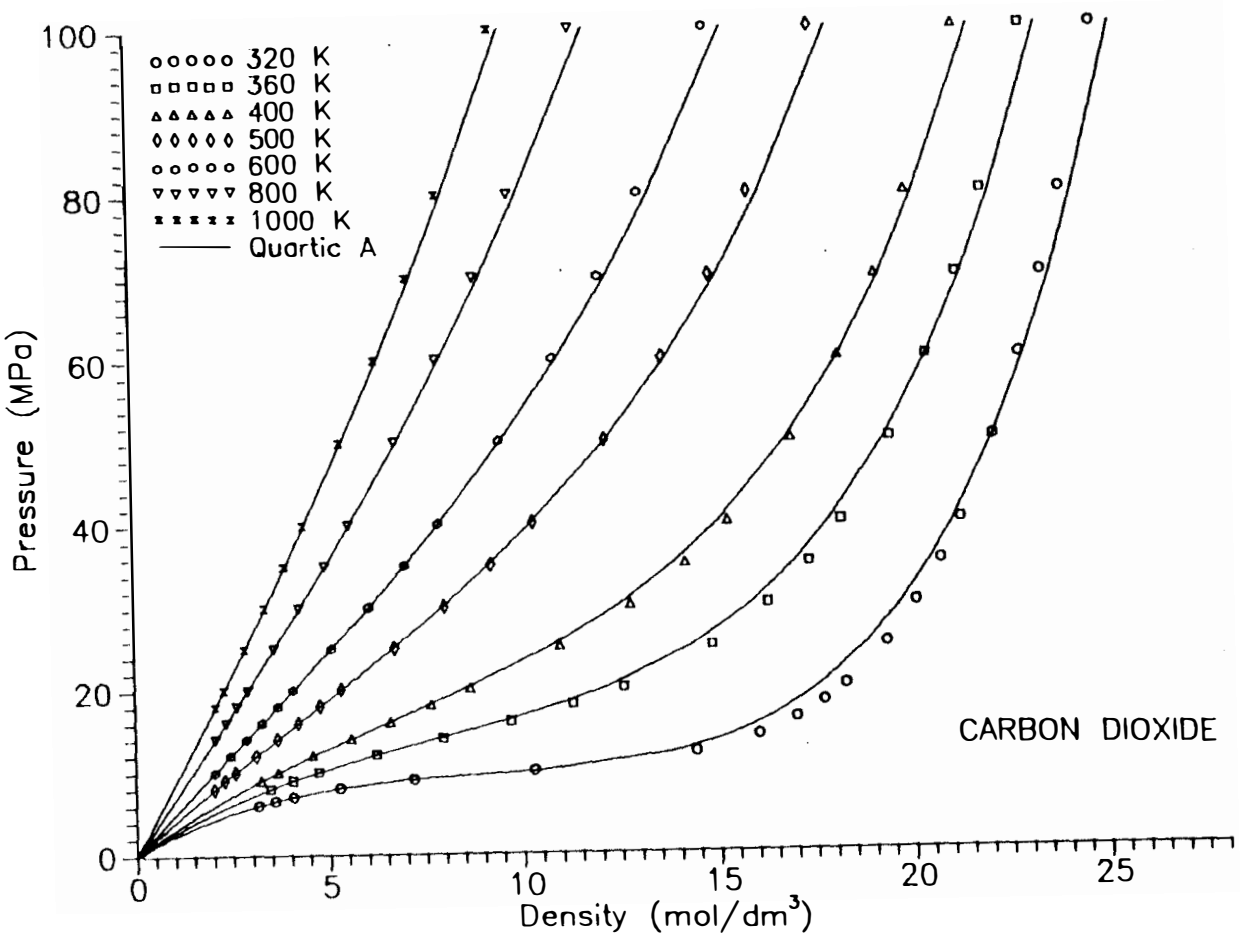

Figure 4.3: Pressure-density calculations for Carbon Dioxide.
Data Source: Angus et al. *International Tables of the Fluid State: Carbon Dioxide*, Permagon Publishing Co., 1976.

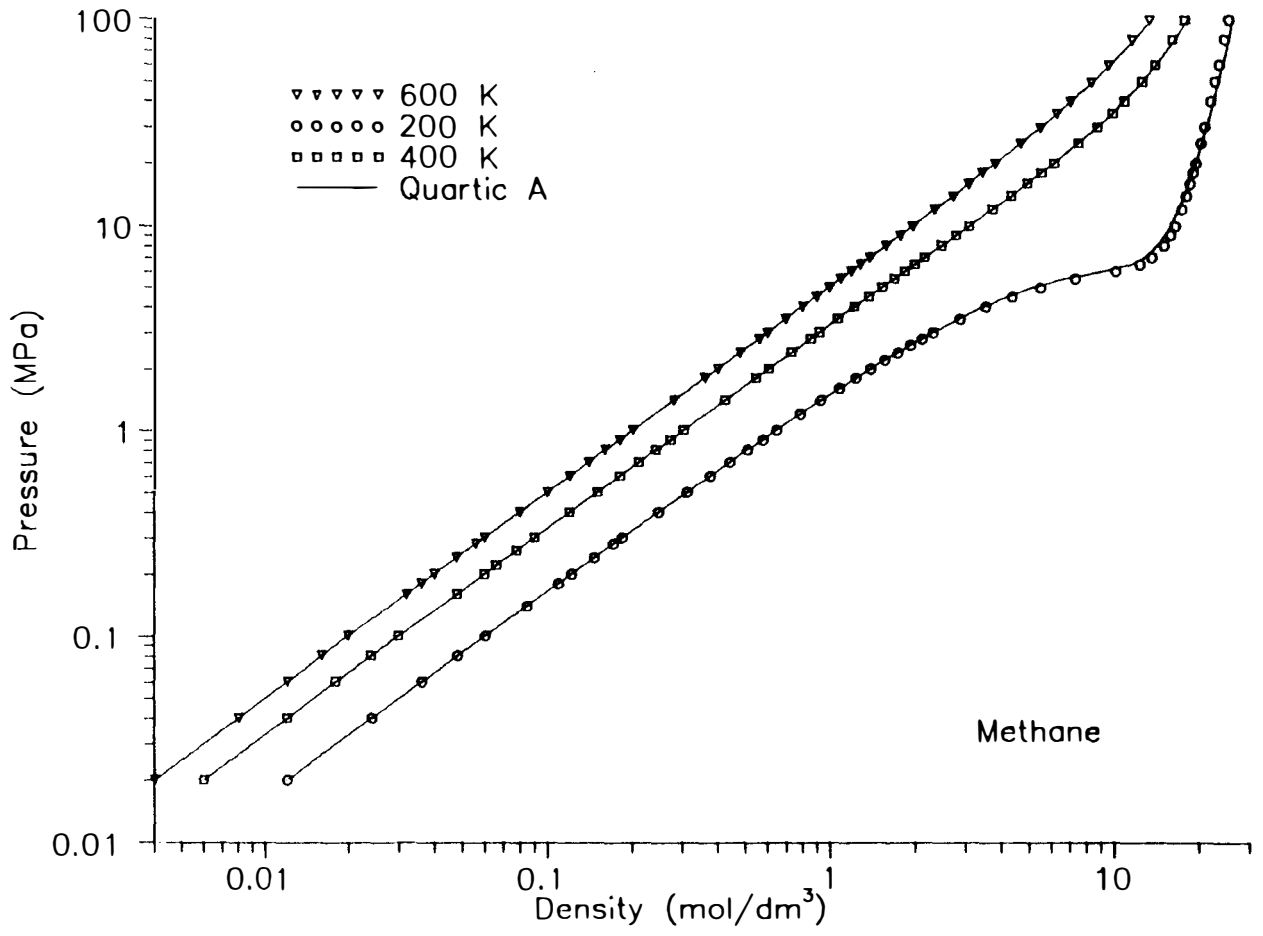

Figure 4.4: Pressure-density calculations for Methane.
Data Source: Younglove et al. *J. Phys. Chem. Ref. Data*, 16:577, 1987.

Table 4.5: Pure component physical properties of fluids used in testing the equation of state [120].

Fluid	Critical Temperature (K)	Critical Volume dm^3/mol	Acentric Factor	Data Source
Carbon Monoxide	132.9	0.0932	0.066	[121]
Ethylene	282.4	0.1304	0.089	[122]
Benzene	562.2	0.259	0.212	[123]

EOS is accurate over a large pressure and density range.

The two-phase envelope calculations for ethane and n-octane can be seen in Figures 4.5 and 4.6. Figures 4.7 and 4.8 show the residual enthalpy calculations for oxygen and n-Butane. Figure 4.9 shows the second virial coefficient calculations for various fluids. The new EOS (Quartic A) does not reproduce the second virial coefficients with high accuracy at subcritical temperatures. Figure 4.10 shows the vapor pressure calculations for n-Nonane by EOS Quartic A. The performance of Quartic A is outstanding for all the properties except the second virial coefficient at subcritical temperatures.

The new EOS was tested for three fluids which had not been used in regressing the constants : Carbon monoxide, Ethylene and Benzene. Using the three parameters of the pure fluids, given in Table 4.5, the new EOS (Quartic A) determined $P - \rho - T$ behavior for these three fluids remarkably well. Figures 4.11, 4.12, 4.13 and 4.14 show the various density and thermodynamic property calculations for these fluids.

Table 4.6 shows the critical points of some fluids calculated from Quartic A. These were calculated by locating the pressure, temperature and density which satisfied Equa-

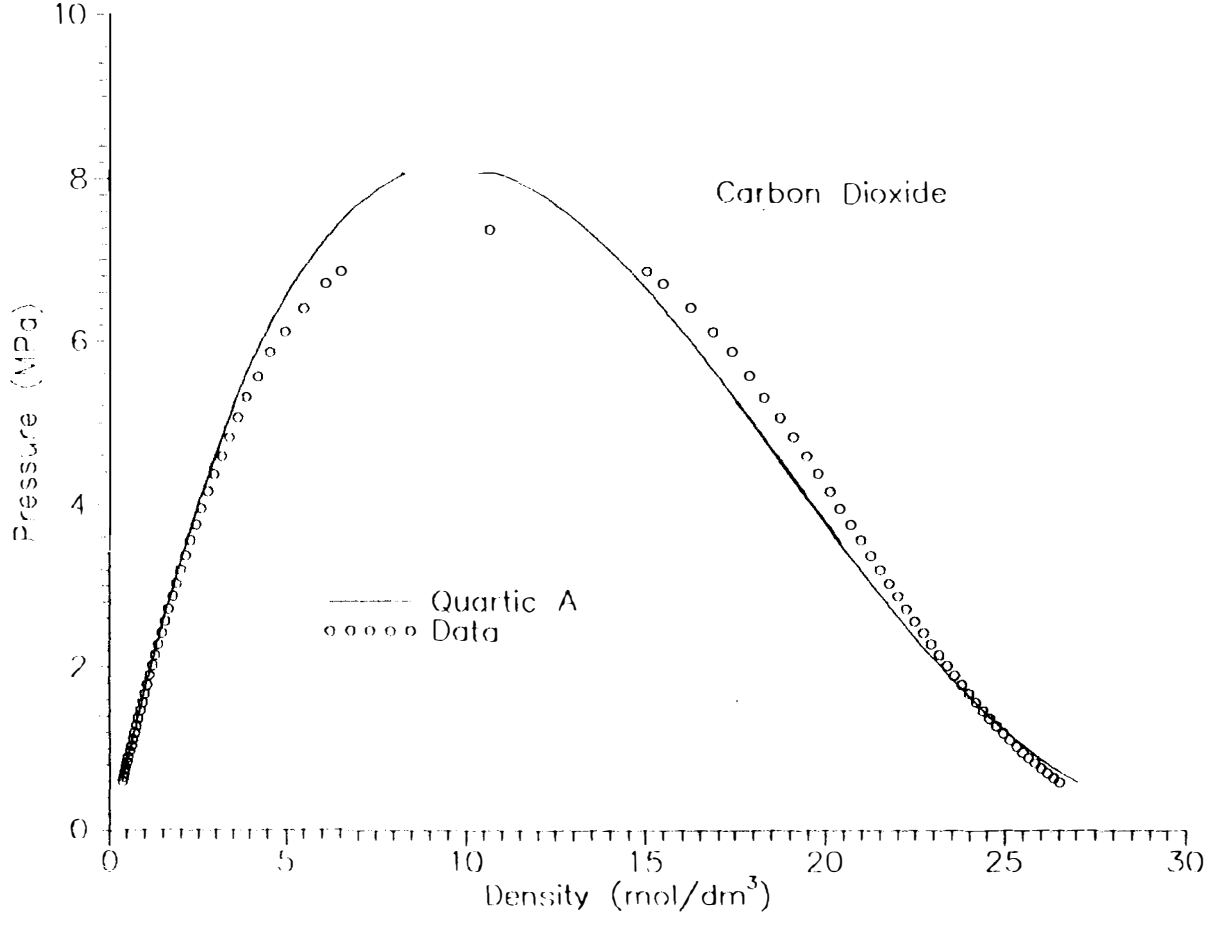

Figure 4.5: Saturated VLE calculations for Carbon Dioxide.
Data Source: Angus et al. *International Tables of the Fluid State: Carbon Dioxide*, Permagon Publishing Co., 1976.

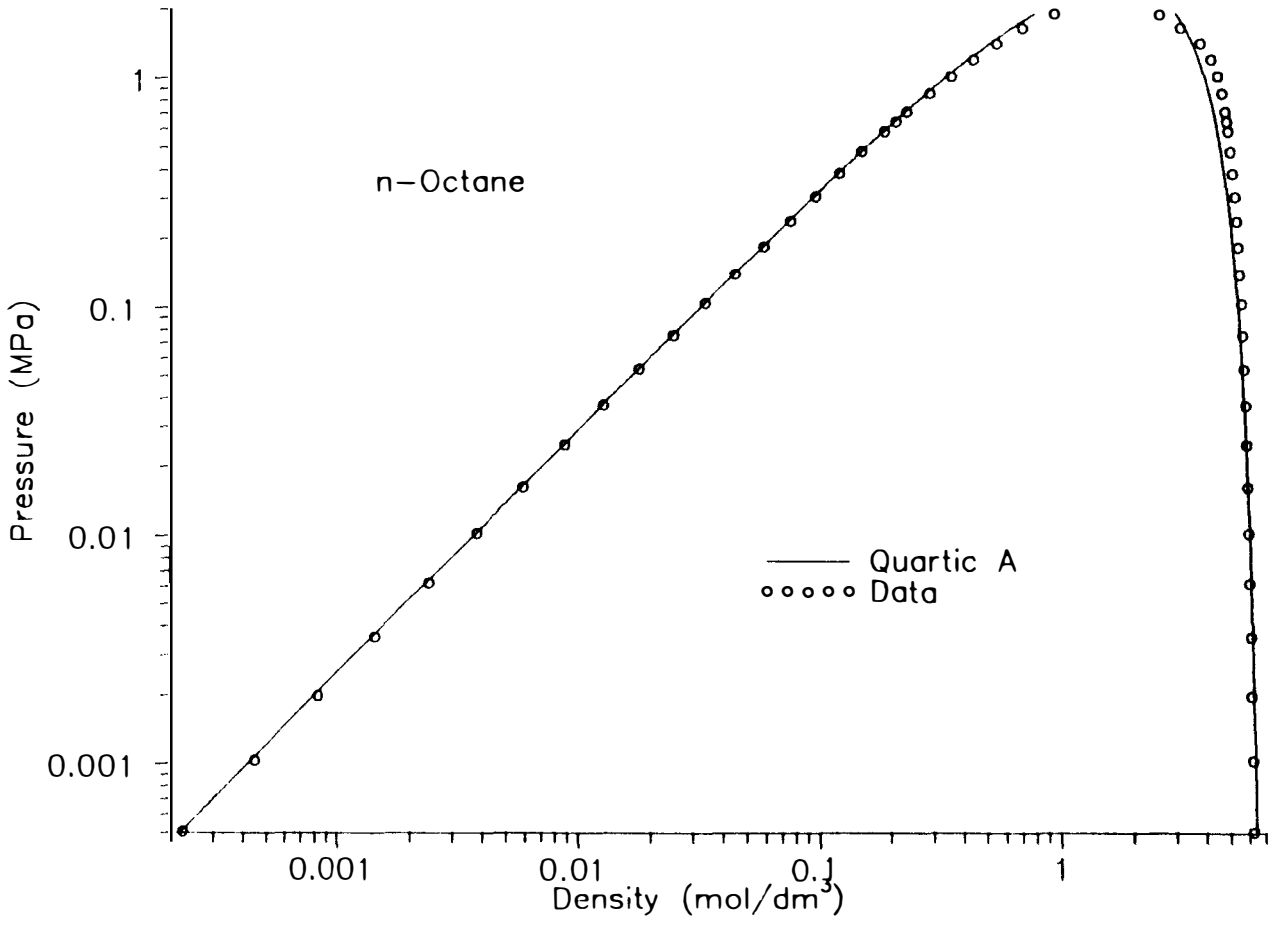

Figure 4.6: Saturated VLE calculations for n-Octane.
Data Source: Starling, K. E., *Fluid Thermodynamic Properties of Light Petroleum Substances*, Gulf Publishing Co., 1973.

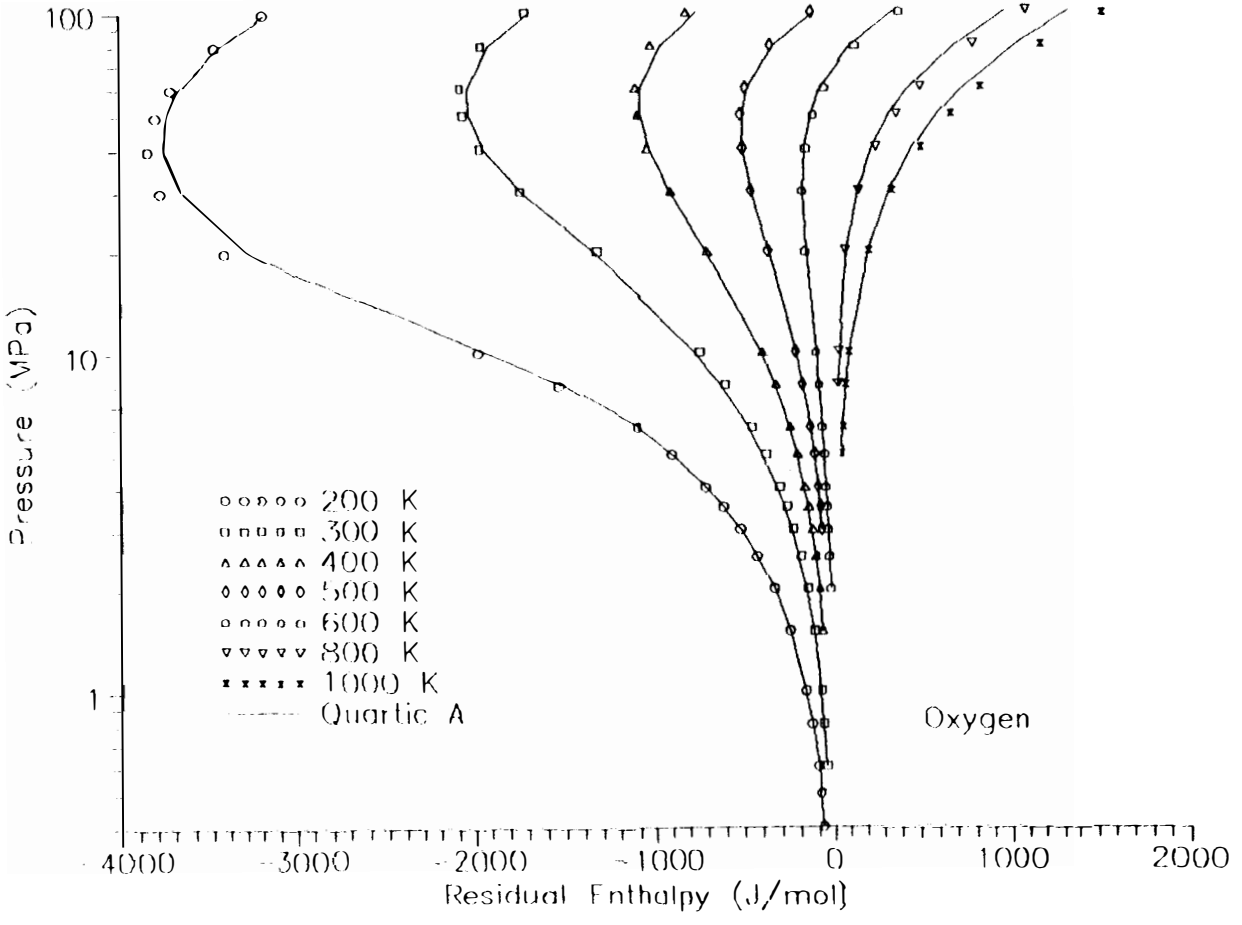

Figure 4.7: Residual enthalpy calculations for Oxygen.
Data Source: Vargaftik, N. B., *Tables on the Thermodynamic Properties of Liquids and Gases*, Hemisphere Publishing Corp., 1975.

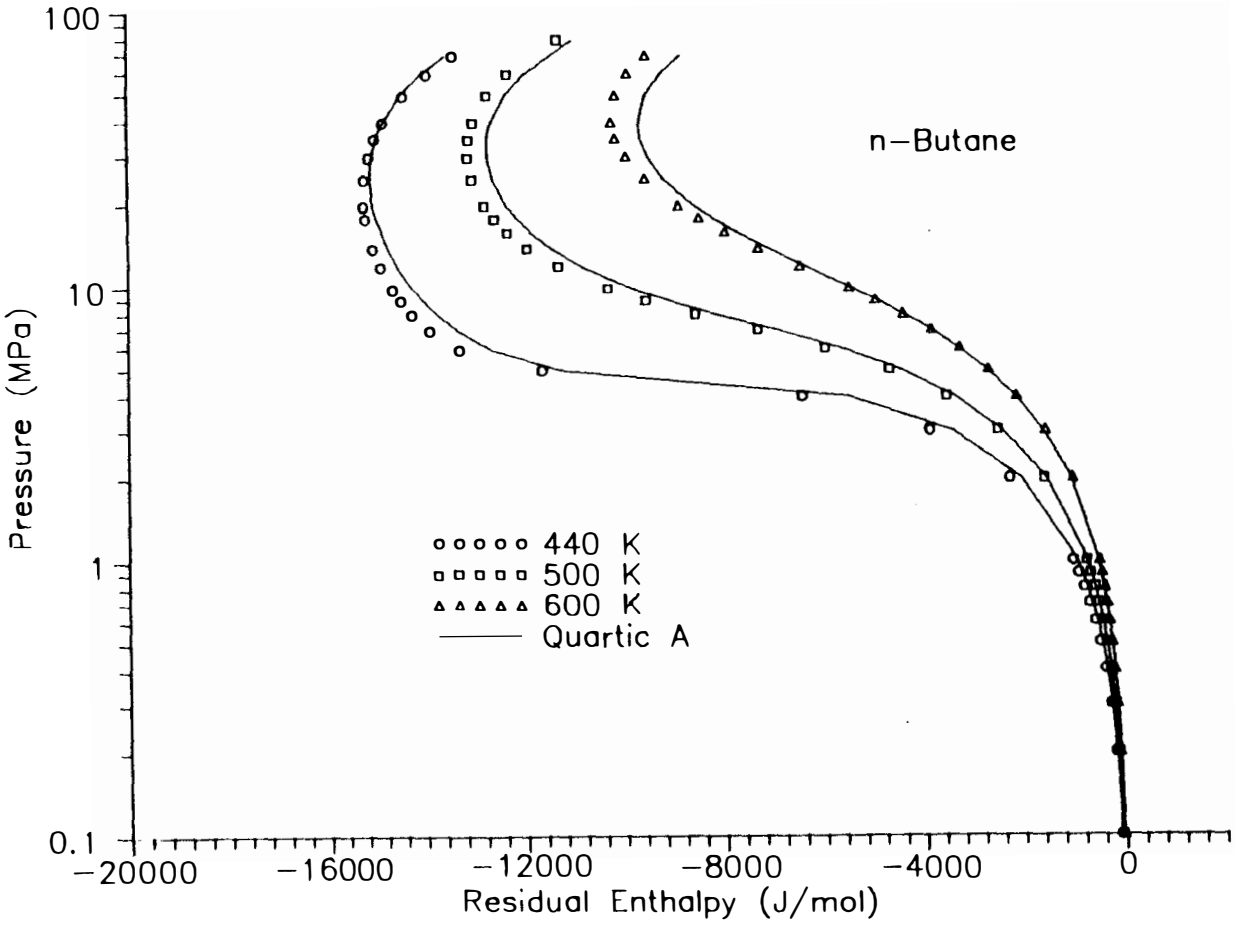

Figure 4.8: Residual enthalpy calculations for n-Butane.
Data Source: Younglove et al. *J. Phys. Chem. Ref. Data*, 16:577, 1987.

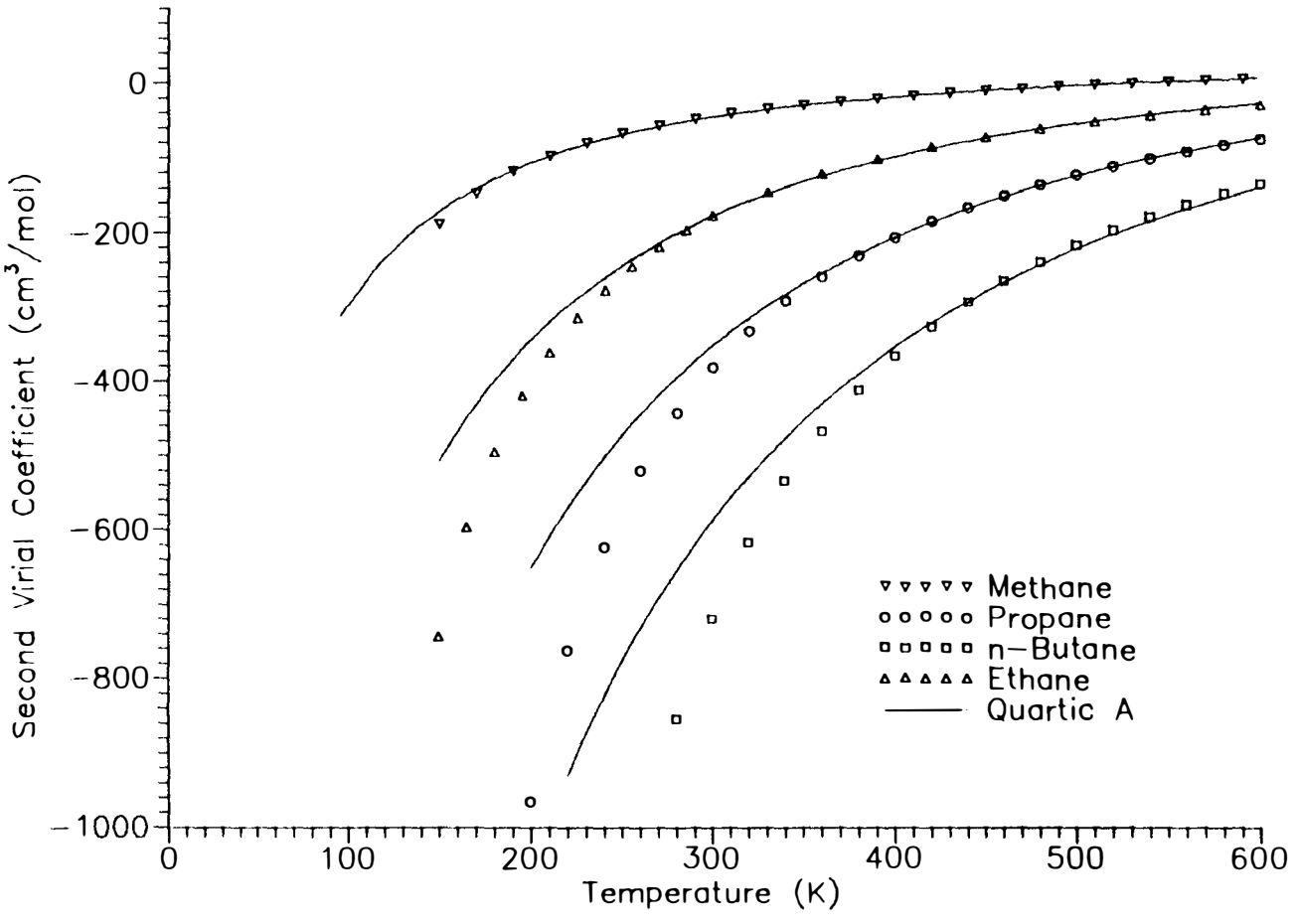

Figure 4.9: Second Virial coefficient prediction by the new equation of state.
Data Source: Younglove et al. *J. Phys. Chem. Ref. Data*, 16:577, 1987.

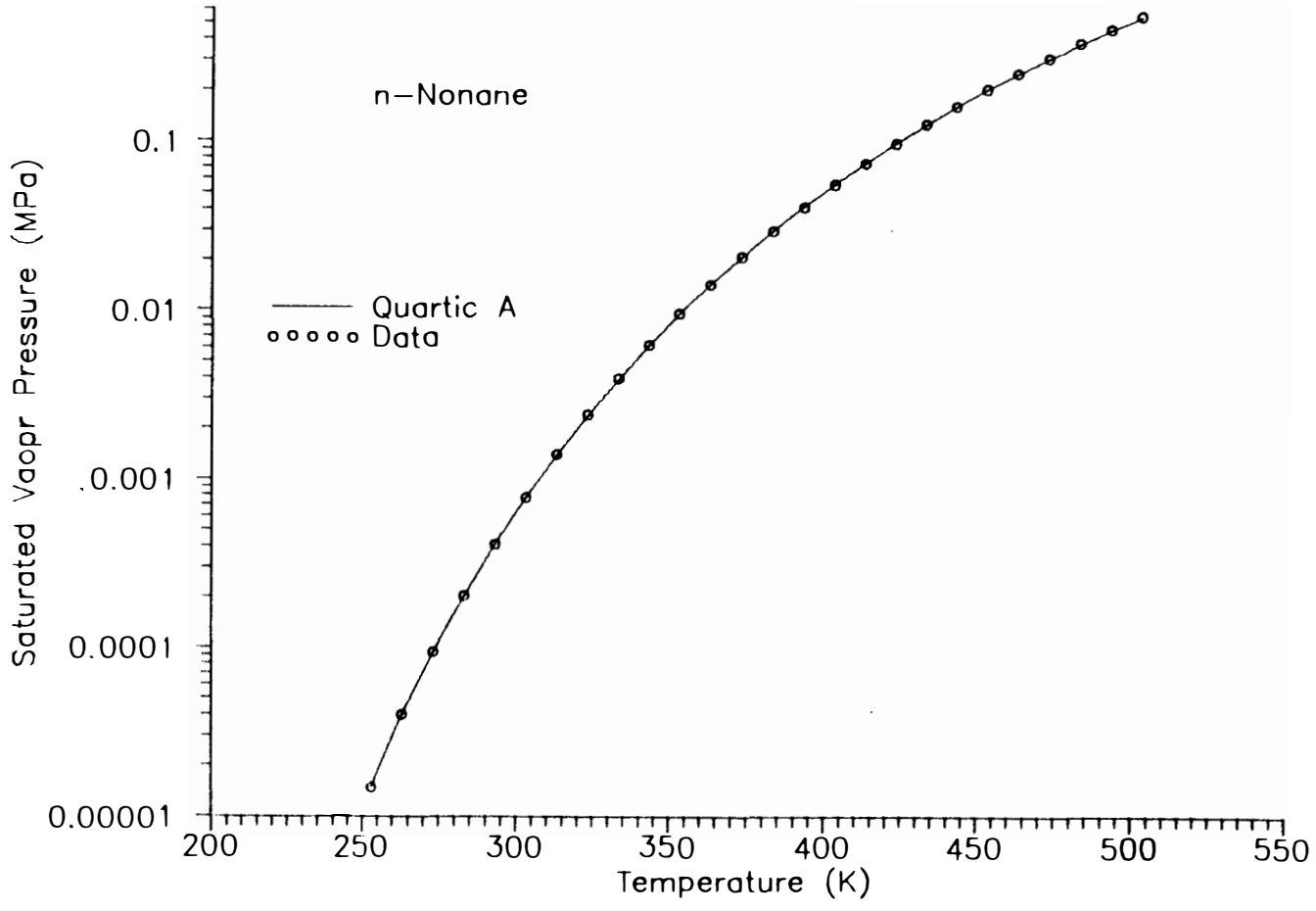

Figure 4.10: Vapor pressure predictions for n-Nonane.
Data Source: Vargaftik, N. B., *Tables on the Thermodynamic Properties of Liquids and Gases*, Hemisphere Publishing Corp., 1975.

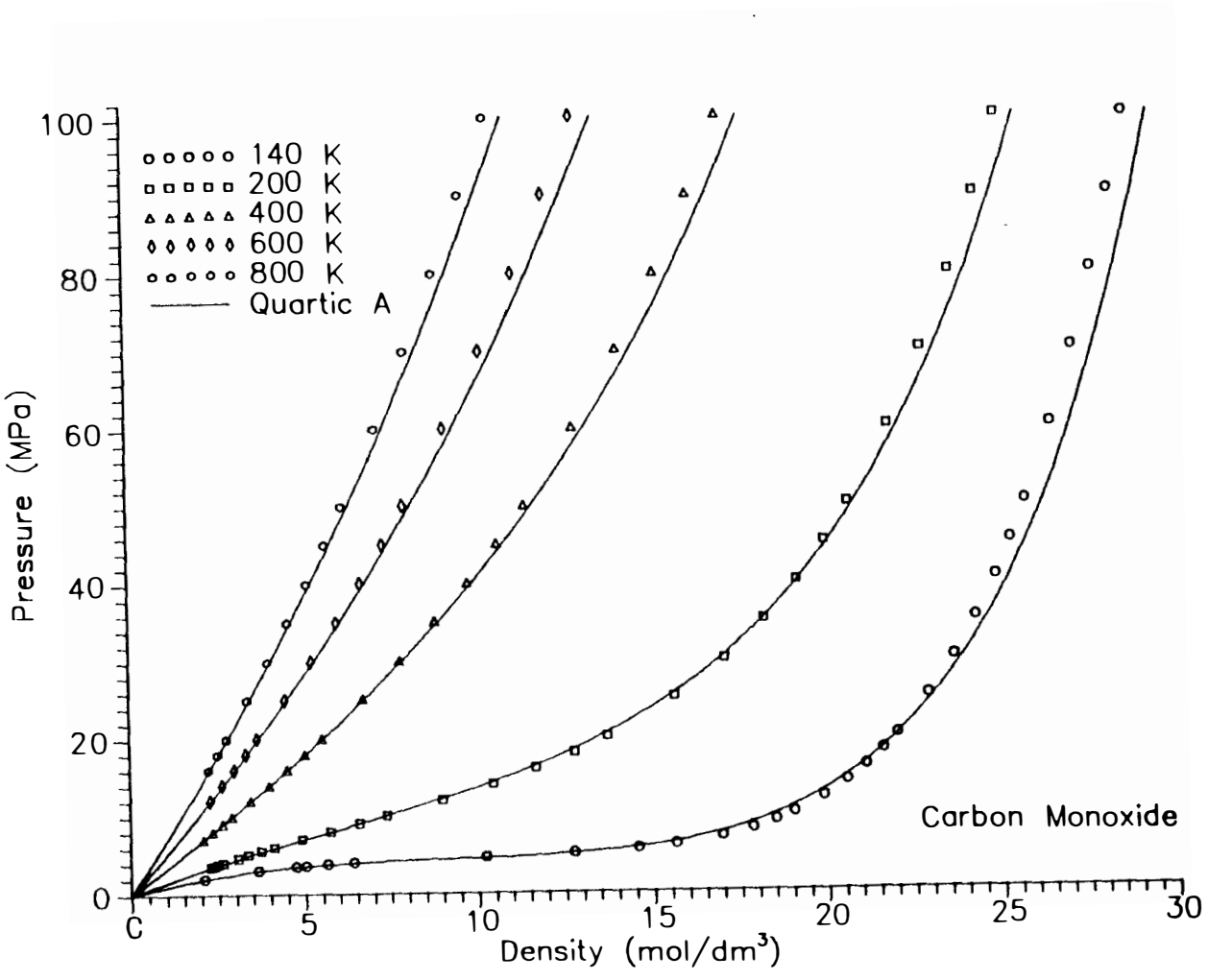

Figure 4.11: Pressure-density calculations for Carbon Monoxide

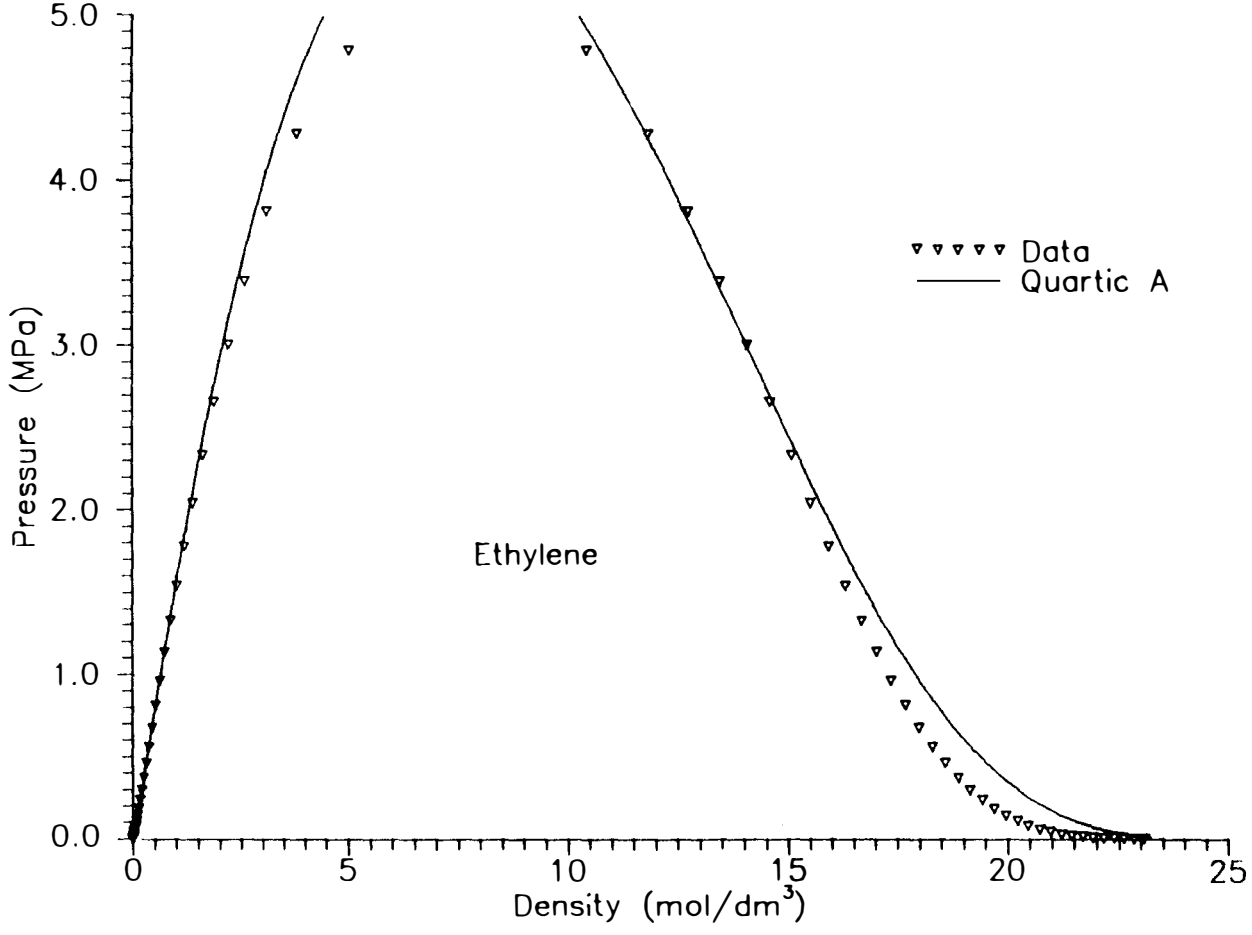

Figure 4.12: Saturated VLE calculations for Ethylene

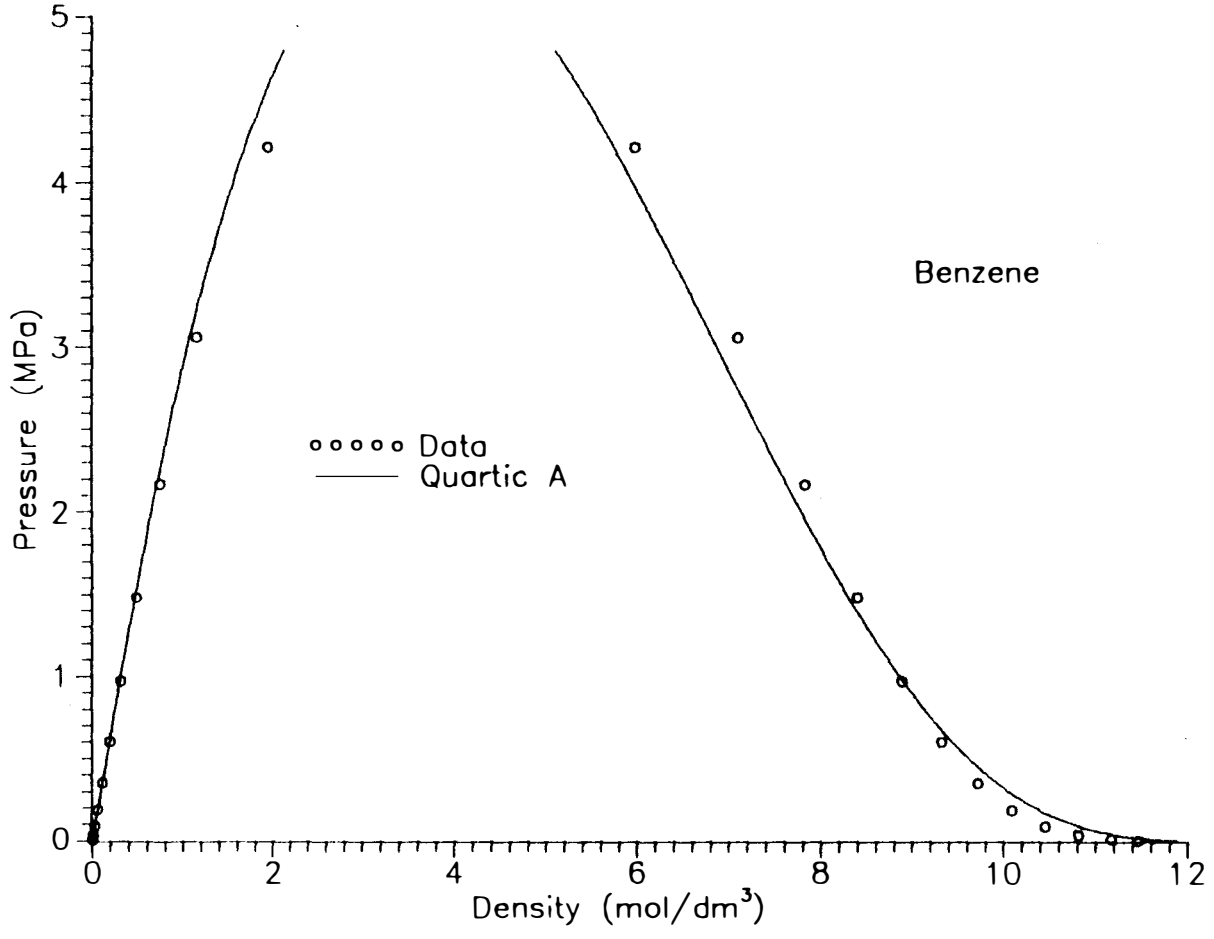

Figure 4.13: Saturated VLE calculations for Benzene

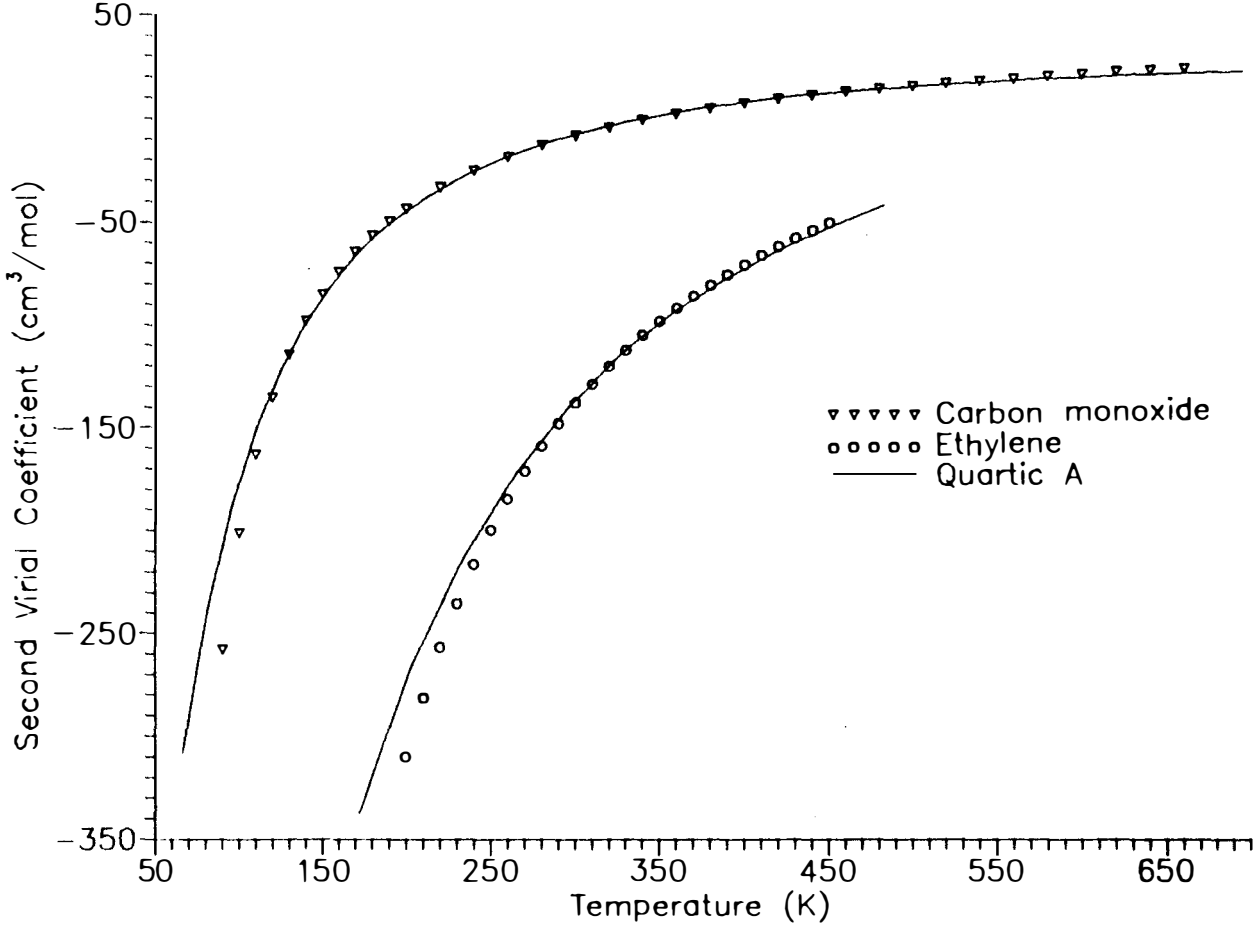

Figure 4.14: Second Virial coefficient calculations

Table 4.6: Calculated critical properties using Quartic A

Fluid	Critical Pressure		Critical Temperature		Critical Density	
	MPa	% Error	K	% Error	mol/dm^3	% Error
Argon	5.278	8.38	152.90	1.39	12.42	−6.97
Methane	5.038	9.52	193.16	1.45	9.40	−6.75
Nitrogen	3.696	9.03	128.17	1.56	10.38	−6.74
n-Butane	4.254	11.95	433.71	2.00	3.56	−9.26
CO_2	8.170	10.70	310.20	2.01	9.59	−9.95
n-Heptane	2.933	7.04	550.58	1.90	1.99	−14.12

$$\% \text{ Error } = \left(\frac{C^{calc} - C^{exp}}{C^{exp}} \right) 100$$

where

C^{exp} is the experimental critical property,

C^{calc} is the calculated critical property

tions (2.5) and (2.6). The critical temperature calculated by the quartic EOS is approximately 2 % greater than the true critical temperature of the fluid. The proposed rules used for the identification of roots (section 3.3) can lead to large errors in the temperature range 1.0 T_r to 1.03 T_r and density range of $0.8\rho_c$ to $1.2\rho_c$.

Comparision of the new EOS with the Peng-Robinson equation of state and Kubic's quartic equation were made. The performance of the new EOS is substantially better than either of them. Both, the PR and Kubic EOS's overpredict densities at high pressures and supercritical temperatures. Density calculations for argon at supercritical temperatures by all the equations of state can be seen in Figure 4.15. At temperatures above $3T_r$ all the equations of state seem to perform equally for all fluids.

At subcritical temperatures, the new EOS performs better particularly for liquid density calculations. For argon, the PR equation predicts too high a liquid density at lower reduced temperatures as seen in Figure 4.16. For normal hydrocarbons, as the chain length of the molecules increases from methane to n-octane, the performance of the PR EOS becomes comparable to that of the new EOS for orthobaric liquid densities and saturated vapor pressures. Figure 4.17 compares the two-phase envelope calculations for the various equations of state with the data for n-butane. The new EOS outperforms the PR and the Kubic's quartic EOS in the compressed liquid region as seen in Figure 4.18. Kubic's EOS shows incorrect orthobaric liquid density calculations at low reduced temperatures as shown in Figure 4.19. Figure 4.20 shows the large errors in saturated vapor pressure calculations by the Kubic EOS for propane at $T_r < 0.5$.

Table 4.7 shows the AAD summary for various physical and thermodynamic properties calculated by Quartic A, the Peng-Robinson and Kubic's quartic equation of state. The AAD summary was generated using the data of all the sixteen fluids used in the

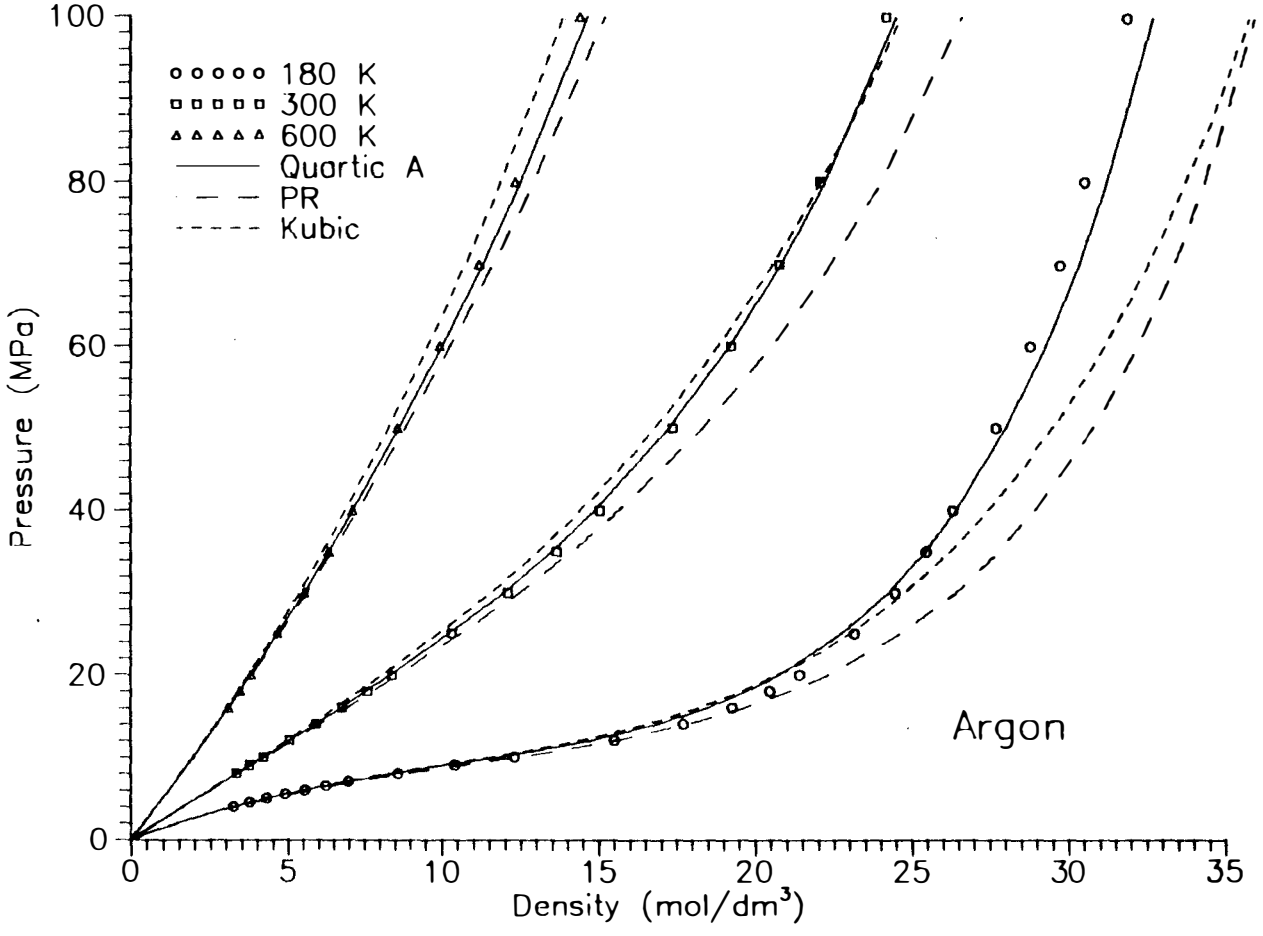

Figure 4.15: Pressure-density calculations for Argon.
Data Source: Stewart et al. *J. Phys. Chem. Ref. Data*, 18:640, 1989.

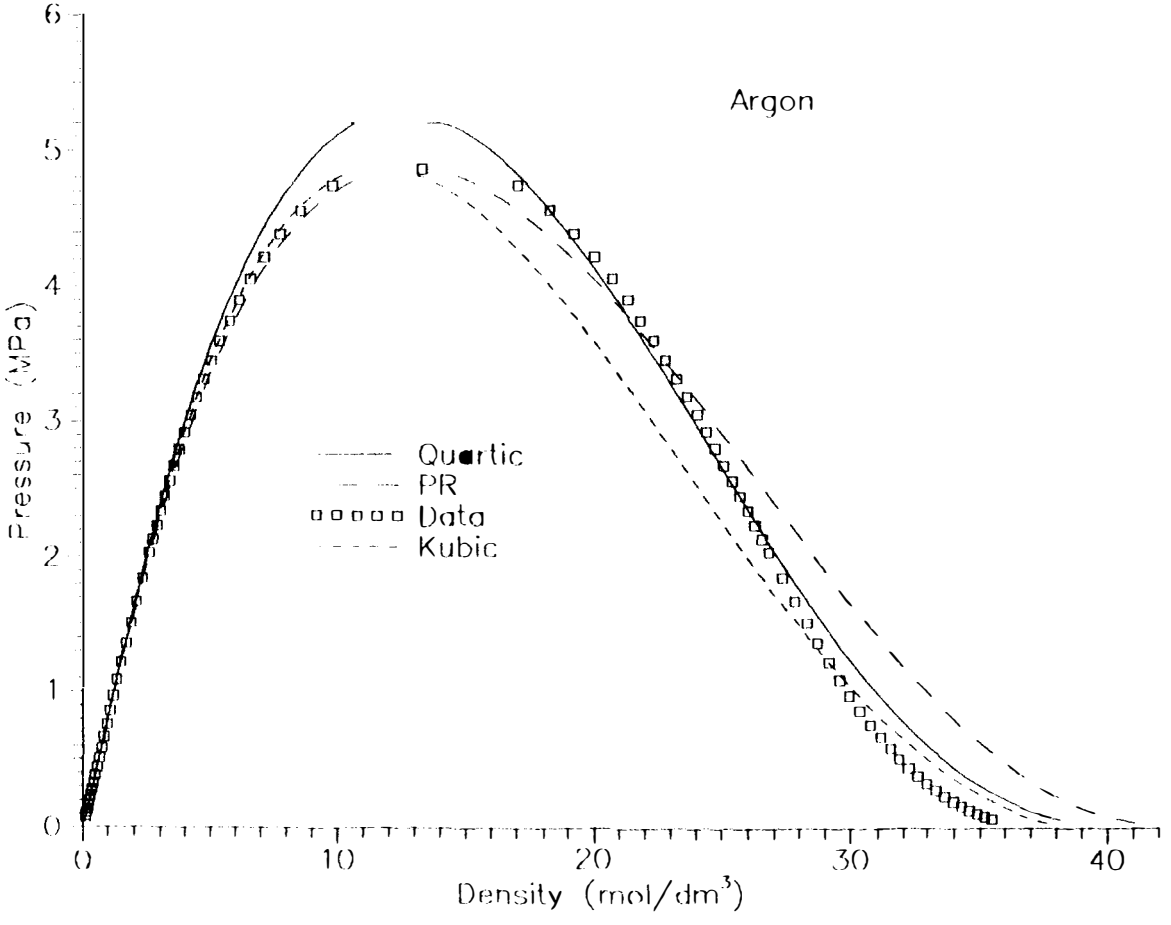

Figure 4.16: Comparision of saturated VLE calculations for Argon.
Data Source: Stewart et al. *J. Phys. Chem. Ref. Data*, 18:640, 1989.

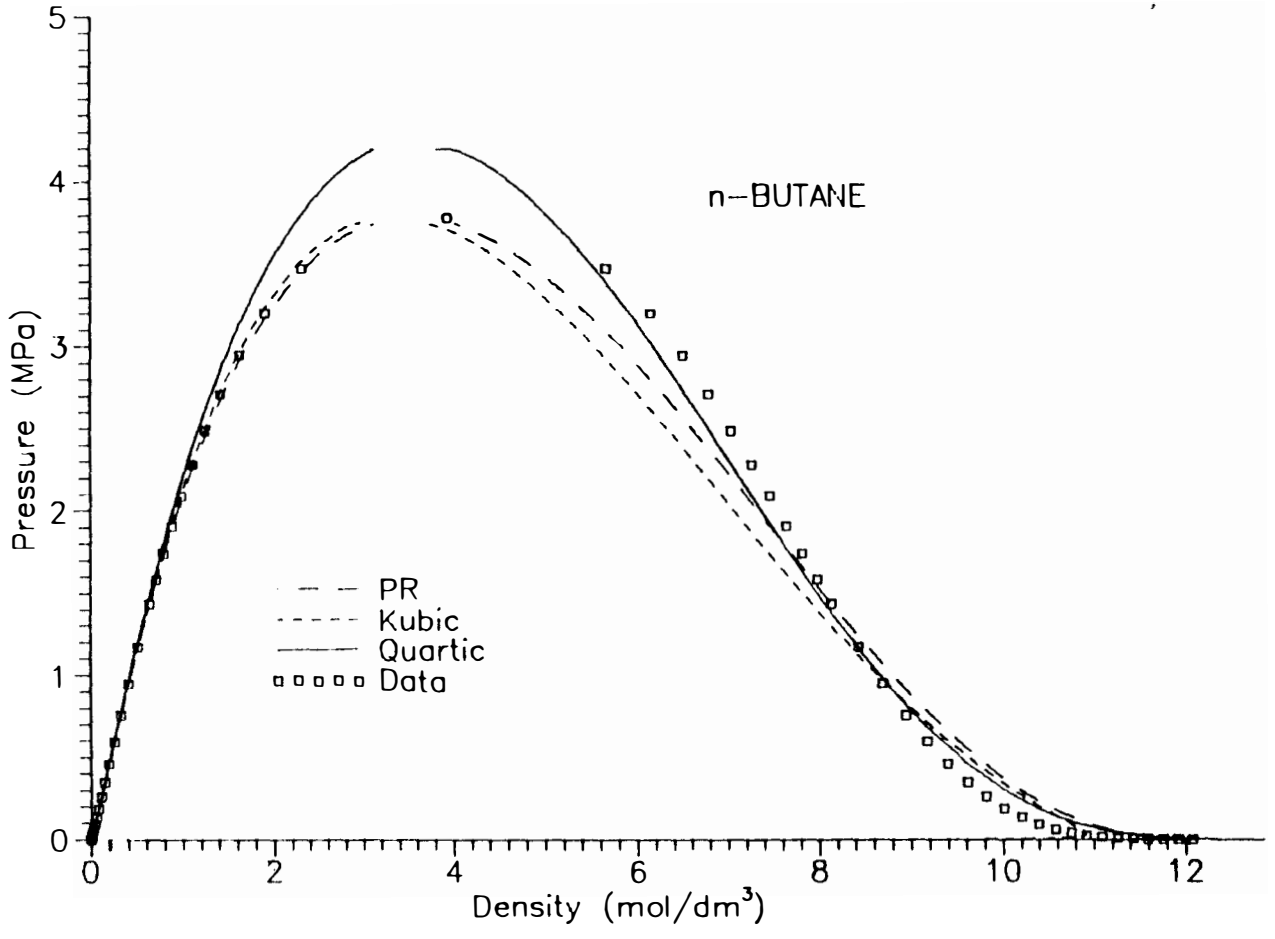

Figure 4.17: Comparision of saturated VLE calculations for n-Butane.
Data Source: Younglove et al. *J. Phys. Chem. Ref. Data*, 16:577, 1987.

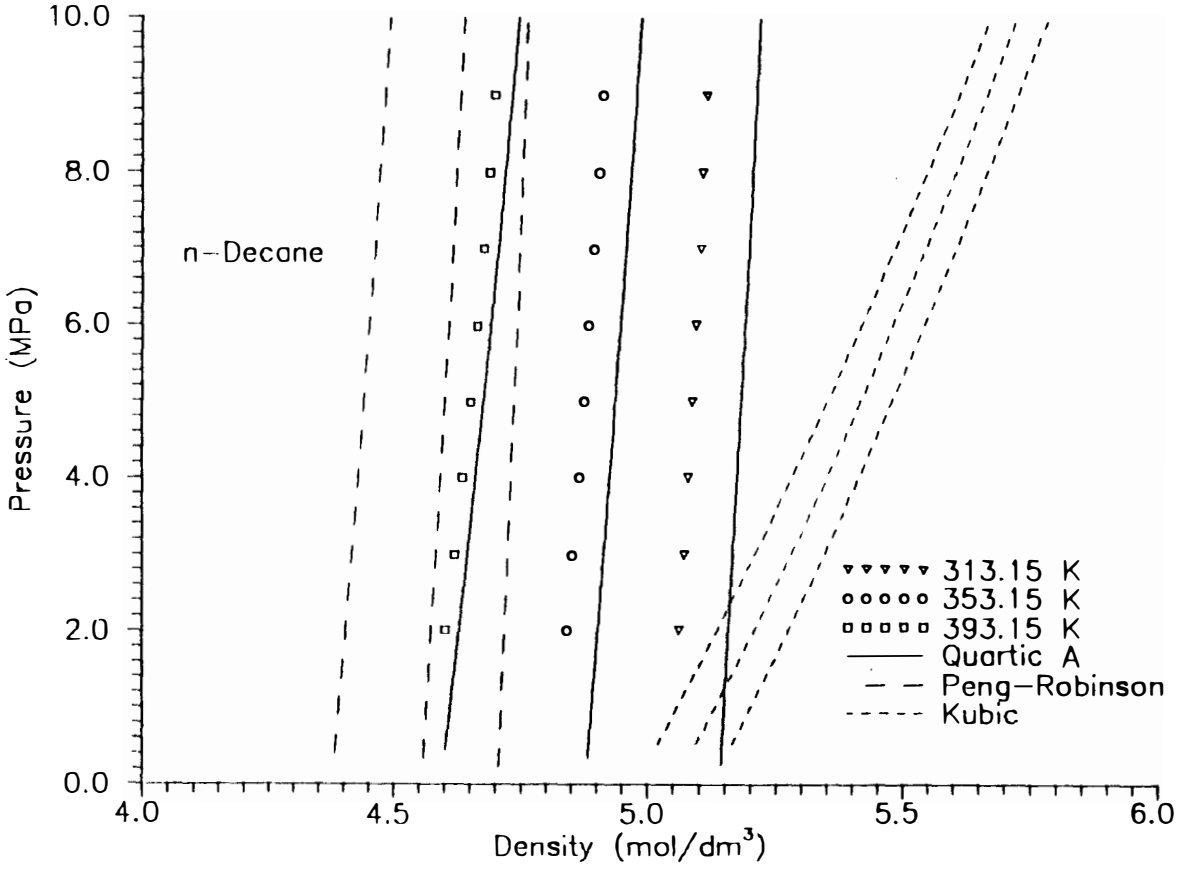

Figure 4.18: Comparision of compressed liquid calculations for n-Decane.
Data Source: Vargaftik, N. B., *Tables on the Thermodynamic Properties of Liquids and Gases*, Hemisphere Publishing Corp., 1975.

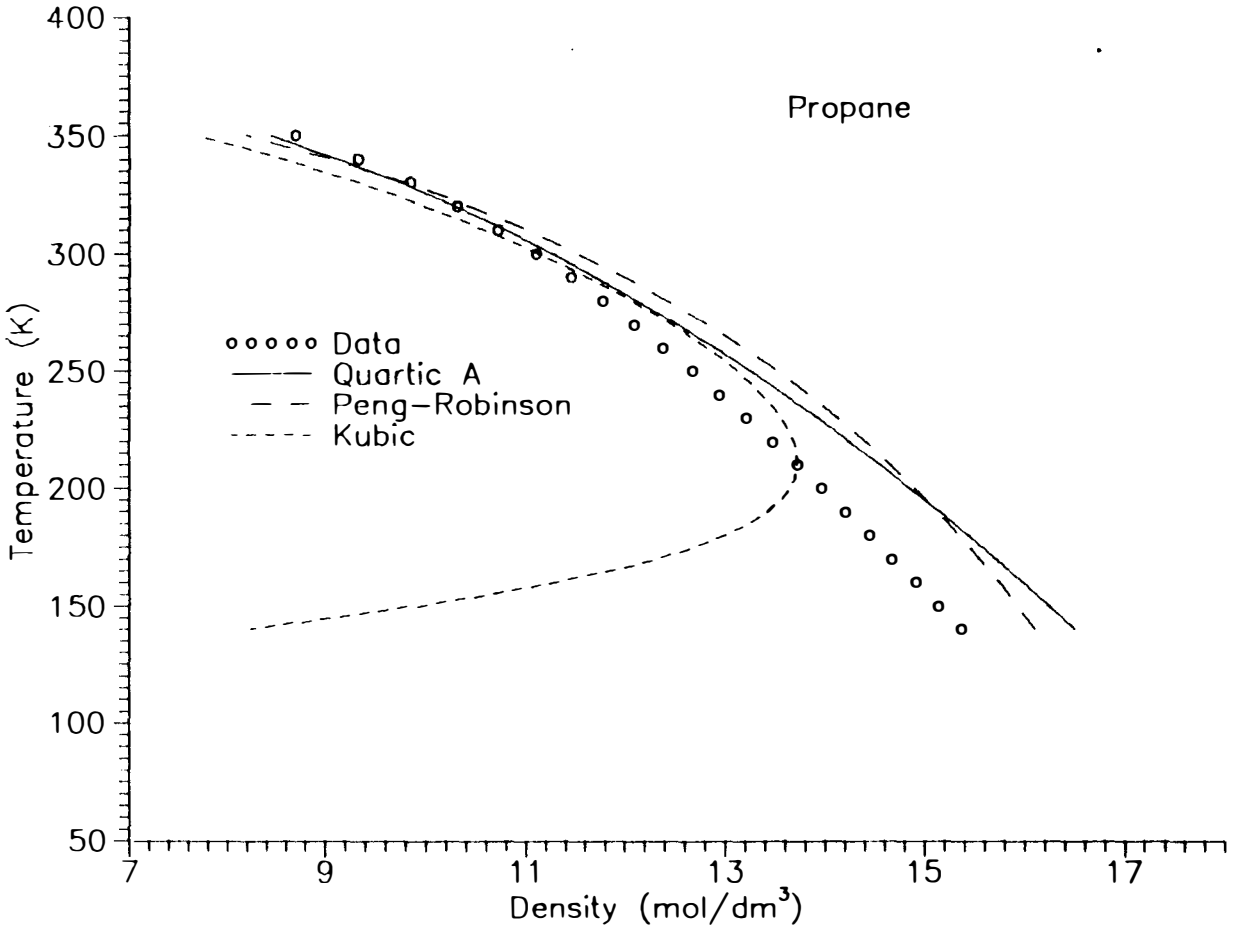

Figure 4.19: Comparision of saturated liquid calculations for Propane.
Data Source: Younglove et al. *J. Phys. Chem. Ref. Data*, 16:577, 1987.

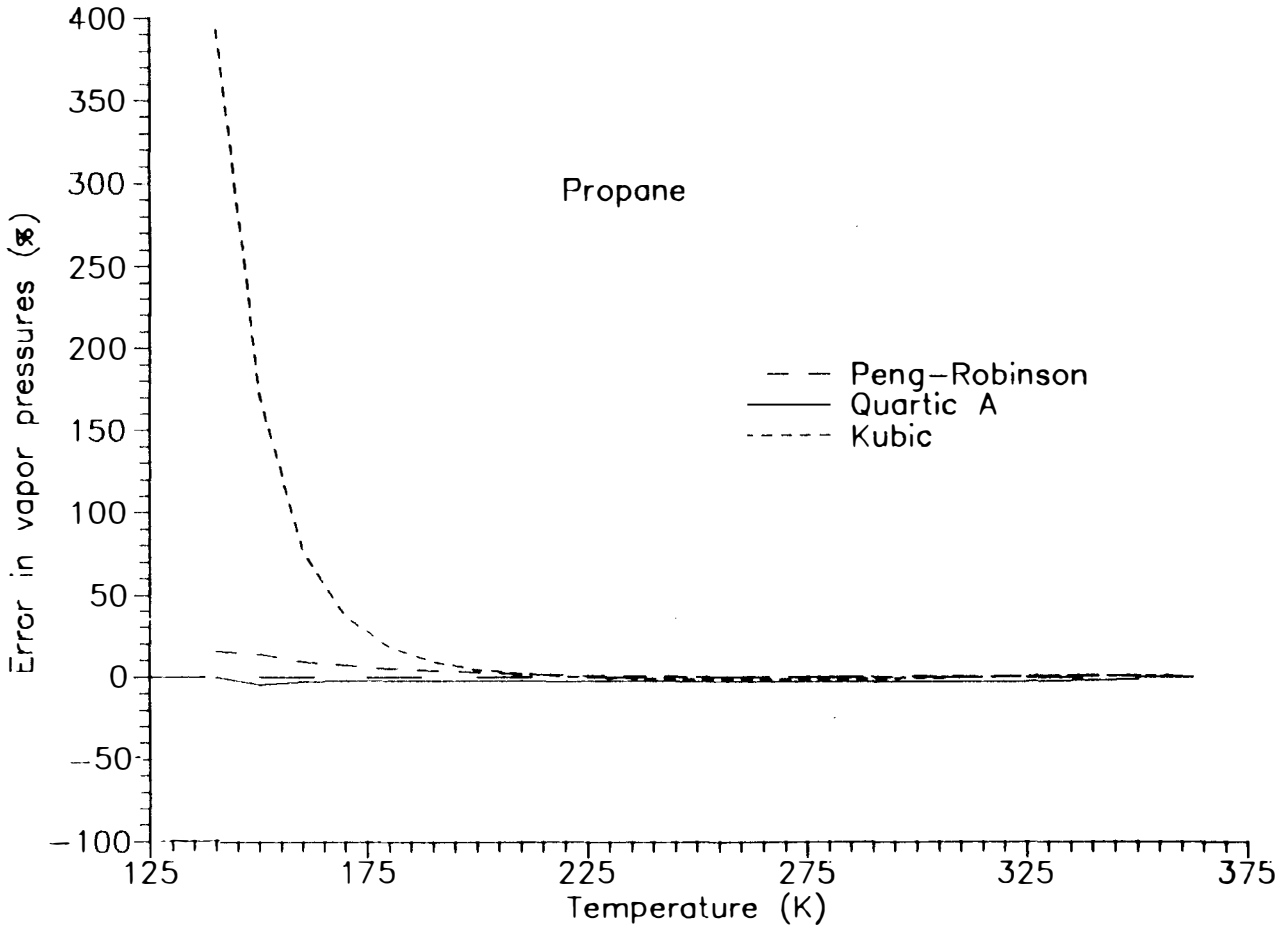

Figure 4.20: Errors in vapor pressure calculations for Propane.
Data Source: Younglove et al. *J. Phys. Chem. Ref. Data*, 16:577, 1987.

Table 4.7: Comparison of physical and thermodynamic property AAD summary

Thermodynamic property	Quartic A AAD (%)	Peng-Robinson AAD (%)	Kubic's Quartic AAD (%)	No. of Data points
P_{sat}	1.52	1.31	118.3	409
ρ_{sv}	2.00	2.20	130.0	409
ρ_l	3.46	6.31	5.78	581
ρ_g	0.60	1.67	1.58	2763
B_{vir}	6.09	46.46	48.04	537
H_r	4.03	22.27	13.18	1204

regressions. It can be seen from Table 4.7 that Quartic A is remarkably superior to the other two equations of state. The Peng-Robinson equation of state is slightly better than quartic A with regards to saturated vapor calculations. Kubic's quartic equation shows large AAD's for saturated vapor pressures and saturated vaopr density calculations. As pointed out earlier, these large errors arise only at $T_r < 0.5$. It is not surprising to find a large improvement in second virial coefficient and residual enthalpy calculations. This is because some second virial coefficient and residual enthalpy data was used in the regressions performed to obtain the constants of the new equation of state. Thus, on the whole the new equation of state (Quartic A) is more accurate than the Peng-Robinson and Kubic's quartic equation of state.

The EOS (Quartic A) needs ω in addition to T_c and ρ_c. It might appear that the value of the critical pressure, P_c, has to be known. This would be so because the critical pressure of a fluid is needed for the calculation of ω. The critical density of a substance

is much more difficult to measure experimentally than its critical pressure. Hence, the critical pressures of a large number of substances have been determined experimentally, whereas their critical densities have not been determined. In such cases the quartic equation of state can be treated as a T_c , P_c, and ω dependent equation of state by using the following relationships.

$$Z_c^* = 0.291 - 0.008\omega$$
$$V_c^* = \frac{Z_c^* R T_c}{P_c} \tag{4.1}$$

where

Z_c^* is the calculated fluid compressibility, and

V_c^* is the calculated fluid critical volume.

Thus, an approximate value for V_c can be obtained from the value of P_c and ω. This approximate value of V_c can be used along with T_c and ω to calculate thermodynamic and physical properties of a fluid. The equation of state that used used the approximate value of V_c, with the constants given by those for Quartic A (Table 4.3), will be called Quartic C. Appendix D gives an detailed comparisons of the AAD's for various thermodynamic properties by the different equations of state. It can be seen from Appendix D that Quartic C is as good as Quartic A. For simple and normal fluids, where Equation (4.1) does not generate large errors in the calculated critical volume, Quartic C may be used.

CHAPTER 5

Conclusions and Recommendations

The generalized quartic equation of state, developed for pure fluids, is remarkably superior to the existing cubic and quartic equations of state. The repulsive interactions between molecules were modelled using a mathematically simplified approximation of accurate hard sphere equations of state. An empirical term was used to model the repulsive interactions. The new equation of state is a general equation and can be used for a number of simple non-polar or slightly polar fluids and normal fluids. The equation of state requires only three properties of a fluid to determine the various physical and thermodynamic properties over a wide temperature and pressure range. These three properties are the critical density, the critical temperature and the acentric factor of the fluid. Various constants in the equation of state were determined using nonlinear regressions and properties of 16 pure fluids.

The new equation of state is theoretically more correct as it attempts to model the attractive and repulsive forces between molecules accurately. One of the roots of the quartic equation is always less than the close packed volume of the fluid and thus it has no physical meaning. The remaining three roots behave like the roots of a cubic equation. Thus, the roots of the new equation of state can be found easily and assigned unequivocally. The equation of state assumes a spherical hard core and a fixed temperature dependence of the hard core volume for all molecules.

The quartic equation of state was tested for temperatures up to 1000 K and pressures

up to 100 MPa. It was found to be more accurate than the Peng-Robinson and Kubic's quartic equation of state, particularly, at high pressures. The performance of the new equation of state is not quite so accurate near the critical point of the fluid. This is because the predicted critical compressibility of the fluid is about 10 % larger than the experimentally observed value. Large errors in density calculations may result in the near critical region (within $\pm 3\%$ of T_c and $\pm 10\%$ of P_c). This is a small region in the $P-\rho-T$ space where the equation of state is less accurate. The remarkable performance of the equation of state in the remaining $P-\rho-T$ space makes the equation of state attractive for use.

For an equation of state to calculate accurate thermodynamic and physical properties of a fluid it does not have to be mathematically complex. Mathematical approximations together with correct interpretation and understanding of physical phenomena can lead to a simple, yet accurate equation of state.

Recommendations

The recommendations for future work on the quartic equation of state are

1. Test the equation of state for a large number of pure fluids. This would include about 30 fluids which are nonpolar or slightly polar.

2. Extend the equation of state to polar fluids.

   Polar fluids have dipole moments which lead to additional attractive forces between molecules. The dipole moment could be used as the fourth property in addition to the critical volume, critical temperature and acentric factor to characterize polar fluids. The equation of state parameters a and c can be made functions

of dipole moments. Regressions with polar fluid data can be used to determine the dependence of a and c on the dipole moment.

3. Extend the equation of state to mixtures. The van der Waals one fluid mixing rules may be used readily to test the EOS's performance for mixtures.

4. Mathematically show that the fourth root of the quartic EOS will have no physical meaning for a wide range of fluids, fluid mixtures, pressures, temperatures and densities. Fourier and Budan's theorem or Sturm's theorem [124] may be used to do this. The exact number of real roots in a given interval can be determined using Sturm's theorem. Both the methods rely on the sign and magnitude of the coefficients of the quartic polynomial. As the coefficients of the quartic EOS are functions of temperature and pressure, it is not an easy task to use these theorems over a large range of temperatures and pressures.

5. The hard core volume of a fluid was fixed to a constant times the critical volume of a fluid. The temperature dependence of the hard sphere volume of the fluid was assumed to be independent of the nature of the fluid. Dependence of both these quantities on the nature of the fluid may present a more realistic approach to extending the equation of state to different types of fluids.

6. Temperature dependence of the parameters a needs to be modified to correct for the less accurate second virial coefficient calculations at low reduced temperatures. At subcritical temperatures the second virial coefficient becomes more negative rapidly as the temperature decreases. The functional form used for α is not capable of such an rapid decline with decreasing temperatures. A different functional

form for α might improve second virial coefficient calculations at subcritical temperatures.

BIBLIOGRAPHY

BIBLIOGRAPHY

[1] Rowlinson J. S.
J. D. van der Waals: On the continuity of the gaseous and liquid states.
North-Holland, 1988.

[2] O. Redlich and J.N. S. Kwong.
On the thermodynamics of solutions. V. An equation of state. Fugacities of gaseous solutions.
Chem. Revs., 233–244, 1949.

[3] G. Soave.
Equilibrium constants from a modified Redlich-Kwong equation of state.
Chem. Eng. Sci., 27:1197–1203, 1972.

[4] D.-Y. Peng and D.B Robinson.
A new two-constant equation of state.
Ind. Eng. Chem. Fundam., 15:59–64, 1976.

[5] M. M. Abbot.
Cubic equations of state: an interpretive review.
In K. C. Chao and R. L. Jr. Robinson, editors, *Advances in Chemistry Series. Equations of State in Engineering and Research*, pages 47–70, Am. Chem. Soc., Washington, D.C., 1979.

[6] R. Stryjek and J. H. Vera.
Prsv : an improved peng-robinson equation of state for pure compounds and mixtures.
Can. J. Chem. Eng., 64:323–333, 1986.

[7] Y. Adachi and H. Sugie.
Derivative method to develop a cohesion parameter of a cubic equation of state.
J. Chem. Eng. Japan., 20:424–426, 1987.

[8] Y. Adachi and H. Sugie.
The controlling quantity in cubic equation of state for the heat of vaporization calculations.
J. Chem. Eng. Japan., 20:190–192, 1987.

[9] G. A. Melhem, R. Saini, and B. M. Goodwin.
A modified Peng-Robinson equation of state.
Fluid Phase Equilibria, 47:189–237, 1989.

[10] E. Usdin and J. C. McAuliffe.
A one parameter family of equations of state.
Chem. Eng. Sci., 31:1077–1084, 1976.

[11] J. J. Martin.
Cubic equations of state - which?
Ind. Eng. Chem. Fundam., 18:81–97, 1979.

[12] G. Schmidt and H. Wenzel.
A modified van der Waals type equation of state.
Chem. Eng. Sci., 35:1503–1512, 1980.

[13] A. Harmens and H. Knapp.
Three-parameter cubic equation of state for normal substances.
Ind. Eng. Chem. Fundam., 19:291–294, 1980.

[14] G. Heyen.
Liquid and vapor properties from a cubic equation of state.
2nd World Congress of Chem. Eng. Montreal, 41–46, 1981.

[15] N. C. Patel and A. S. Teja.
A new cubic equation of state for fluids and fluid mixtures.
Chem. Eng. Sci., 37:463–473, 1982.

[16] W. L. Jr. Kubic.
A modification of the Martin equation of state for calculating vapor-liquid equilibria.
Fluid Phase Equilibria, 9:79–97, 1982.

[17] R. Freze, J.-L. Chevalier, A. Peneloux, and E. Rauzy.
Vapor-liquid equilibria calculations for normal fluid systems using a new cubic equation of state.
Fluid Phase Equilibria, 15:33–66, 1983.

[18] Yu J. M., Y. Adachi, and B. C.-Y. Lu.
Selection and design of cubic equations of state.
In K. C. Chao and R. L. Jr. Robinson, editors, *ACS Symposium series 300, Equations of State: Theories and Applications*, pages 537–559, Am. Chem. Soc., Washington, D. C., 1986.

[19] J. M. Yu, B. C.-Y. Lu, and Y. Iwai.
Simultaneous calculation of VLE and saturated liquid and vapor volumes by means of a 3P1T cubic eos.
Fluid Phase Equilibria, 37:207–222, 1987.

[20] Y. Iwai, M. R. Margerum, and B. C.-Y. Lu.
A new three parameter eos for polar fluids and fluid mixtures.
Fluid Phase Equilibria, 42:21–41, 1988.

[21] Y. Adachi, B. C.-Y. Lu, and H. Sugie.
Three-parameter equations of state.
Fluid Phase Equilibria, 11:29–48, 1983.

[22] T. M. Guo, H. Kim, H. M. Lin, and K. C. Chao.
Cubic Chain-of-Rotators equation of state for polar fluids.
Fluid Phase Equilibria, 24:43–61, 1985.

[23] M. A. Trebble and P. R. Bishnoi.
Development of a new four-parameter cubic equation of state.
Fluid Phase Equilibria, 35:1–18, 1987.

[24] Y. Adachi and H. Sugie.
Development of a five parameter equation of state.
Fluid Phase Equilibria, 28:119–136, 1986.

[25] S. Salerno, M. Cascella, May D., P. Watson, and D. Tassios.
Prediction of vapor pressures and saturated volumes witha simple cubic equation of state: Part I : A reliable database.
Fluid Phase Equilibria, 27:15–34, 1986.

[26] M. A. Trebble and P. R. Bishnoi.
Accuracy and consistency comparisons of ten cubic equations of state for polar and non-polar compounds.
Fluid Phase Equilibria, 29:1–18, 1986.

[27] P. H. Salim and M. A. Trebble.
A modified Trebble-Bishnoi equation of state: Thermodynamic consistency revisited.
Fluid Phase Equilibria, 65:59–71, 1991.

[28] D. Zudkevitch and J. Joffe.
Correlation and prediction of vapor-liquid equilibria with the Redlich-Kwong equation of state.
AIChEJ, 16:112–119, 1970.

[29] L. Yarborough.
Application of a generalized equation of state to petroleum reservoir fluids.
In *Advances in Chemistry Series No. 182, Equations of State in Engineering and Research.*, pages 385–439, Am. Chem. Soc., 1979.

[30] R. W. Morris and E. A. Turek.
Optimal temperature dependent parameters for the Redlich-Kwong equation of state.
In *ACS Symposium series 300, Equations of State: Theories and Applications.*, pages 389–405, Am. Chem. Soc., 1986.

[31] A. Z. Panagiotopoulos and S. K. Kumar.
A generalized technique to obtain pure component parameters for two-parameter equations of state.
Fluid Phase Equilibria, 27:77–88, 1985.

[32] L. A. Cisternas.
A simple and accurate technique to obtain pure component parameters for three-parameter equations of state.
Fluid Phase Equilibria, 39:75–87, 1988.

[33] A. Peneloux, E. Rauzy, and R. Freze.
A consistent volume correction for Redlich-Kwong Soave volumes.
Fluid Phase Equilibria, 8:7–23, 1982.

[34] P. M. Mathias, T. Naheiri, and E. M. Oh.
A density correction for the peng-robinson equation of state.
Fluid Phase Equilibria, 47:77–87, 1989.

[35] W. L. Jr. Kubic.
A quartic hard chain equation of state for normal fluids.
Fluid Phase Equilibria, 31:35–56, 1986.

[36] W. L. Jr. Kubic.
Application of the quartic hard chain equation of state to polymer mixtures.
Fluid Phase Equilibria, 31:56–, 1986.

[37] G. Soave.
A non-cubic equation of state for PVT and phase equilibrium calculations (pure compounds).
Fluid Phase Equilbria, 56:39–57, 1990.

[38] B. E. Poling, E. A. Grens II, and J. M. Prausnitz.
Thermodynamic properties from a cubic equation of state : avoiding trivial roots and spurious derivatives.
Ind. Eng. Chem. Process Des. Dev., 20:127–130, 1981.

[39] A. Asselineau, G. Bogdanic, and J. Vidal.
A versatile algorithm for calculating vapor-liquid equilibria.
Fluid Phase Equilibria, 3:273–290, 1979.

[40] R. Gosset, G. Heyen, and B. Kalitventzeff.
An efficient algorithm to solve cubic equations of state.
Fluid Phase Equilibria, 25:51–64, 1986.

[41] J. S. Rowlinson and F. L. Swinton.
Liquids and Liquid Mixtures.
Butterworths Press, 1982.

[42] N. F. Carnahan and K. E. Starling.
Equation of state for nonattracting rigid spheres.
J. Chem. Phys., 51:635– 636, 1969.

[43] B. J. Alder and T. E. Wainwright.
Studies in molecular dynamics. ii. behavior of a small number of elastic spheres.
J. Chem. Phys., 33:1439–1451, 1960.

[44] K. R. Hall.
Another hard-sphere equation of state.
J. Chem. Phys., 57:2252–2254., 1972.

[45] J. J. Erpenbeck and W. W. Wood.
Molecular dynamics calculations of the hard sphere equation of state.
J. Stat. Phys., 35:321–340., 1984.

[46] Y. Zhou and G. Stell.
Equations of state for hard sphere fluids.
Int. J. Thermophys., 9:953–963., 1977.

[47] R. M. Gibbons.
The scaled particle theory for particles of arbitrary shape.
Mol. Phys., 17:81–86, 1969.

[48] R. M. Gibbons.
The scaled particle theory for mixtures of hard convex particles.
Mol. Phys., 18:809–816, 1970.

[49] T. Boublik.
Statistical thermodynamics of convex molecule fluids.
Mol. Phys., 27:1415–1427, 1974.

[50] T. Boublik.
Hard convex body equation of state.
J. Chem. Phys., 63:4084, 1975.

[51] I. Nezbeda, J. Pavlicek, and S. Labik.
Thermodynamic properties of pure hard sphere, spherocylinder and dumbell fluids.
Coll. Czech. Chem. Commun., 44:3555–3565, 1979.

[52] P. A. Monson and M. Rigby.
Virial equation of state for rigid spherocylinders.
Mol. Phys., 35:1337–1342., 1978.

[53] I. Nezbeda and T. Boublik.
On the possible equivalence of hard convex molecule fluids.
Mol. Phys., 51:1443–1447, 1984.

[54] K.-H. Naumann, Y. P. Chen, and T. W. Leland.
Conformal-solution-theorie fur mischungen konvexer molekule.
Ber. Bunsenges. Phys. Chem., 85:1029–1033, 1981.

[55] E. G. Azevedo and J. M. Prausnitz.
Effects of molecular size and shape on thermodynamic properties of fluid mixtures.
Fluid Phase Equilibria, 41:109–125, 1988.

[56] B. Alder, D. A. Young, and M. A. Mark.
Studies in molecular dynamics. X. corrections to the augmented van der Waals theory of the square well fluid.
J. Chem. Phys., 56:3013–3029, 1972.

[57] S. S. Chen and A. Kreglewski.
Applications of the augmented van der Waals theory of fluids. I. Pure fluids.
Ber. Bunsenges. Phys. Chem., 81:1048–1052, 1977.

[58] N. F. Carnahan and K. E. Starling.
Intermolecular repulsions and the equation of state for fluids.
AIChEJ, 18:1184–1189., 1972.

[59] S. Beret and J. M. Prausnitz.
Perturbed hard-chain theory : an equation of state for fluids containing small or large fluids.
AIChEJ, 21:1123–1132, 1975.

[60] M. D. Donohue and J. M. Prausnitz.
Perturbed hard chain theory for fluid mixtures : Thermodynamic properties for mixtures in natural gas and petroleum technology.
AIChEJ, 24:849–860, 1978.

[61] R. De Santis, F. Gironi, and L. Marrelli.
Vapor-liquid equilibrium from a hard-sphere equation of state.
Ind. Eng. Chem., Fundam.:183–189, 1976.

[62] R. Nakamura, J. F. Breedveld, and J. M. Prausnitz.
Thermodynamic properties of gas mixtures containing polar and nonpolar components.
Ind. Eng. Chem., Process Des. Dev., 15:557–564, 1976.

[63] L. R. Oellrich, H. Knapp, and J. M. Prausnitz.
A simple perturbed-hard-sphere equation of state applicable to subcritical and supercritical temperatures.
, *Fluid Phase Equilibria*, 2:163–171, 1978.

[64] M. D. Donohue and P. Vimalchand.
The perturbed-hard-chain-theory. extensions and applications.
Fluid Phase Equilibria, 40:185–211, 1988.

[65] P. R. Bienkowski and K. C. Chao.
Hard cores of molecules of simple fluids.
J. Chem. Phys., 62:615–619, 1975.

[66] P. R. Bienkowski and K. C. Chao.
A generalized hard-sphere augmented virial equation of state.
AIChEJ, 19:167–173, 1973.

[67] P. Svejda and F. Kohler.
A generalized van der Waals equation of state. I. Treatment of molecular shape in terms of the Boublik-Nezbeda equation.
Ber. Bunsenges. Phys. Chem., 87:672–680, 1983.

[68] B. Marchand, M.-J. Huron, and J. Vidal.
Pure component vapor pressure from a carnahan-starling equation of state : theoretically based temperature law for the attractive term.
Fluid Phase Equilibria., 9:105–117, 1982.

[69] J. Vidal.
Mixing rules and excess properties in cubic equations of state.
Chem. Eng. Sci., 33:787–791, 1978.

[70] M. J. Huron and J. Vidal.
New mixing rules in simple equations of state for representing vapor- liquid equilibria for strongly non-ideal mixtures.
Fluid Phase Equilibria, 3:255–271, 1979.

[71] K. M. Won.
Phase equilibria of high-boiling organic solutes in compressed supercritical fluids-equation of state with new mixing rule.
In *Chemical Engineering at Supercritical Fluid Conditions*, pages 323–340, Ann Arbor Science., 1983.

[72] G. Soave.
Improvement of the van der Waals equation of state.
Chem. Eng. Sci., 39:357–369, 1984.

[73] K. Tochigi, K. Kurihara, and K. Kojima.
Prediction of high pressure vapor-liquid equilibria with mixing rule using the ASOG group contribution method.
J. Chem. Eng. Jpn., 18:60–65., 1988.

[74] K. Tochigi, K. Kurihara, and K. Kojima.
Prediction of ternary vapor-liquid equilibria by mixing rule containing regular solution and residual excess free energy terms.
Fluid Phase Equilibria, 42:105–115., 1988.

[75] A. Pandit and R. P. Singh.
Vapor-liquid equilibria calculations for polar mixtures with mixing rule using ASOG group contribution method.
Fluid Phase Equilibria, 33:1–12, 1987.

[76] G. Soave.
Infinite-pressure excess functions and VLE K values from liquid-phase activity coefficients.
Fluid Phase Equilibria, 31:147–152, 1986.

[77] J. Mollerup.
A note on the derivation of mixing rules from excess Gibbs energy models.
Fluid Phase Equilibria, 25:323–327, 1986.

[78] P. A. Gupte, P. Rasmussen, and A. Fredenslund.
A new group-contribution equation of state for vapor-liquid equilibria.
Ind. Eng. Chem. Fundam., 25:636–645, 1986.

[79] B. L. Larsen, P. Rasmussen, and A. Fredenslund.
A modified UNIFAC group-contribution model for prediction of phase equilibria and heats of mixing.
Ind. Eng. Chem. Res., 26:2274–2286, 1987.

[80] R. Stryjek and J. H. Vera.
Prsv : an improved peng-robinson equation of state with new mixing rules for strongly nonideal mixtures.
Can. J. Chem. Eng., 64:334–339, 1986.

[81] K. Kurihara, K. Tochigi, and K. Kojima.
Mixing rule containing regular solution ans residual excess free energy.
J. Chem. Eng. Jpn., 20:227–231, 1987.

[82] J. Mollerup.
A note on excess gibbs energy models, equations of state and the local composition concept.
Fluid Phase Equilibria, 7:121–138, 1981.

[83] W. B. Whiting and J. M. Prausnitz.
Equations of state for the strongly nonideal fluid mixtures: application of the local compositions toward density-dependent mixing rules.
Fluid Phase Equilibria, 9:119–147, 1982.

[84] L. L. Lee, T. H. Chung, and K. E. Starling.
A molecular theory for the thermodynamic behaviour for polar mixtures. I. The statistical-mechanical local-composition model.
Fluid Phase Equilibria, 12:105–124, 1983.

[85] S. I. Sandler.
The generalized van der Waals partition function. I. Basic theory.
Fluid Phase Equilibria, 19:233–257, 1985.

[86] K.-H. Lee, M. Lombardo, and S. I. Sandler.
The generalized van der Waals partition function. II. Application to the square-well fluid.
Fluid Phase Equilibria, 21:177–196, 1985.

[87] K.-H. Lee, S. I. Sandler, and N. C. Patel.
The generalized van der Waals partition function. III. Local composition models for a mixture of equal size square-well molecules.
Fluid Phase Equilibria, 25:31–49, 1986.

[88] K.-H. Lee and S. I. Sandler.
The generalized van der Waals partition function IV. Local composition models for mixtures of unequal-size molecules.
Fluid Phase Equilibria, 34:113–147, 1987.

[89] S. B. Kanchanakpan, Lee L. L., and C. H. Twu.
Equations of state for nonspherical molecules based on the distribution function theories.
In K. C. Chao and R. L. Jr. Robinson, editors, *ACS Symposium series 300: Equations of State: Theories and Applications.*, pages 132–155, Am. Chem. Soc., 1986.

[90] L. L. Lee.
A molecular theory of solubility parameters: Generalization to polar fluid mixtures.
Fluid Phase Equilibria, 35:77–91, 1987.

[91] T. Boublik.
Excess entropy of the systems of molecules differing in size and shape.
Collect. Czech. Chem. Commun., 48:192–198, 1983.

[92] B. L. Beegle, M. Modell, and R. C. Reid.
Thermodynamic stability criterion for pure substances and mixtures.
AIChEJ, 20:1200–1206, 1974.

[93] R. C. Reid and B. L. Beegle.
Critical point criterion in legendre transform notation.
AIChEJ, 23:726–732, 1977.

[94] D.-Y. Peng and D. B. Robinson.
A rigourous method for predicting the critical properties of multicomponent systems from an equation of state.
AIChEJ, 23:137–144., 1977.

[95] R. A. Heidemann and A. M. Khalil.
The calculation of critical points.
AIChEJ, 26:769–779, 1980.

[96] M. L. Michelsen and R. A. Heidemann.
Calculation of critical points from two-constant equations of state.
AIChEJ, 27:521–523, 1981.

[97] G. T. Hong, M. Modell, and J. W. Tester.
Binary phase diagrams from a cubic equation of state.
In *Chemical Engineering at Supercritical Fluid Conditions*, pages 263–321, Ann Arbor Science., 1983.

[98] D. D. Palenchar, R. M. Erickson and Leland T. W.
Prediction of binary critical loci by cubic equations of state.
In *ACS Symposium series 300, Equations of State: Theories and Applications.*, pages 132–155, Am. Chem. Soc., 1986.

[99] R. J. Sadus and C. L. Young.
Application of hard convex body and hard sphere equations of state to the critical properties of binary mixtures.
Fluid Phase Equilibria, 39:89–99, 1988.

[100] D. E. Mainwaring, R. J. Sadus, and C. L. Young.
Prediction of binary and ternary critical properties using Dieter's equation, hard sphere and hard convex equations of state.
Fluid Phase Equilibria, 42:85–103, 1988.

[101] L. E. Baker, A. C. Pierce, and K. D. Luks.
Gibbs energy analysis of phase equilibria.
Soc. Pet. Eng. J., 731–742, 1982.

[102] M. L. Michelsen.
The isothermal flash problem. Part I. Stability.
Fluid Phase Equilibria, 9:1–19, 1982.

[103] M. L. Michelsen.
The isothermal flash problem. Part II. Phase split calculation.
Fluid Phase Equilibria, 9:20–40, 1982.

[104] M. L. Michelsen.
Calculation of critical points and phase boundaries in the critical region.
Fluid Phase Equilibria, 16:57–76, 1984.

[105] M. L. Michelsen.
Some aspects of multiphase calculations.
Fluid Phase Equilibria, 30:15–29, 1986.

[106] R. Dohrn and J. M. Prausnitz.
A simple perturbation term for the carnahan starling equation of state.
Fluid Phase Equilibria, 61:53–69., 1990.

[107] I. Nezbeda and K. Aim.
Perturbed hard-sphere equations of state of real fluids. ii. effective hard-sphere diameters and residual properties.
Fluid Phase Equilibria, 17:1–18, 1984.

[108] A. Bondi.
Physical Properties of Molecular Liquids, Crystals and Glasses.
Wiley, 1968.

[109] J. E. Jr. Dennis, D. M. Gay, and R. E. Welsch.
Algorithm 573. NL2SOL-an adaptive nonlinear least-squares algorithm.
ACM Trans. Math. Soft., 7:369–383., 1981.

[110] J. A. Nelder and R. Mead.
A simplex method for function minimization.
The Computer Journal., 308–313, 1972.

[111] J. C. Nash and M. Walker-Smith.
Nonlinear parameter estimation.
Marcel Dekker, Inc., 1987.

[112] J. V. Sengers and Levelt Sengers J. M. H.
Thermodynamic behaviour of fluids near the critical point.
Ann. Rev. Phys. Chem., 37:1986, 1986.

[113] T. E. Daubert and R. P. Danner.
Physical and Thermodynamic Properties of Pure Chemicals. Vols 1-4.
Hemisphere Publishing Corp., 1989.

[114] R. B. Stewart and R. T. Jacobsen.
Thermodynamic properties of argon from triple point to 1200 k with pressures to 1000 mpa.
J. Phys. Chem. Ref. Data, 18:640–798., 1989.

[115] N. B. Vargaftik.
Tables on the Thermophysical Properties of Liquids and Gases.
Hemisphere Publishing Corporation, 1975.

[116] R. T. Jacobsen, R. B. Stewart, and M. Jahangiri.
Thermodynamic properties of nitrogen from freezing line to 2000 k with pressures to 1000 mpa.
J. Phys. Chem. Ref. Data, 15:735–909., 1986.

[117] B. A. Younglove and J. F. Ely.
Thermophysical properties of fluids.ii. methane, ethane, propane, isobutane and normal butane.
J. Phys. Chem. Ref. Data, 16:577–794., 1987.

[118] S. Angus, B. Armstrong, and K. M. de Rueck.
International Tables of the Fluid State Carbon Dioxide.
Permagon Pub. Co., 1976.

[119] K. E. Starling.
Fluid Thermodynamic Properties for Light Petroleum Systems.
Gulf Publishing Company., 1973.

[120] R. C. Reid, J. M. Prausnitz, and B. E. Poling.
The Properties of Gases and Liquids.
McGraw Hill Book Company, 4th edition, 1987.

[121] R. D. Goodwin.
Carbon monoxide thermophysical properties from 68 to 1000 K at pressures to 100 MPa.
J. Chem. Phys. Ref. Data, 14:849, 1985.

[122] M. Jahangiri, R. T. Jacobsen, and R. B. Stewart.
Thermodynamic properties of ethylene from the freezing line to 450 k at pressures to 260 mpa.
J. Phys. Chem. Ref. Data, 15:593–625., 1986.

[123] R. D. Goodwin.
Benzene thermophysical properties from 279 to 900 K at pressures to 1000 bar.
J. Chem. Phys. Ref. Data, 17:1541, 1988.

[124] W. S. Burnside and A. W. Panton.
The Theory of Equations with an Introduction to the Theory of Binary Algebraic Forms. Vol 1.
Dover Publications, Inc., 1912.

[125] J. R. Young.
Theory and solution of equations of higher order.
Souter and Law, 1843.

[126] H. W. Turnbull.
Theory of Equations.
Oliver and Boyd., 1952.

[127] M.-J. Ko.
Solubility studies on the antibiotic Penicillin V using supercritical fluids.
Master's thesis, University of Tennessee, 1989.

[128] R. W. Miller and R. W. Richard.
Flow Measurement Engineering Handbook.
McGraw Hill Book Company, New York, 1983.

[129] A. Barton.
Handbook of Solubility Parameters and Other Cohesive Parameters.
CRC Press, Inc., 1983.

[130] R. W. Pike.
Optimization for Engineering Systems.
Van Nostrand Reinhold Comapny, 1986.

[131] J. G. Kirkwood and F. P. Buff.
The statistical mechanical theory of solutions. I.
J. Chem. Phys., 19:774–, 1951.

[132] J. P. O'Connell.
Thermodynamic properties of solutions based on correlation functions.
Mol. Phys., 20:27—33., 1971.

[133] A. Ben-Naim.
Water and Aqueous Solutions, Introduction to a Molecular Theory.
Plenum Press, 1974.

[134] H. D. Cochran, L. L. Lee, and D. M. Pfund.
Application of the kirkwood-buff theory of solutions to dilute supercritical mixtures.
Fluid Phase Equilibria., 34:219–234., 1987.

[135] D. M. Pfund, L. L. Lee, and H. D. Cochran.
Application of the kirkwood–buff theory of solutions to dilute supercritical mixtures. ii. the excluded volume and local composition models.
Fluid Phase Equilibria., 39:161–192., 1988.

[136] H. D. Cochran, D. M. Pfund, and L. L. Lee.
Theoretical models of thermodynamic properties of supercritical solutions.
Sep. Sci. Tech., 23:2031–2047., 1988.

[137] J. K. Lee and J. A. Barker.
Surface structure and surface tension: perturbation theory and monte carlo calculation.
J. Chem. Phys., 60:1976–1980, 1974.

[138] A. Z. Panagiotopoulos, N. Quirke, M. Stapleton, and D. J. Tildesley.
Phase equilibria by simulation in the gibbs ensemble: alternative derivation, generalization and application to mixture and membrane equilibria.
Mol. Phys., 63:527–545, 1988.

[139] J. J. De Pablo and J. M. Prausnitz.
Phase equilibria for fluid mixtures from the monte-carlo simulation.
Fluid Phase Equilibria, 53:177–189, 1989.

[140] D. J. Adams.
Chemical potential of hard-sphere fluids by monte carlo methods.
Mol. Phys., 28:1241–1252., 1974.

[141] L. A. Rowley, D. Nicholson, and N. G. Parsonage.
Monte carlo grand canonical ensemble calculation in a gas-liquid transition region for 12-6 argon.
J. Comput. Phys., 17:401–414., 1975.

[142] D. J. Adams.
Grand canonical ensemble monte carlo for a lennard-jones fluid.
Mol. Phys., 29:307–311, 1975.

[143] L. A. Rowley, D. Nicholson, and N. G. Parsonage.
Grand ensemble monte carlo studies of physical adsorption: i. results for multilayer adsoption of 12-6 argon in the field of a plane homogeneous solid.
Mol. Phys., 31:365–387., 1976.

[144] L. A. Rowley, D. Nicholson, and N. G. Parsonage.
Grand ensemble monte carlo studies of physical adsorption: ii. the structure of the adsorbate. critique of theories of multilayer adsorption for the 12-6 argon on a plane homogeneous solid.
Mol. Phys., 31:389–407, 1976.

[145] D. J. Adams.
Calculating the low temperature vapour line by monte carlo.
Mol. Phys., 32:647–657., 1976.

[146] D. J. Adams.
Calculating the high temperature vapour line by monte carlo.
Mol. Phys., 37:211–221., 1979.

[147] M. Mezei.
A cavity based (t, v, μ) monte carlo method for the computer simulation of fluids.
Mol. Phys., 40:901–906., 1980.

[148] J. P. Valleau and K. L. Cohen.
Primitive model electrolytes. i. grand canonical monte carlo computations.
J. Chem. Phys., 72:5935–5941, 1980.

[149] J. Yao, R. A. Greenkorn, and K. C. Chao.
Monte carlo simulation of the grand canonical ensemble.
Mol. Phys., 46:587–594, 1982.

[150] M. Noucer and K. S. Shing.
Grand canonical monte carlo simulation for the solubility calculation in supercritical extraction.
Mol. Simul., 2:55–68, 1989.

[151] M. P. Allen and D. J. Tildesley.
Computer Simulation of Liquids.
Oxford University Press, Oxford, 1987.

[152] J. J. Nicholas, K. E. Gubbins, W. B. Street, and D. J. Tildesley.
Equation of state for the lennard-jones fluid.
Mol. Phys., 37:1429–1454, 1979.

[153] P. G. Debendetti and I. B. Petsche.
Solute-solvent interactions in infinitely dilute supercritical mixtures: A molecular dynamic investigation.
J. Chem. Phys., 91:7075–, 1989.

APPENDICES

APPENDIX A

Theory of Quartic Equations

Several authors [125], [124], [126] have discussed and reviewed the properties of a quartic equation. Ferrari and Descartes independently proposed techniques to solve the quartic equation analytically. Both the techniques lead to the same results. The analytical solution of the quartic equation is described below. Consider the quartic equation

$$lx^4 + 4mx^3 + 6nx^2 + 4ox + p = 0 \tag{A.1}$$

Equation (A.1) can be transformed using the substitution $z = lx + b$ to

$$z^4 + 6Hz^2 + 4Gz + 2lI - 3H^2 = 0 \tag{A.2}$$

where

$$H = ln - m^2 \tag{A.3}$$

$$I = lp - 4mo + 3n^2 \tag{A.4}$$

$$G = l^2o - 3lmn + 2m^3 \tag{A.5}$$

Equation (A.2) can be further reduced to the "reducing cubic" of the quartic equation, which is

$$4l^3\theta^3 - Il\theta + J = 0 \tag{A.6}$$

where

$$J = lnp + 2mno - lo^2 - pm^2 - n^3 \tag{A.7}$$

Let θ_1, θ_2 , and θ_3 be the three roots of Equation (A.6). The solution for z is given by

$$z_1 = lx_1 + m = +\sqrt{m^2 - ln + l^2\theta_1} + \sqrt{m^2 - ln + l^2\theta_2} - \frac{G}{2\sqrt{m^2 - ln + l^2\theta_1}\sqrt{m^2 - ln + l^2\theta_2}} \tag{A.8}$$

$$z_2 = lx_2 + m = -\sqrt{m^2 - ln + l^2\theta_1} + \sqrt{m^2 - ln + l^2\theta_2} + \frac{G}{2\sqrt{m^2 - ln + l^2\theta_1}\sqrt{m^2 - ln + l^2\theta_2}} \tag{A.9}$$

$$z_3 = lx_3 + m = +\sqrt{m^2 - ln + l^2\theta_1} - \sqrt{m^2 - ln + l^2\theta_2} + \frac{G}{2\sqrt{m^2 - ln + l^2\theta_1}\sqrt{m^2 - ln + l^2\theta_2}} \tag{A.10}$$

$$z_4 = lx_4 + m = -\sqrt{m^2 - ln + l^2\theta_1} - \sqrt{m^2 - ln + l^2\theta_2} - \frac{G}{2\sqrt{m^2 - ln + l^2\theta_1}\sqrt{m^2 - ln + l^2\theta_2}} \tag{A.11}$$

where

θ_1 and θ_2 are any two roots of "reducing cubic" Equation (A.6),

z_1, z_2, z_3, and z_4 are the four roots of Equation (A.2), and

x_1, x_2, x_3, and x_4 are the four desired roots of Equation (A.1).

The roots of the "reducing cubic" can be easily found analytically. The roots of the quartic Equation (A.1) satisfy the following relationships also :

$$x_1 + x_2 + x_3 + x_4 = -\frac{4m}{l} \tag{A.12}$$

$$x_1x_2x_3x_4 = \frac{p}{l} \tag{A.13}$$

The nature of the roots obtained on solving depends on the discriminant of the quartic equation. The discriminant of a quartic equation is given by

$$\Delta = I^3 - 27J^2 \tag{A.14}$$

Depending on whether the discriminant is positive, negative, or zero, the following conclusions regarding the nature of the roots may be drawn :

1. When $\Delta = 0$, Equation (A.1) has equal roots. Four distinct cases may lead to this :

   (a) when only two roots are equal, in which case $I \neq 0$ and $J \neq 0$.

   (b) when three roots are equal, in which case $I = 0$, and $J = 0$, separately.

   (c) when two pairs of roots are equal, in which case $G = 0$, and $l^2 I - 12H^2 = 0$.

   (d) when all the roots are equal, in which case $I = 0$, $J = 0$, and $H = 0$ separately.

2. when $\Delta < 0$, there are two real roots and two complex roots.

3. when $\Delta > 0$, the roots are either all real or all imaginary.

At the critical point of the fluid the quartic equation of state should have at least three roots which are equal. In this case condition 1(b) must be satisfied, i.e. I and J must be equal to zero independently. This provides an alternative set of equations, which could be used to correlate the equation of state parameters a, c, d, and e to the critical properties of the fluid. Unfortunately, setting I and J equal to zero leads to a set of equations which are too complicated to be solved easily. A simple procedure to determining the relationship between the equation of state parameters a, c, d, e and the

critical properties of the fluid is described below. Assuming that three roots in volume are equal at the critical point, the quartic equation can be written as

$$(V - V_c)^3 \left(V - \hat{V}\right) = 0 \tag{A.15}$$

$$\left(V^3 - 3V^2V_c + 3VV_c^2 - V_c^3\right)\left(V - \hat{V}\right) = 0 \tag{A.16}$$

$$V^4 + V^3\left(-3V_c - \hat{V}\right) + V^2\left(3V_c^2 + 3V_c\hat{V}\right) + V\left(-V_c^3 - 3V_c^2\hat{V}\right) + V_c^3\hat{V} = 0 \tag{A.17}$$

Comparison of the coefficients of (A.17) with the quartic equation of state (3.10) gives the following equations :

$$q_3 = \left(-3V_c - \hat{V}\right) \tag{A.18}$$

$$q_2 = \left(3V_c^2 + 3V_c\hat{V}\right) \tag{A.19}$$

$$q_1 = \left(-V_c^3 - 3V_c^2\hat{V}\right) \tag{A.20}$$

$$q_0 = V_c^3\hat{V} \tag{A.21}$$

Also, equation A.12 gives

$$3V_c + \hat{V} = -q_3 \tag{A.22}$$

Using Equation (A.22) to eliminate $\hat{V}$ from Equations (A.18) through (A.21) and solving the resulting equations simultaneously gives the same relationships between d, a, e, and c and the critical properties of the fluid as obtained previously (Equations (3.15), (3.16) and (3.17)). Thus, it is not necessary to know the fourth root of the quartic EOS at the critical point beforehand. This procedure is simpler and leads to considerable time savings when compared with using Equations (2.5) and (2.6) on the quartic EOS (3.9).

APPENDIX B

Detailed description of the pure component data used in regressions and their sources

Table B.1: Detailed description of the pure component data used in regressions and their sources

Fluid	Property	Temperature Range (K)	Pressure Range (MPa)	Number of Data points
Argon	P_s	84 – 140		29
	ρ_{sv}	84 – 140		29
	ρ_l	84 – 140		29
	ρ_g	180 – 1000	0 – 100	344
	B_{vir}	160 – 740		70
	H_r	400 – 1000		125
Krypton	P_s	116 – 204		44
	ρ_{sv}	116 – 204		44
	ρ_l	116 – 204		44
	ρ_g	250 – 1000	0 – 100	161
Xenon	P_s	164 – 280		30
	ρ_{sv}	164 – 280		30
	ρ_l	164 – 280		30
	ρ_g	290 – 800	0 – 100	138
	B_{vir}	300 – 1000		71

Table B.1 (cont'd)

Fluid	Property	Temperature Range (K)	Pressure Range (MPa)	Number of Data points
Oxygen	P_s	56 – 152		49
	ρ_{sv}	56 – 152		49
	ρ_l	56 – 152		49
	ρ_g	180 – 1000	0 – 100	225
	B_{vir}	155 – 1000		91
	H_r	400 – 1000		109
Nitrogen	P_s	64 – 117		54
	ρ_{sv}	64 – 117		54
	ρ_l	64 – 117		54
	ρ_g	150 – 1000	0 – 100	330
	B_{vir}	140 – 720		69
	H_r	200 – 1000		213
Methane	P_s	100 – 180		24
	ρ_{sv}	100 – 180		24
	ρ_l	100 – 180		24
	ρ_g	200 – 600	0 – 100	290
	B_{vir}	200 – 820		58
	H_r	200 – 600		180

Table B.1 (cont'd)

Fluid	Property	Temperature Range (K)	Pressure Range (MPa)	Number of Data points
Ethane	P_s	140 – 350		18
	ρ_{sv}	140 – 350		18
	ρ_l	140 – 350		18
	ρ_g	380 – 600	0 – 100	400
	B_{vir}	380 – 700		61
	H_r	400 – 600		123
Propane	P_s	170 – 410		22
	ρ_{sv}	170 – 410		22
	ρ_l	170 – 410		22
	ρ_g	440 – 600	0 – 70	288
	B_{vir}	430 – 700		51
	H_r	500 – 600		95
n-Butane	P_s	130 – 300		47
	ρ_{sv}	130 – 300		47
	ρ_l	130 – 300		47
	ρ_g	320 – 600	0 – 70	251
	B_{vir}	310 – 600		49
	H_r	400 – 600		92

Table B.1 (cont'd)

Fluid	Property	Temperature Range (K)	Pressure Range (MPa)	Number of Data points
Carbon	P_s	220 – 290		36
Dioxide	ρ_{sv}	220 – 290		36
	ρ_l	220 – 290		36
	ρ_g	320 – 1000	0 – 100	336
	B_{vir}	310 – 1000		66
	H_r	320 – 1000		267
n-Pentane	P_s	299 – 455		29
	ρ_{sv}	299 – 455		29
	ρ_l	299 – 455		69
n-Hexane	P_s	266 – 494		43
	ρ_{sv}	266 – 494		43
	ρ_l	266 – 494		43
n-Octane	P_s	277 – 533		27
	ρ_{sv}	277 – 533		27
	ρ_l	277 – 533		27
n-Nonane	ρ_l	303 – 573	0 – 20	42
	P_s	253 – 503		26
n-Decane	ρ_l	313 – 393	0 – 10	48
	P_s	263 – 523		27
n-Undecane	ρ_l	303 – 573	0 – 100	42

APPENDIX C

Equation of State Constants for Quartic B

Table C.1: Equation of state constants obtained by regressions (Quartic B)

Parameter		Parameter	
a_{r0}	1.89174	X_{21}	0.13384
a_{r1}	0.10750	X_{22}	0.93831
a_{r2}	0.36104	X_{31}	−0.27418
c_{r0}	3.83684	X_{32}	2.34329
c_{r1}	−1.52948	X_{41}	0.06054
c_{r2}	2.86499	X_{42}	−3.83132
e_{r0}	0.95260	X_{51}	0.12630
e_{r1}	−0.96445	X_{52}	0.53155
e_{r2}	2.23649	X_{61}	0.02886
d^*	0.0000	X_{62}	−0.04436
β_r^*	0.175	X_{71}	−0.54554
k_0^*	1.2865	X_{72}	−0.63484
k_1^*	2.8225		

* These quantities were kept fixed during regressions.

The equation of state is completely specified by the set of Equations (3.9), (3.19), (3.20), (3.22), (3.23), (3.18) and equations (3.32) through (3.39).

APPENDIX D

Comparison of Average Absolute Deviations of Various Physical and Thermodynamic Properties Calculated using Different Equations of State

Table D.1: AAD's calculated using different equations of state

Fluid	Property	Quartic A AAD (%)	Quartic C AAD (%)	Peng-Robinson AAD (%)	Kubic AAD (%)	No. of data pts
Argon	P_s	0.14	0.34	0.51	1.49	29
	ρ_{sv}	1.89	1.55	1.14	1.75	29
	ρ_l	4.11	4.39	9.68	3.78	29
	ρ_g	0.39	0.4	1.55	1.3	344
	B_{vir}	6.97	6.78	55.84	52.66	56
	H_r	7.06	7.11	53.91	32.41	125
Krypton	P_s	0.81	0.5	0.57	1.33	46
	ρ_{sv}	1	1.43	2.48	1.61	46
	ρ_l	4.03	3.72	8.55	5.05	46
	ρ_g	0.64	0.62	2.26	1.8	161
Xenon	P_s	1.54	0.73	0.39	1.1	30
	ρ_{sv}	0.84	1.16	1.7	0.97	30
	ρ_l	3.53	3.17	7.45	4.34	30
	ρ_g	1.45	1.12	2.7	2.7	138
	B_{vir}	4.53	4.84	139		

Table D.1 (cont'd)

Fluid	Property	Quartic A AAD (%)	Quartic C AAD (%)	Peng-Robinson AAD (%)	Kubic AAD (%)	No. of data pts
Oxygen	P_s	1.38	1.33	1.39	11.66	49
	ρ_{sv}	1.27	1.3	2.19	11.7	49
	ρ_l	6.05	5.99	10.74	6.18	49
	ρ_g	0.58	0.58	2.14	1.23	225
	B_{vir}	4.64	4.63	30.8	14.36	91
	H_v	4.4	4.39	32.51	15.87	109
Nitrogen	P_s	0.59	1.72	0.64	1.23	54
	ρ_{sv}	1.42	1.14	1.14	1.26	54
	ρ_l	4.39	5.42	10.41	3.43	54
	ρ_g	0.64	0.72	1.92	1.35	330
	B_{vir}	5.35	5.29	30.07	10.51	69
	H_v	4.85	4.97	39.87	23.54	213
Methane	P_s	2.49	2.17	1.44	0.45	24
	ρ_{sv}	2.41	2.18	3.46	1.25	24
	ρ_l	4.54	4.32	9.06	5.43	24
	ρ_g	0.63	0.62	1.88	1.59	290
	B_{vir}	3.4	3.35	49.47	36.07	58
	H_v	4.17	4.29	17.28	6.52	180

Table D.1 (cont'd)

Fluid	Property	Quartic A AAD (%)	Quartic C AAD (%)	Peng-Robinson AAD (%)	Kubic AAD (%)	No. of data pts
Ethane	P_s	1.35	2.35	1.34	7.83	18
	ρ_{sv}	2.34	2.34	1.52	8.09	18
	ρ_l	3.47	3.97	6.74	6.04	18
	ρ_g	0.4	0.44	1.15	1.02	400
	B_{vir}	6.28	6.44	14.38	16.11	61
	H_v	2.83	3.02	8.17	4.07	123
Propane	P_s	1.28	2.42	2.67	31.34	23
	ρ_{sv}	1.95	2.17	3.4	31.32	23
	ρ_l	3.44	4.06	5.43	9	23
	ρ_g	0.86	0.98	2.07	2.73	288
	B_{vir}	5.47	5.71	12.76	18.09	41
	H_v	2.71	3.02	6.84	6.08	95
n-Butane	P_s	1.49	1.62	1.98	987	47
	ρ_{sv}	1.31	1.31	2.34	1088	47
	ρ_l	3.72	3.72	4.28	17.59	47
	ρ_g	0.63	0.63	1.36	1.52	251
	B_{vir}	9.1	9.1	13.51	17.64	39
	H_v	3.87	3.88	6.07	6.55	92

Table D.1 (cont'd)

Fluid	Property	Quartic A AAD (%)	Quartic C AAD (%)	Peng-Robinson AAD (%)	Kubic AAD (%)	No. of data pts
Carbon	P_s	0.44	1.01	0.54	1.5	36
Dioxide	ρ_{sv}	3.27	2.54	1.28	2.21	36
	ρ_l	1.81	1.72	2.98	3.99	36
	ρ_g	0.43	0.46	0.85	1.46	336
	B_{vir}	5.49	4.77	17.64	178	66
	H_v	2.81	2.9	10.18	8.33	267
n-Pentane	P_s	4.53	1.95	0.95	2.07	29
	ρ_{sv}	2.77	1.61	1.14	1.41	29
	ρ_l	4.75	3.05	3.56	8.404	69
n-Hexane	P_s	1.52	1.16	1.12	1.44	43
	ρ_{sv}	1.61	2.35	1.83	1.88	43
	ρ_l	3.06	3.02	2.51	4.2	43
n-Octane	P_s	1.5	1.16	2.09	1.18	27
	ρ_{sv}	3.32	2.35	2.02	1.42	27
	ρ_l	5.61	3.02	5.59	4.28	27
n-Nonane	ρ_l	2.07	1.96	2.94	41.82	42
n-Decane	ρ_l	1.3	0.57	5.71	27.73	48
n-Undecane	ρ_l	2.39	1.77	5.27	39.29	42

APPENDIX E

Modelling of Solubility of Penicillin V in Supercritical CO_2

The β-lactam antibiotics represent the largest group of commercially available antibiotics. The penicillins are an important class of the β-lactam antibiotics. Of the large number of penicillins known, Penicillin V (phenoxymethyl penicillin) is used most widely. Penicillins are high molecular weight substances characterized by high polarity, low volatility, and thermal lability. The classical separation and purification process for antibiotics has been a series of solvent extractions, purification steps and finally product crystallization. Some of the purification techniques used are ion exchange, carbon adsorption and chromatography. These separation and purification processes can entail up to 60 processing steps and account for as much as 80 % of the expense of an antibiotic production operation. Supercritical fluid extraction could reduce the cost of the antibiotic separation and purification process. This could be accomplished by extracting the antibiotic from the fermentation broth or by purifying the antibiotic once it has been precipitated. The solubility of Penicillin V in supercritical CO_2 has been determined [127] experimentally. The pressures ranged from 7.987 MPa to 28.02 MPa and the temperatures were 314.85 K, 324.85 K, and 334.85 K. The experimental solubility data was corrected for the wet gas flow meter correction [128]. The corrected solubility of Penicillin V is shown in Table E.1.

The quartic equation of state developed in this research was not extended and tested for mixtures. Hence, it could not be used for modelling the solubility of Penicillin V. The

Table E.1: Solubility of Penicillin V in CO_2

Temperature (K)	Pressure (MPa)	Solubility (mole fraction)
314.85	8.076	$6.23E-05$
	9.014	$9.70E-05$
	11.468	$1.77E-04$
	14.397	$2.13E-04$
	17.299	$2.68E-04$
	20.773	$3.28E-04$
	24.254	$3.73E-04$
	28.045	$4.32E-04$
324.85	7.987	$5.87E-05$
	9.124	$9.94E-05$
	11.578	$2.03E-04$
	14.349	$2.45E-04$
	17.072	$3.08E-04$
	20.814	$4.01E-04$
	24.144	$4.37E-04$
	27.962	$5.01E-04$
334.85	8.014	$5.45E-05$
	9.172	$9.23E-05$
	11.743	$2.15E-04$
	14.397	$3.12E-04$
	17.141	$3.91E-04$
	20.780	$4.33E-04$
	24.068	$5.20E-04$
	28.017	$5.76E-04$

solubility of Penicillin V in supercritical CO_2 was correlated using the Peng-Robinson equation of state and the Kirkwood-Buff theory.

E.1 Peng-Robinson Equation of State

At equilibrium, the fugacities of the individual species in the two phases have to be the same. For a solid solute in equilibrium with a fluid (supercritical solvent), the fugacity of the solute (2) in the solid phase has to be same as the fugacity of the solute in the fluid phase. Similarly, the fugacity of the solvent (1) has to be the same in the supercritical fluid phase and the solid phase.

Denoting the solid phase by the superscript s and the fluid phase by superscript scf, we can write

$$f_2^s = f_2^{scf} \tag{E.1}$$

where

f_2^s is the fugacity of the solute in the solid phase,

f_2^{scf} is the fugacity of the solute in the fluid phase.

It is assumed that carbon dioxide has no solubility in the solid phase. Thus, the solid phase can be treated as a pure solid and its fugacity is given by

$$f_2^s = \phi_2^{sat} P_2^{sat} \exp\left(\int_{P_2^{sat}}^{P} \frac{v_2^{solid}}{RT} dP\right) \tag{E.2}$$

where

f_2^s is the fugacity coefficient of the saturated vapor,

$P_2^{sat}$is the saturated vapor pressure of the solid,

v_2^{solid} is the molar volume of the solid solute,

$P$is the pressure of the system,

$T$is the temperature of the system.

The fugacity of the solid in the fluid phase is given by

$$f_2^{scf} = y_2 \phi_2^{scf} P \tag{E.3}$$

where

y_2 is the solubility of the solute in the fluid phase,

ϕ_2^{scf} is the fugacity of the solute in the fluid phase.

The fugacity of the solid in the fluid phase can be calculated using an equation of state. The solubility of the solid can then be calculated by using Equations (E.1) and (E.2), and (E.3), and is given by :

$$y_2 = \frac{\phi_2^{sat} P_2^{sat}}{P \phi_2^{scf}} \exp\left(\int_{P_2^{sat}}^{P} \frac{v_2^{solid}}{RT} dP\right) \tag{E.4}$$

The Peng-Robinson equation of state[94] was used to model the solubility of penicillin V in CO_2. The fugacity of the solute in the fluid phase can be calculated using the Peng-Robinson equation of state. To use the Peng-Robinson equation of state the critical properties (T_c and P_c) and the acentric factor (ω) of the solute and the solvent must be known. As none of these properties have been reported for Penicillin V, they were estimated using known group contribution techniques. The solid molar volume was also

Table E.2: Estimated physical properties of Penicillin V

Physical property	Estimated value	Technique of estimation
T_c	921.7 K	Fedor's method [120]
P_c	1.72 MPa	Ambrose's method [120]
T_b	733.8 K	Ambrose's method [120]
ω	1.1676	Lee-Kessler Correlation [120]
V_s	231.7 $cm^3/gmol$	Group-contribution method [129]

Table E.3: Estimated vapor pressure of Penicillin V

Temperature (K)	P_{sat} (MPa)
314.85	$5.53E-11$
324.85	$1.50E-10$
334.85	$3.83E-10$

calculated using a group contribution technique and was assumed to be constant over the temperature range of interest. The vapor pressures of Penicillin V were estimated using the modified Clausius-Clapeyron equation. Table E.2 and E.3 give the estimated physical properties of Penicillin V. The fugacity coefficient ϕ_2^{scf}, derived from the Peng-Robinson equation of state, for the component 2 of a binary mixture is given by

$$\ln\left(\phi_2^{scf}\right) = \frac{b_2}{b_m}(Z_m - 1) - \ln(Z_m - B) -$$

$$\left(\frac{A_m}{2\sqrt{2}B_m}\right)\left[\left(\frac{2\sum_{j=1}^{2} x_j a_{2j}}{a_m}\right)-\frac{b_2}{b_m}\right]\ln\left(\frac{Z_m+(2+\sqrt{2})B_m}{Z_m-(2-\sqrt{2})B_m}\right) \quad \text{(E.5)}$$

where

$$A_m = \frac{a_m P}{R^2 T^2}$$

$$B_m = \frac{b_m P}{RT}$$

$Z_m = \frac{v_m P}{RT}$ is the compressibility of the mixture,

$$b_m = x_1 b_1 + x_2 b_2$$

$$a_m = \sum_{j}^{2}\sum_{i}^{2} x_i x_j a_{ij}$$

$$a_{ij} = (1-k_{ij})\sqrt{a_i a_j}$$

The compressibility Z_m can be calculated by solving the Peng-Robinson equation of state using the mixture parameters a_m and b_m. The binary interaction parameter k_{ij} is obtained by regression of the experimental solubility data to the solubility calculated using Equations (E.4) and E.5. The average absolute deviation (AAD) for the mol fraction y_2 is minimized in the regressions.

$$AAD = \frac{1}{N}\sum_{i}^{N}\left|\frac{y_i^{exp}-y_i^{cal}}{y_i^{exp}}\right| \quad \text{(E.6)}$$

where

$N$is the number of data points,

y_i^{cal} is the calculated solubility of the solute as mole fraction,

y_i^{exp} is the experimentally solubility of the solute as mole fraction.

Table E.4: Regressed binary interaction coefficients for the Peng-Robinson equation of state for the system Carbon Dioxide (1) - Penicillin V (2)

Temperature (K)	k_{12}	SSE[a]	AAD (%)
314.85	0.173	$3.06E-8$	37.85
324.85	0.160	$5.22E-8$	42.46
334.85	0.147	$1.42E-7$	54.38

[a]

$$SSE = \sum \left[\left(y_i^{exp} - y_i^{calc} \right)^2 \right]$$

Thus, the independent variables are pressure P and temperature T and the dependent variable is the mole fraction y_2.

The objective function E.6 is a convex function. Hence, a golden section search method [130] was used to find k_{ij}. As k_{ij} is a function of temperature, all the three isotherms were regressed individually. The results of regression are shown in table E.4. Figure E.1 shows the plot of the experimental data and the solubility calculated using the Peng-Robinson equation of state.

E.2 Kirkwood-Buff theory

The Kirkwood-Buff theory [131] is a general statistical mechanical theory of solutions, applicable to solutions with all types of intermolecular interactions. Kirkwood and Buff used the theory of the grand canonical ensemble to relate the fluctuations in concentrations of the components to the derivatives of their chemical potentials. They also related these concentration fluctuations to the integrals of the radial distribution

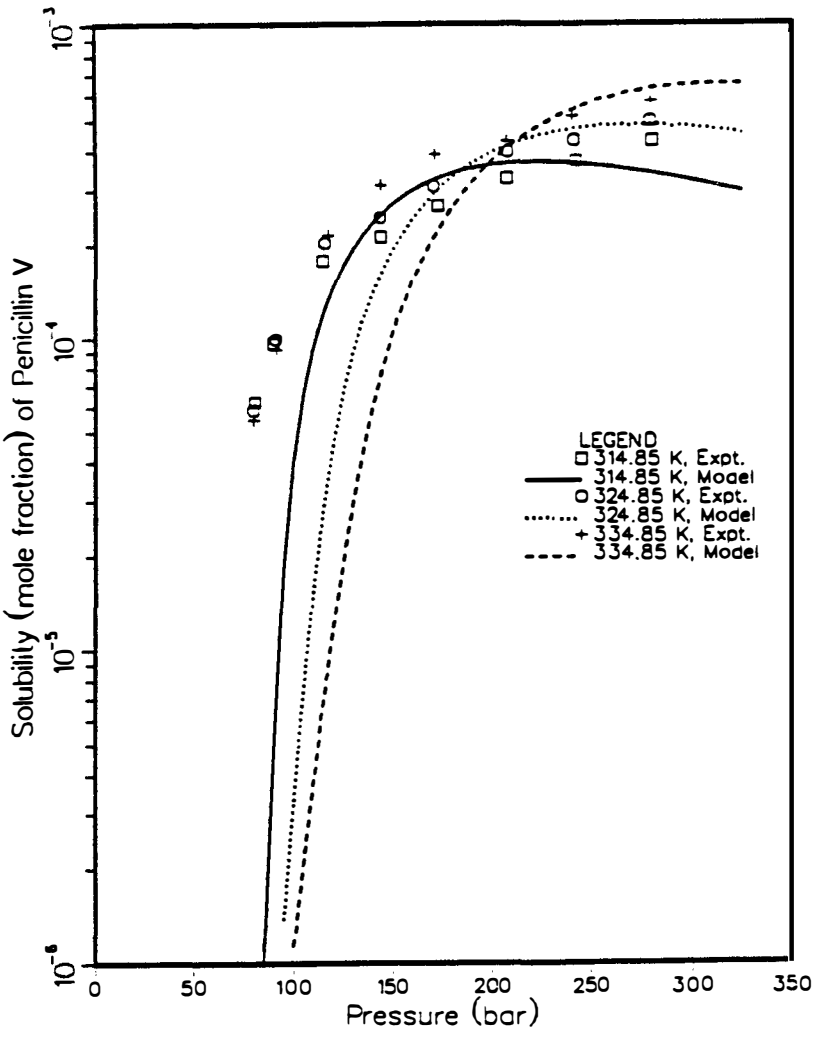

Figure E.1: Peng-Robinson calculations for the solubility of Penicillin V in CO_2

functions of the different types of molecular pairs present in the solution. The derivatives of the chemical potential with respect to the concentrations were used to obtain the partial molar volumes. The Kirkwood-Buff theory is valid in the bulk phases as well as near the critical point. This theory has been applied by O'Connell [132] to dilute solutions. Ben-Naim [133] gives a simplified and detailed explanation of the theory and its applications. The Kirkwood fluctuation integral G_{12} given by

$$G_{12} = \int_0^\infty (g_{12} - 1)\ 4\pi r^2 dr \tag{E.7}$$

where

g_{12} is the spatial pair correlation function for the interaction between the species 1 and 2,

r is the spatial separation between 1 and 2.

The quantity $\rho_1 G_{12}$ represents the average excess number of particles 1 around b relative to the bulk phase. Cochran et al.[134, 135, 136] have shown that at infinite dilution the isothermal variation in the number density of a solute 1, ρ_1, with pressure, P, in a solvent 2 at equilibrium with a pure solid phase is given by

$$\left(\frac{kT}{\rho_1}\right)_T d\rho_1 = \left(G_{12}^0 + \bar{v}_1\right) dP \tag{E.8}$$

where

kT is the Boltzmann's constant times the temperature,

G_{12}^0 is the solute-solvent Kirkwood fluctuation integral at infinite dilution,

$\bar{v}_1$ is the partial molecular volume of the solute 1,

ρ_1 is the number density of the solute.

They further showed that the solubility of the solid solute near infinite dilution can be expressed by

$$\left(\frac{\partial \ln y_1}{\partial \rho_2}\right)_T = \frac{(G_{12}^0 + \bar{v}_1)}{(1 + \rho_2^0 G_{22}^0)} - \frac{1}{\rho_2^0} \tag{E.9}$$

where

y_1 is the solute mole fraction in the fluid phase,

ρ_2^0 is the number density of the solvent,

G_{22}^0 is the solvent-solvent Kirkwood fluctuation integral at infinite dilution.

G_{22}^0 can be obtained from an accurate equation of state for the pure solvent.

$$G_{22}^0 = \frac{(kT\rho_2^0 \chi_2^0 - 1)}{\rho_2^0} \tag{E.10}$$

where

χ_2^0 is the isothermal compressibility of the pure solvent.

They used a local composition model to derived the expression for the solute solvent fluctuation integral as

$$G_{12}^0 = aG_{22}^0 + V_{12} \exp\left(b_0 + \frac{b_1}{T}\right) - V_{12} \tag{E.11}$$

where b_0, b_1 and $V12$ are adjustable parameters and a is given by

$$a = \frac{V_{12}}{V_{c2}} \sqrt{\frac{T_{c1}}{T_{c2}}} \tag{E.12}$$

where

V_{c2} is the critical molecular volume of the solvent,

T_{c2} is the critical temperature of the solvent, and

T_{c1} is the critical temperature of the solute.

Substituting the Equations (E.11) and (E.10) into (E.9) and integrating it, gives the resulting solubility expression for the solute in the fluid phase.

$$\begin{aligned} \ln(y_1) &= \ln\left(\frac{P_1^{sat}}{P}\right) + \ln\left(Z_2^0\right) - a\ln\left(\frac{f_2^0}{\rho_2^0 kT}\right) \\ &\quad + \left[v_1^{solid} + V_{12}\exp\left(b_0 + \frac{b_1}{T} - V_{12}\right)\right]\left(\frac{P - P_1^{sat}}{kT}\right) \end{aligned} \tag{E.13}$$

where

Z_2^0 is the compressibility of the pure solvent,

f_2^0 is the fugacity of the pure solvent, and

P_1^{sat} is the saturated vapor pressure of the solute at the temperature T.

The advantages of using the Kirkwood-Buff model are that it only needs the vapor pressure, the critical temperature and the solid density to correlate the solubility. The adjustable parameters b_0, b_1 and V_{12} are obtained by regression of the solubility data to the solubility calculated using Equation (E.13). The sum of squares of the error (SSE) in the experimental and calculated mole fraction y_1. is minimized in the regressions.

$$SSE = \sum_i^N \left[\left(y_i^{exp} - y_i^{calc}\right)^2\right] \tag{E.14}$$

Table E.5: Regressed parameters for the Kirkwood Buff model for the system Carbon dioxide (1) - Penicillin V (2)

V_{12} cm^3/mol	b_0	b_1 (Kelvin)	SSE	AAD (%)
497.7	4.06	-1264	$2.26E-7$	44.35

where

N is the number of data points,

y_i^{cal} is the calculated solubility of the solute as mole fraction,

y_i^{exp} is the experimentally solubility of the solute as mole fraction.

The independent variables are the pressure P and the temperature T. As the objective function (E.14) is not a smooth function of the parameters being estimated. Hence, a nonlinear least squares [109] method was used to find b_0, b_1 and V_{12}. As the temperature dependence is built within the model, all the three isotherms were regressed simultaneously. The results of regression are shown in Table E.5. Figure E.2 shows the plot of the experimental data along with the solubility calculated using the Kirkwood-Buff local composition model.

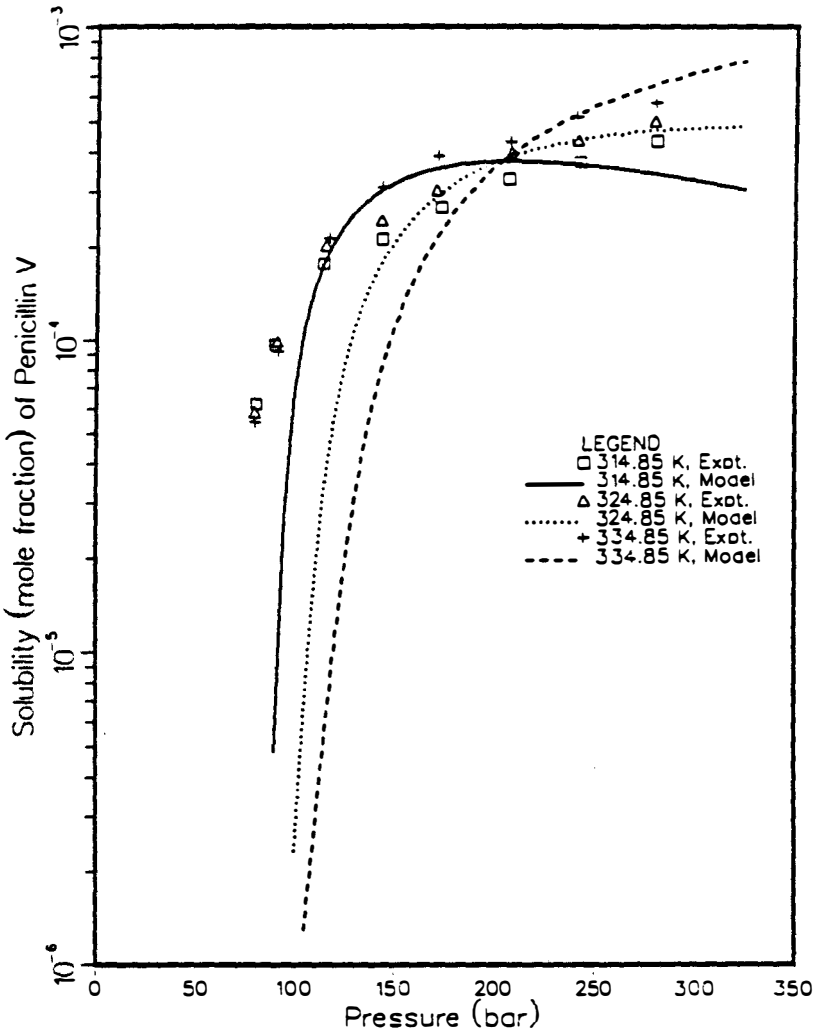

Figure E.2: Kirkwood-Buff calculations for the solubility of Penicillin V in CO_2

APPENDIX F

Grand Canonical Monte Carlo Simulations

While many problems in statistical mechanics cannot be solved exactly, introducing some approximations may lead to an approximate solutions. Computer simulations can essentially provide exact results for problems in statistical mechanics which can only be solved approximately using analytical techniques. Molecular simulation is the study of the behavior of an assembly of molecules using a computer. Monte Carlo and molecular dynamics are the most widely used techniques in molecular simulations. Molecular simulations have been widely used to predict the thermodynamic properties of fluids. Monte Carlo simulations make extensive use of random number generators, and are easier to program on the computer. Molecular dynamics simulations solve the classical equations of motion for a set of molecules, but are difficult to program on the computer. Monte Carlo simulations are computationally more intensive than Molecular dynamic simulations.

A majority of the reported Monte Carlo simulations have been restricted to either the canonical (constant N, V, T) ensemble or the isothermal-isobaric (constant N, P, T) ensemble. Simulations in the canonical (NVT) ensemble are the easiest to program; however isothermal- isobaric (NPT) ensemble simulations describe more realistic thermodynamic systems. Neither of the techniques can be used to determine the Gibbs and Helmholtz free energy of the system of molecules. Simulations of two-phase coexistence [137] and phase transitions cannot be performed satisfactorily in the NVT and NPT

ensembles. Recently simulations in the Gibbs ensemble [138], [139], have been reported.

The Gibbs ensemble simulation method provides a powerful technique to determine the two- phase coexistence curves of fluids and fluid mixtures. The grand canonical Monte Carlo simulations have the advantage of directly providing the thermodynamic properties, such as the Helmholtz free energy of the fluid. The Helmholtz free energy can only be obtained by integrations in an NVT or NPT ensemble simulation. Based on the observed fluctuations in the energy, pressure, and the number of particles in the grand canonical ensemble, a number of thermodynamic properties can be calculated. These include, isothermal compressibility, the Kirkwood fluctuation integrals, and partial molar volumes (in the case of mixtures).

Adams [140] reported the first simulations in the grand canonical ensemble. He used a hard sphere fluid for his simulations. This technique was extended by Rowley [141] and independently, by Adams [142] to a Lennard-Jones fluid. Rowley, Nicholson and Parsonage [143, 144] further extended this technique to study the adsorption of argon on a solid surface. To determine the thermodynamic properties of the two-phase coexistence curve of a Lennard-Jones fluid, Adams [145] used simulations in the grand canonical ensemble and canonical ensemble. The critical temperature of a pure Lennard- Jones fluid was estimated using these simulations [146]. Mezei [147] reported a cavity-based grand canonical Monte Carlo technique that allowed the simulations to be extended to higher densities. Using grand canonical Monte Carlo simulations, Valleau et al. [148] studied the behavior of electrolytes in aqueous solutions. Yao [149] reported grand canonical Monte Carlo simulations on pure Lennard-Jones fluids. Recently, grand canonical ensemble simulations have been performed for mixtures in the near vapor-liquid critical region [150] . The solvent is highly compressible in supercritical fluid solutions close to

the critical point of the solvent. This can also be characterized by large density fluctuations in the SCF solution. Only simulations in the grand canonical ensemble would permit such large fluctuations in density. Hence GCMC simulations of supercritical fluid solutions might provide considerable insight into the clustering phenomena.

F.1 Monte Carlo Simulations

Computer simulations provide a direct link between the microscopic characteristics of a system (the interactions between atoms, molecular geometry, etc) and the macroscopic properties of interest (transport properties, PVT and thermodynamic properties, etc). Computer simulations have been used to study phenomena occurring at high temperatures or pressures which are difficult or impossible to study experimentally. The results of computer simulations have been used to test various statistical mechanical theories and may also be compared with those of a real experiment.

The microscopic state of a system at equilibrium can be specified in terms of the positions, the momenta and the interactions between the set of particles that constitute the system. For Monte Carlo simulations the momenta of the particles need not be specified. The interactions between the particles are often characterized by simpler and idealized pair potentials. For example the Lennard-Jones 12-6 potential

$$v^{LJ}(r) = 4\epsilon \left(\left(\frac{\sigma}{r} \right)^{12} - \left(\frac{\sigma}{r} \right)^{6} \right) \tag{F.1}$$

where

$v^{LJ}(r)$ is the pair potential between the particles separated by a distance r,

ϵ is the characteristic intermolecular potential,

σ is the characteristic intermolecular distance.

serves as an idealized pair potential reflecting the essential features of real interactions.

Computer simulations are usually performed on a small number of particles, between 10 and 10,000 in a cubical box. In simulations with small number of particles surface effects become important and a true comparison of results with a bulk fluid is not possible. This problem can be overcome by implementing periodic boundary conditions [151]. An infinite lattice is formed by replicating the cubic box throughout the space. As particles in the original box move during the course of the simulation, its periodic images in each of the neighboring images move exactly in the same manner. As a molecule moves out of the central box, its periodic image will enter the central box through the opposite face. Thus the central box has no walls at the boundary and therefore no surface effects come into play. As the neighboring images are identical to the central box, only the particle movement in the central box need to be examined. Figure F.1 shows a two dimensional representation of such a periodic boundary condition. As particle 1 leaves the central box its periodic image 1' enters the central box from the opposite side.

The properties of such a small, infinitely periodic, system will be the same as the macroscopic system it represents, if the particles in the central box are far enough to be unable to sense their periodic images. That is, as long as the particles in the central box do not interact with their periodic images, this microscopic system represents the macroscopic system. For a Lennard- Jones fluid, a box of length $L = 6\sigma$ is large enough to represent the macroscopic state when the periodic boundary conditions are applied to it. For a cube of side L, the periodicity will suppress any density waves

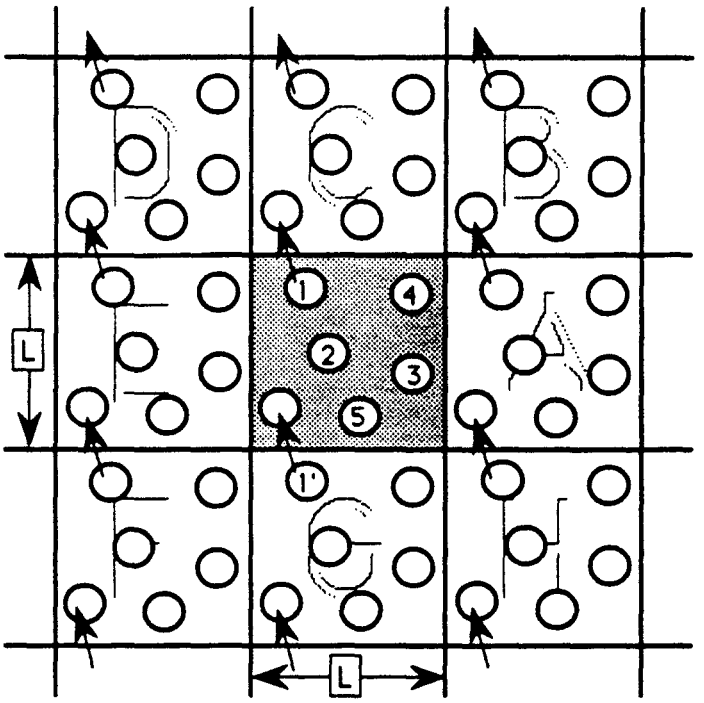

Figure F.1: Two dimensional representation of periodic boundary conditions

with a wavelength greater than L. Hence, it would not be possible to simulate a liquid close to the gas-liquid critical point, where the range of density fluctuations tend to very large. In Monte Carlo simulations, calculation of the potential energy of the microscopic system is an important step. Assuming pairwise additivity, the interaction of a particle 1 with all the remaining $N-1$ particles in the simulation box has to be accounted for. In principle, interaction between particles 1 and images of other particles in the neighboring boxes should be taken into account. By making the molecule 1 the center of a region which has the same size and shape as the simulation box, the molecule 1 is then said to interact only with particles whose centers lie within this region. This is called the 'minimum image convention'. Thus by the convention of the minimum image distance, one uses the shortest distance between the particle 1 and one of the images of the other particles in calculating the potential energy. Figure F.2 shows the minimum image convention applied to a two dimensional system. The pairwise additivity of particulate interactions involves $\frac{1}{2}N(N-1)$ terms in order to calculate the potential energy. For short- range forces, where the largest contribution to the potential energy comes from the neighbors close to the molecule of interest, a spherical cutoff is employed. That is, the pair potential $v(r)$ is set to zero for $r > r_c$, where r_c is the cutoff distance. Long-range corrections have to applied to the calculated properties such as potential energy and the pressure to correct for the spherical cutoff.

In equilibrium statistical mechanics ensemble averages of any mechanical quantity $f(\mathbf{x})$ is obtained by the integral

$$\langle f \rangle = \int \cdots \int f(\mathbf{x})\, \rho(\mathbf{x})\, d\mathbf{x} \tag{F.2}$$

where

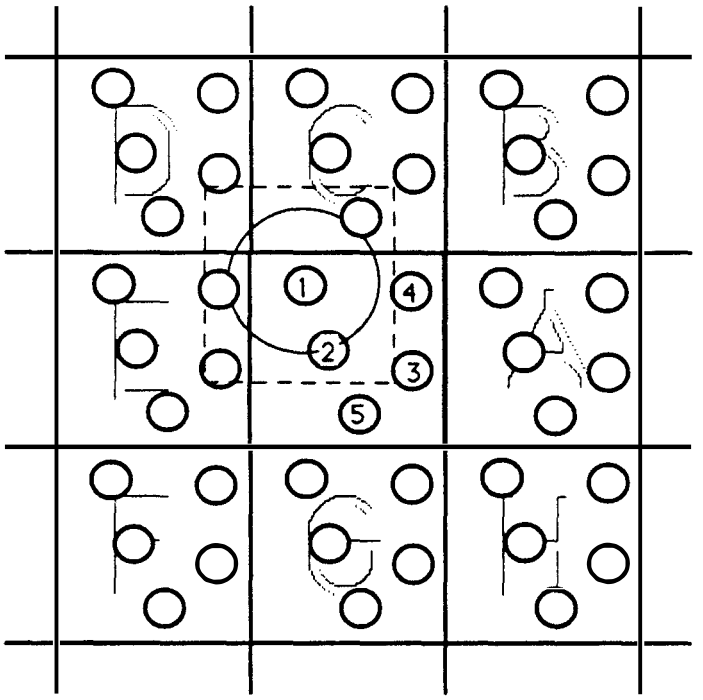

Figure F.2: Two dimensional representation of the 'minimum image convention'

$\rho(\mathbf{x})$ is the ensemble's probability density function,

$\mathbf{x}$ is a m dimensional vector defining the microscopic state of the system.

The Monte Carlo method estimates the average $\langle f \rangle$ as

$$\langle f \rangle = \frac{1}{n} \sum_{i=1}^{n} f[\mathbf{x}(t)]\, \rho(\mathbf{x}(t)) \tag{F.3}$$

where

$\mathbf{x}(t)$ represents a sequence of discrete states with $t = 1, \ldots i, j, \ldots n$,

n is the total number of discrete states over which the average was estimated.

In Monte Carlo estimation of an average like Equation (F.3), random numbers are used to generate the state $t = 1, \ldots i, j, \ldots n$. In Monte Carlo simulation of molecular systems, the state of the system is synonymous with the configuration of the system. Special sampling methods known as importance sampling are used in the statistical-mechanical applications of Monte Carlo. Importance sampling techniques choose random numbers generated from the distribution r (x), which allows the function evaluation to be concentrated in the region of space that make important contributions to the integral. However, as $\rho(\mathbf{x})$ is not a known quantity one cannot use the importance sampling method directly to calculate the average (F.3). If the successive sample states of a system are chosen to form a Markov chain, rather than to be independent samples, only the ratios of $\rho(\mathbf{x})$ for the successive states is needed to evaluate F.3. Any state j generated in this procedure depends only on the preceding state i, i.e. the one from which the

new state was generated. The transition from state j to i is occurs with a probability π_{ij} , which is also called the transition probability. A transition matrix consists of the transition probabilities π_{ij} as its elements. Additionally, π_{ij} is independent of the state j which requires that

$$\sum_{j=1}^{n} \pi_{ij} = 1 \qquad \text{for all } i \tag{F.4}$$

(F.5)

For the chain average $\langle f \rangle$ to be equal to equal to the ensemble average the following conditions have to be satisfied :

1. Ergodicity condition: i and j are any two admissible states and there are (say) k steps involved in going from i to j, then there exists an k-step transition probability π_{ij}^{k} which is non-zero. Thus every state can eventually be reached from another state.

2. Steady state condition :

$$\sum_{j=1}^{n} \rho_i \pi_{ij} = \rho_j \qquad \text{for all } j \tag{F.6}$$

Thus, the Monte Carlo procedure requires a selection of a transition probability scheme (a transition matrix) which satisfies the ergodicity and steady state conditions. Following the selection of such a scheme, the realization of the corresponding Markov chain can be used to estimate the average. A transition matrix can be selected such that it satisfies the principle of microscopic reversibility :

$$\rho_i \pi_{ij} = \rho_j \pi_{ji} \tag{F.7}$$

The most commonly used scheme for Monte Carlo simulations is that of Metropolis et al. If i and j are distinct states, the Metropolis solution considers two cases

$$\pi_{ij} = \begin{cases} \alpha_{ij} & \text{if } \rho_j \geq \rho_i \quad i \neq j \\ \alpha_{ij} \frac{\rho_j}{\rho_i} & \text{if } \rho_j < \rho_i \quad i \neq j \end{cases} \tag{F.8}$$

$$\pi_{ij} = 1 - \sum_{j=i} \pi_{ji} \tag{F.9}$$

In the case of Monte Carlo simulations, the state of the system is characterized by the positions of the particles and its total potential energy (i.e. its configuration). The original Metropolis method was applied to systems with a constant number of molecules. The states i and j differed only in the positions of the molecules. Thus, the transition from state i to j resulted by the displacement of a particle. The new state was accepted if

1. The probability density function of the new state ρ_j was greater than in the original state ρ_i.

2. A random number generated uniformly in the interval (0,1) is less than $\frac{\rho_j}{\rho_i}$ when ρ_j is less than ρ_i.

If neither of the conditions stated above are satisfied, the transition from state i to j is rejected.

F.2 Simulations in the Grand Canonical Ensemble

In the grand canonical ensemble, the limiting distribution ρ is proportional to the grand canonical partition function. The transition from state i to j can be either of the three types shown below:

1. a particle is displaced;

2. a particle selected at random, is destroyed;

3. a particle is created at a random position in the fluid.

The particle displacement is handled using the normal Metropolis method shown above. The ratios of the probabilities of the two states is given by

$$\frac{\rho_j}{\rho_i} = \exp\left(-\beta\,\Delta U_{ji}\right) \tag{F.10}$$

where

ΔU_{ji} is the change in the potential energy between state j and i.

If the particle displacement leads to a configuration with a lower potential energy, the new configuration is accepted. Alternatively, if the new configuration has a higher potential energy, then the new state is accepted with a probability $\frac{\rho_j}{\rho_i}$ which is given by Equation (F.10). In this case, a random number is generated uniformly on $(0,1)$. If the random number is less than F.10, the move is accepted. This can be summarized by saying that the particle displacement is accepted with the probability

$$min\left(1\ ,\ \exp\left(-\beta\,\Delta\,U_{ji}\right)\right) \tag{F.11}$$

If state j is obtained from state i by the destruction of a particle, the probabilities of the two states is

$$\frac{\rho_j}{\rho_i} = \exp\left(-\beta\,\Delta U_{ji} + \ln\left(\frac{N}{zV}\right)\right) \tag{F.12}$$

where

z is the chemical activity of the particle,

N is the number of particles in the original state i,

V is the volume of the simulation cell.

The destruction move is accepted with the probability

$$min\,(1\ ,\ \exp\,(-\beta\,\Delta\,U_{ji})) \tag{F.13}$$

If state j is obtained from state i by the creation of a particle, the probabilities of the two states is

$$\frac{\rho_j}{\rho_i} = \exp\left(-\beta\,\Delta\,U_{ji} + \ln\left(\frac{zV}{N+1}\right)\right) \tag{F.14}$$

where

N is the number of particles in the original state i.

The creation step is accepted with the probability

$$min\left(1, \exp\left(-\beta\,\Delta U_{ji} + \ln\left(\frac{zV}{N+1}\right)\right)\right) \tag{F.15}$$

In order to satisfy the condition of microscopic reversibility, the probability of an attempted creation α_c must equal the probability of an attempted destruction α_d. It is common practice to employ

$$\alpha_c = \alpha_d = \alpha_m = \frac{1}{3} \tag{F.16}$$

α_m is the probability of an attempted move or displacement of a particle. α_d is the probability of an attempted destruction of a particle. α_c is the probability of an attempted creation of a particle. Adams proposed a thermodynamic consistency check

for the pure fluid GCMC simulations based on the criteria for mechanical stability. For mechanical stability

$$\frac{\beta_T \gamma_V}{\alpha_P} = 1 \tag{F.17}$$

where

β_T is the isothermal compressibility of the fluid,

γ_V is the thermal pressure coefficient of the fluid,

α_P is the coefficient of thermal expansion of the fluid.

must be satisfied. Adams derived the expressions for calculating the isothermal compressibility, the pressure expansivity and the coefficient of thermal expansion from the average quantities and their cross moments obtained from a GCMC simulation.

In the case of a binary mixture the grand canonical partition function is given by

$$\Xi(V,T,\mu_1,\mu_2) = \sum_{N_1,N_2=0}^{\infty} \exp\left(\frac{N_1\mu_1 + N_2\mu_2}{kT}\right) \frac{V^{N_1+N_2}}{N_1!N_2!\Lambda_1^{3N_1}\Lambda_2^{3N_2}} \tag{F.18}$$

where

Ξ is the grand canonical ensemble partition function for the binary system,

V is the volume of the ensemble,

T is the temperature of the ensemble,

N_i is the number of molecules of species i ,

μ_i is the chemical potential of species i ,

Λ_i is the de Broglie wavelength of species i.

For performing simulations of a binary mixture in the grand canonical ensemble, the Markov chain is generated using a limiting distribution proportional to

$$\exp\left[\begin{array}{l} -\beta U_N + \beta N_1\mu_1 + \beta N_2\mu_2 + (N_1+N_2)\ln V \\ -3N_1\ln\Lambda_1 - 3N_2\ln\Lambda_2 - \ln N_1! - \ln N_2! \end{array}\right] \tag{F.19}$$

The average number of particles $\langle N_1\rangle$ and $\langle N_2\rangle$ depend on the chemical potentials μ_1 and μ_2 respectively. The algorithm used to perform GCMC simulations for a binary mixture is essentially the same as described above. The type of particle to be created or destroyed has to be specified during the creation or destruction moves. When attempting to destroy a particle, a particle is picked at random irrespective of its type. This results in a destruction probability of a species proportional to the its mole fraction. When creating a new particle, it is chosen to be of type 1 or 2 with an probability proportional to the mole fraction of the type chosen. This satisfies the condition of microscopic reversibility (F.7) for each of the individual species. The criteria for accepting new states are as follows :

- Particle displacement is accepted with the probability

$$\min\left(1\ ,\ \exp\left(-\beta\,\Delta\,U_{ji}\right)\right) \tag{F.20}$$

- Particle creation is accepted with the probability

$$\min\left(1\ ,\ \exp\left(-\beta\,\Delta U_{ji} + \ln\frac{z_k V}{N_k+1}\right)\right) \tag{F.21}$$

where

k is the type of particle being created.

N_k is the number of particles of type k in the original state.

- Particle destruction is accepted with the probability

$$\min\left(1\ ,\ \exp\left(-\beta\,\Delta U_{ji} + \ln\frac{N_k}{z_k V}\right)\right) \tag{F.22}$$

where

k is the type of particle being destroyed.

N_k is the number of particles of type k in the original state.

The realization of the Markov chain is achieved by generating a large number of successive states starting from an initial state. The new states are generated either by displacement, addition or destruction of particle. If the new state is accepted as per the conditions stated above, it is called an accepted state and is used in calculation of the average quantity. If the transition from state i to j was rejected the original state is retained and is also counted as another state in calculating the average . The number of accepted states has to be large in order that the MC estimate of $\langle f \rangle$ has the required precision. GCMC simulations for a pure Lennard-Jones fluid have not been reported at temperatures slightly above the critical temperature ($kT/\epsilon = 1.40$) and at reduced densities ($\rho\,\sigma^3$) of about 0.35. A cubical box to hold a total of 864 particles at a density of was chosen as the simulation box. Periodic boundary conditions and the minimum image convention were implemented in the simulations. The Lennard-Jones potential was cutoff at 6σ and appropriate long-range corrections were applied for the potential

Table F.1: Summary of the pure fluid simulation and comparison with the Nicholas equation of state at $\frac{kT}{\epsilon} = 1.40$ and $\rho\,\sigma^3 \approx 0.33$.

	Simulation (P)	Nicholas EOS [152]
ρ^*	0.33 ± 0.03	0.33
$\frac{P}{\rho^* kT}$	0.4061 ± 0.1	0.3727
$\frac{U}{\langle N \rangle kt}$	-1.5471 ± 0.14	-1.6257
$\frac{\mu}{kT}$	-2.5136	-2.5257

energy and the pressure in the cell. GCMC simulations were performed at $kT/\epsilon = 1.40$ and $\rho\,\sigma^3 \approx 0.33$ to evaluate the thermodynamic consistency of such an simulation. The chemical potential of the fluid needed to get the required density had to be obtained by trial and error. The Nicholas et al. [152] equation of state for the Lennard-Jones fluid predicted a reduced chemical potential (μ/kT) of -2.5257 for a reduced temperature of 1.35 and a reduced density of 0.34. The results of the simulation are shown in Table F.1. A thermodynamic consistency of 1.011 was obtained which showed that simulations could be performed at these conditions. In other simulations of near-critical systems with a fixed number of molecules, it has been found that clustering of molecules in the simulation box leads to a depletion in the number of molecules at the edges of the box. This is clearly seen when the number of excess molecules (above the bulk average) surrounding a selected molecule is plotted against the radius within which the excess molecules are counted. Figure F.3 shows the number of excess solvent molecules within a sphere of radius L from the central molecule for the pure fluid GCMC and a pure fluid CEMD [153] simulation. Clearly the GCMC simulation appears to have a more realistic long range behavior.

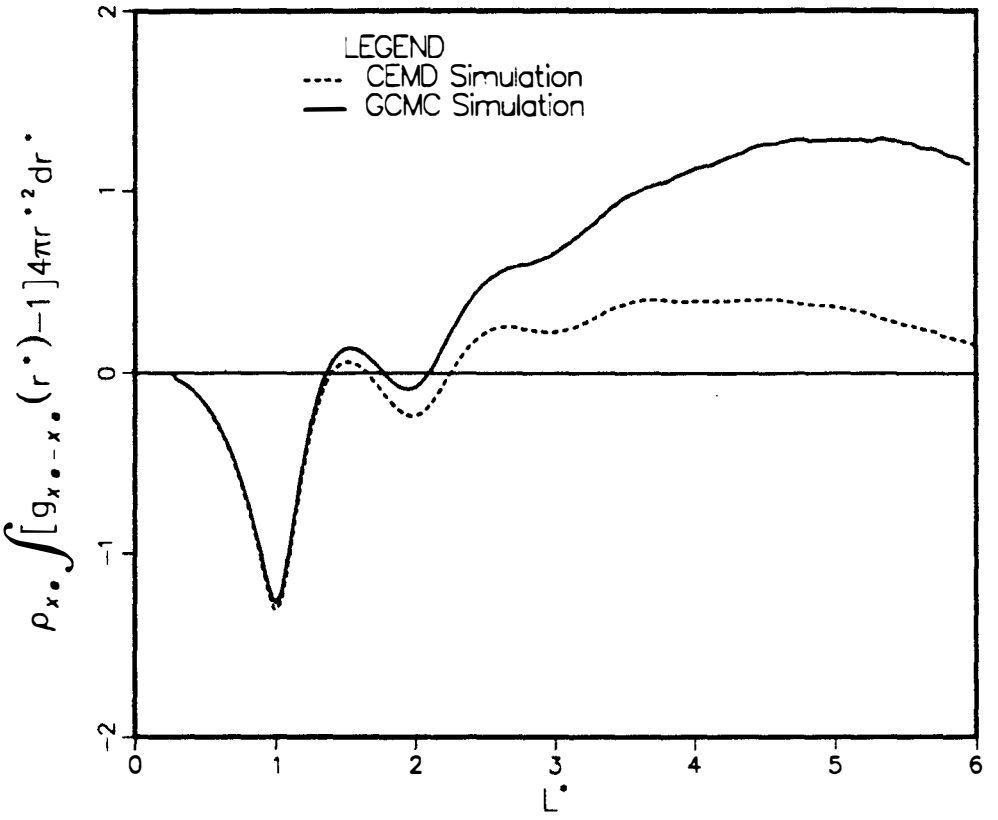

Figure F.3: Number of excess molecules surrounding a selected molecule

Table F.2: Potential Parameters used in the Mixture Simulations

Pair	σ (A)	ϵ/k (K)
Ne-Ne	2.503	24.5
Ne-Xe	3.047	65.1
Xe-Xe	3.591	172.7

GCMC simulations were performed on binary mixtures. The Lennard-Jones pair potential was used to model the interactions between the molecules. The respective Lennard- Jones parameters are shown in Table F.2. For the simulation all the parameters were reduced with respect to the size and potential parameter of the larger molecule. One of the objectives of performing the simulations was to compare the GCMC results with the MD results of Petsche and Debenedetti [153]. Hence, the conditions used in the simulation were very close their conditions. The chemical potentials of the molecules were determined by trial and error to get the approximate ratio of one solute molecule in 863 solvent molecules.

A cubical box to hold a total of 864 particles at a density of $\rho\,\sigma_{22}^3 \approx 0.35$ was chosen as the simulation box. Subscript 2 denotes Xenon and subscript 1 denotes Neon. An equilibriated configuration of 863 solvent molecules (Xenon) and 1 solute molecule (Neon) was used as an starting configuration for performing GCMC simulations. Periodic boundary conditions and the minimum image convention were implemented in the simulations. The Lennard-Jones potential was cutoff at $6\sigma_{22}$ and appropriate long-range corrections were applied for the potential energy and the pressure in the cell. Initial 500,000 accepted configurations were discarded in order to achieve a steady state. Table

Table F.3: Summary of the mixture simulations

Case	T^*	L^*	μ^*_{Ne}	μ^*_{Xe}	n_{acc}	n_{config}
R1	1.40	13.51	+0.737	−1.372	5.3×10^6	18.6×10^6
R2	1.40	13.51	+0.772	−1.413	7.1×10^6	24.0×10^6
R3	1.40	13.51	+0.799	−1.533	4.5×10^6	19.8×10^6

where

L^* is the length of the simulation box,

n_{acc} is the number of new configurations accepted during the simulation,

n_{config} is the number of new configurations attempted during the simulation.

F.3 gives the summarizes the simulations of dilute solutions of Neon(1) in Xenon (2) that were performed.

Table F.4 gives the results of these simulations. Figure F.4 shows the plot of the solvent-solute pair correlation function for the GCMC simulation and CEMD simulation. The agreement between the two methods is good, however, the pair correlation function obtained by the GCMC simulation is more noisier. The Kirkwood fluctuation integrals were calculated from fluctuations in the number of molecules in the simulation cell. These fluctuation integrals were calculated using the formula

$$G_{12} = V\left[\frac{\langle (N_1 N_2\rangle - \langle N_1\rangle \langle N_2\rangle}{\langle N_1\rangle \langle N_2\rangle} - \frac{\delta_{12}}{\langle N_1\rangle}\right] \tag{F.23}$$

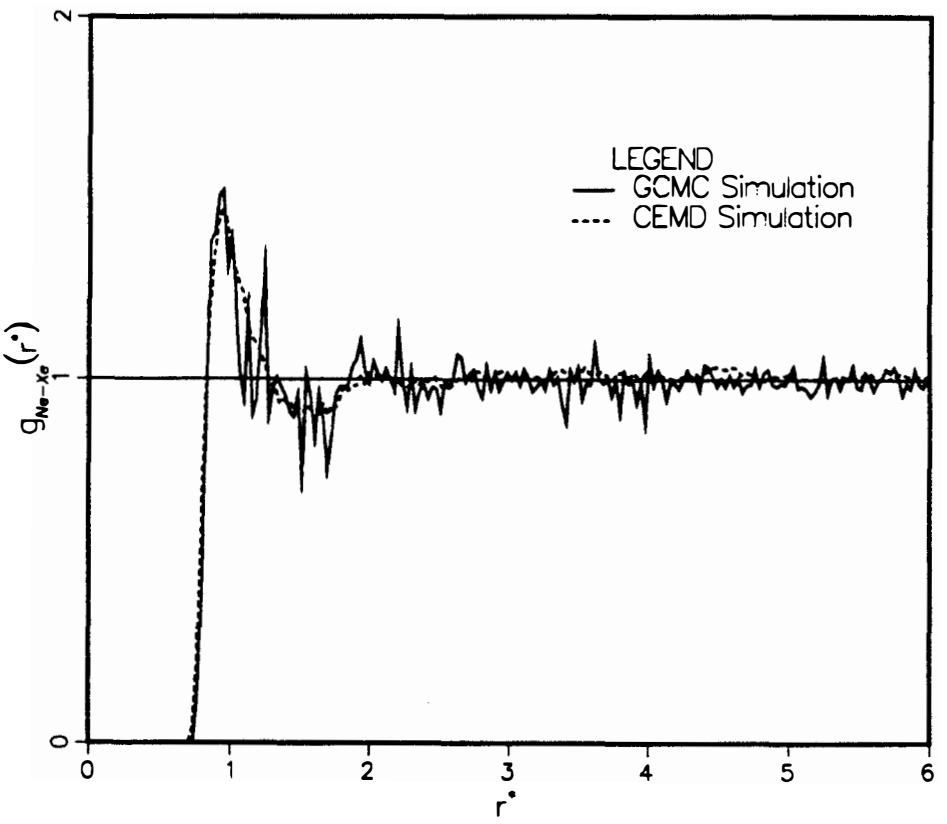

Figure F.4: Ne-Xe pair correlation function

Table F.4: Simulation results for Ne(1) in Xe(2) at $kT/\epsilon_{22} = 1.40$

	R1	R2	R3
$\langle N_{Ne} \rangle$	0.91 ± 0.13	1.02 ± 0.15	1.07 ± 0.16
$\langle N_{Xe} \rangle$	$666. \pm 58.$	$836. \pm 65.$	$972. \pm 50.$
$\langle \rho \sigma_{22}^3 \rangle$	0.27 ± 0.02	0.34 ± 0.03	0.39 ± 0.02
x_{Ne}	0.0014 ± 0.0002	0.0012 ± 0.0002	0.0011 ± 0.0002
$\frac{\langle U \rangle}{\langle N \rangle kT}$	-0.62 ± 0.26	-1.38 ± 0.28	-1.25 ± 0.22
$\frac{\langle P \rangle}{\langle N \rangle kT}$	0.63 ± 0.03	0.45 ± 0.08	0.51 ± 0.04

Table F.5: Summary of fluctuation integrals calculated from the simulations

	R1	R2	R3
$\frac{G_{Ne-Ne}}{\sigma_{22}^3}$	-1259 ± 1530	-1076 ± 3074	-1009 ± 440
$\frac{G_{Ne-Xe}}{\sigma_{22}^3}$	13 ± 13	5 ± 26	1 ± 7
$\frac{G_{Xe-Xe}}{\sigma_{22}^3}$	20 ± 29	13 ± 11	6.6 ± 1

However, the standard error in the calculated fluctuations was very large, making the estimates unreliable. Table F.5 summarizes the results of the fluctuation integral calculations. The standard deviations are based on subaverage of blocks of 5,000,000 configurations each. Hence, these results cannot be used for the calculation of thermodynamic quantities of interest. Attempts to simulate the dilute, attractive supercritical solution of Xenon in Neon in the grand canonical ensemble failed. At $kT/\epsilon = 1.40$ and chemical potentials yielding $\rho\sigma^3 \approx 0.35$, this system appeared to be in a two phase region for compositions near $x_{Xe} = 0.001$.

In general it can be concluded that GCMC simulations appear to be better than CEMD simulations for pure fluids. In the case of dilute repulsive mixtures, qualitative agreement can be found between CEMD simulations and GCMC simulations. However, the results of the GCMC simulations are much noisier than the CEMD simulations. Due to the large standard error in the calculated fluctuation integrals, they do not appear to be of practical value for calculating thermodynamic quantities of mixtures.

VITA

Vinod Mavji Shah was born in Bombay, India on July 19, 1960. He completed his High School studies in 1976 in Bombay. He received the Bachelor of Science degree in Chemistry from The University of Bombay in May 1981. He received another Bachelor of Science (Technology) degree in the Technology of Pharmaceuticals and Fine Chemicals from the University of Bombay in May 1984. He joined The University of Tennessee for the Master's program in Chemical Engineering in January 1987. After passing the Ph.D. qualifying exams he was allowed to bypass the master's program and was admitted to the doctoral program. He intends to continue work on extending the equation of state to a variety of fluids and fluid mixtures.